Integrated Modelling of Distribution Networks for Strategic Valuation of Distributed Energy Resources Deployment and Investment

Yiju Ma

Doctor of Philosophy

A thesis submitted for the degree of Doctor of Philosophy at
The University of Sydney in March, 2021

School of Electrical and Information Engineering
Faculty of Engineering
The University of Sydney

Abstract

Renewable generation such as rooftop photovoltaic (PV) systems constitute an increasingly important part of the electricity supply mix. However, increasing renewable penetration on distribution networks has in many jurisdictions reached levels where network issues have started to emerge, including over-voltages, reverse power flows and phase unbalance. In response to these issues, distribution network service providers (DNSP) have the option to invest in network augmentation such as transformer upgrade and line reconductoring to accommodate the increasing uptake of renewable generation, but it is often expensive and time consuming. On the other hand, flexible distributed energy resources (DER) such as battery energy storage systems (ESS) have the potential to become an economically viable alternative with its continuous cost reduction. However, very little work has assessed the extent to which the behind-the-meter DER investments, equipped by optimisation-based home energy management (HEM) systems, will benefit the network and DNSP. Thus, as DER become increasingly popular in distribution network operation and planning, methods and tools that assess their technical and financial performances are urgently needed. To this end, this thesis carries out a systematic assessment of distribution network with customer-owned and utility-owned DER, focusing on specific related topics including (i) probabilistic impact assessment of schedulable DER such as residential PV-battery systems on distribution networks; (ii) economic assessment on DER investments using *real options valuation* (ROV); and (iii) assessment on policies and regulations for improving network resource allocation and coordination for DER hosting capacity using game theoretic analysis.

In more detail, this thesis develops a novel probabilistic impact assessment framework to study the impact of schedulable DER on LV distribution networks. The application of rooftop PV-battery systems is used to demonstrate the efficacy of the framework. In particular, the proposed framework incorporates ESS operational decisions calculated using HEM systems within Monte Carlo (MC) time series power flow analysis, following a three-step process. First, using available smart meter data, a Bayesian nonparametric model is used to generate statistically-representative synthetic demand and PV profiles for producing thousands of simulation runs to capture the uncertain behaviours of demand and PV generation. Second, to reduce the computation time required by directly solving HEM problems within the MC analysis, a policy function approximation is used to emulate ESS operational decisions for the large pool of synthetic demand and PV profiles. This step makes the simulation of optimisation-based HEM feasible within the MC framework. Third, a comprehensive probabilistic power flow analysis is completed to show the impact of ESS, without any coordination, on reducing network issues

caused by excessive PV generation.

Based on the first contribution, the second contribution is to develop a financial framework that values DER investments that require scheduling. Specifically, ROV is used to design optimal strategies that allow DNSPs to flexibly make contingent decisions to execute real options created by uncertainty. These strategies help DNSPs increase the investment value and reduce the risk exposure. Specific to different types of investments, the integrated ROV framework incorporates network constraints modelled using (i) the probabilistic impact assessment framework to value the DNSP's incentive schemes for supporting residential DER investments; and (ii) an AC optimal power flow model to value grid-scale DER investments. The proposed integrated ROV framework shows that expensive network solutions can be delayed or avoided by strategically arranging and carrying out suitable DER investments.

Third, in addition to the integrated ROV framework that enables DNSPs to assess the DER investments on distribution networks, this thesis also proposes a novel game-theoretic framework that evaluates the efficiency loss in PV investments led by the policies and regulations for improving coordination and allocation of PV hosting capacity (and that of other DER). In particular, the proposed framework simulates the natural uncoordinated process where customers independently invest in PV systems under the recent PV inverter connection standards outlined in AS4777 to maximise their own welfare under limited network hosting capacity. The inefficiency of the PV investments caused by these new standards is reflected by comparing the uncoordinated investment process to an optimal PV sizing problem that maximises the overall network profit.

In summary, the models and tools developed in this thesis enables DNSP to (i) perform technical assessments on DER deployment using a probabilistic impact assessment framework; (ii) strategically evaluate and execute DER investments to increase the value to DNSP using an integrated ROV framework; and (iii) evaluate policies and regulations for improving coordination and allocation for network DER investments via a game theoretic framework.

Statement of Originality

This thesis is composed of my original work, and contains no material previously published or written by another person except where due reference has been made in the text. I have clearly stated the contribution by others to jointly-authored works that I have included in my thesis.

I have clearly stated the contribution of others to my thesis as a whole, including statistical assistance, survey design, data analysis, significant technical procedures, professional editorial advice, financial support and any other original research work used or reported in my thesis. The content of my thesis is the result of work I have carried out since the commencement of my higher degree by research candidature and does not include a substantial part of work that has been submitted to qualify for the award of any other degree or diploma in any university or other tertiary institution.

This work contains fewer than 50,000 words including appendices, bibliography, footnotes, tables and equations and has fewer than 150 figures.

Yiju Ma
July, 2020

Acknowledgments

I would like to express my deepest gratitude to my supervisors, Gregor Verbič and Archie Chapman. You have been very instrumental in my formation as a good researcher and team player. I would like to thank you for the continuous support and encouragement that you have given me throughout my Ph.D candidature. Without your guidance and assistance, I would not have completed my research to a high standard.

I would also like to thank my co-authors – Donald Azualatam, Kevin Swandi, Thomas Power, Daniel Gebbran and Kaveh Paridari – for their help and contributions to the work contained in this thesis. I am also grateful to Samir Gautam, Waqas Hassan, Sadiq Sani, Zahra Rahimpour, Jaysson Guerrero and Bowen Wang, for all the unforgettable moments we have shared together. You are all great friends and mentors to me.

I am thankful to my family, for you emotional support and sacrifices. Finally, my deep and sincere gratitude to my girlfriend, Wenhui Li, for her continuous and unparalleled love, help and support. I remain grateful.

This thesis is dedicated to my family.

List of publications

Below is a list of publications where I was the lead author. These publications have been included in different chapters in this thesis. The numbers in the tables represent the percentage shares of each author's contribution.

The following publication has been incorporated as Chapter 3.

1. **Yiju Ma**, Donald Azuatalam, Thomas Power, Archie C. Chapman and Gregor Verbič, A Novel Probabilistic Framework to Study the Impact of Photovoltaic-battery Systems on Low-Voltage Distribution Networks, *Applied Energy* Issue 254, Number 113669, 2019.

Contributor	Modelling	Analysis	Writing
Yiju Ma	80%	95%	80%
Others	20%	5%	20%

The following publication has been incorporated as Chapter 4.

2. **Yiju Ma**, Kevin Swandi, Archie C. Chapman and Gregor Verbič, Multi-Stage Compound Real Options Valuation in Residential PV-Battery Investment, *Energy* Issue 191, Number 116537, 2019.

Contributor	Modelling	Analysis	Writing
Yiju Ma	80%	95%	90%
Others	20%	5%	10%

The following publication has been incorporated as Chapter 5.

3. **Yiju Ma**, Archie C. Chapman and Gregor Verbič, Strategic Valuation of Compound Options for the Investment in Residential Battery Systems, *Submitted to IEEE Transactions on Power systems*, 2020.

Contributor	Modelling	Analysis	Writing
Yiju Ma	95%	95%	95%
Others	5%	5%	5%

The following publications have been incorporated as Chapter 6.

4. **Yiju Ma**, Mohammad Seydali Seyf Abad, Donald Azuatalam, Gregor Verbič, Archie Chapman, Impacts of Community and Distributed Energy Storage Systems on Unbalanced Low Voltage Networks, Australiasian Universities Power Engineering Conference (AUPEC), Melbourne, 2017.

Contributor	Modelling	Analysis	Writing
Yiju Ma	80%	90%	90%
Others	20%	10%	10%

5. **Yiju Ma**, Gregor Verbič and Archie C. Chapman, Estimating the Option Value of Grid-Scale Battery Systems to Distribution Network Service Providers, *PowerTech*, Milan, 2019.

Contributor	Modelling	Analysis	Writing
Yiju Ma	80%	95%	90%
Others	20%	5%	10%

6. **Yiju Ma**, Gregor Verbič and Archie C. Chapman, Optimal Investment Strategy in Grid-Scale Energy Storage Systems, *Asia-Pacific Solar Research Conference*, 2018.

Contributor	Modelling	Analysis	Writing
Yiju Ma	80%	95%	90%
Others	20%	5%	10%

The following publication has been incorporated as Chapter 7.

7. **Yiju Ma**, Daniel Gebbran, Archie C. Chapman and Gregor Verbič, A Photovoltaic System Investment Game for Assessing Network Hosting Capacity Allocation, *in the Eleventh ACM International Conference on Future Energy Systems* (*e'Energy*), June 2020, pp. 1-9

Contributor	Modelling	Analysis	Writing
Yiju Ma	80%	95%	80%
Others	20%	5%	20%

Contents

Abstract ii

Contents **ix**

List of Figures **xiii**

List of Tables **xvii**

List of Abbreviations **xix**

List of Symbols **xxi**

1 Introduction **1**

1.1 Thesis Structure 7

1.2 Background 8

1.2.1 Probabilistic Impact Assessment Framework 9

1.2.2 Real Options Valuation 11

1.2.3 Integrated ROV Framework considering Network Constraints 13

1.2.4 PV Investment Game 16

2 Literature Review **21**

2.1 Probabilistic Impact Analysis of PV and Energy Storage Systems on Distribution Networks 22

2.1.1 Residential PV-battery Impact Analysis 22

2.1.2 Monte Carlo Approaches 23

2.1.3 Home Energy Management with PV-Battery Systems 24

2.1.4 Residential Solar and Demand Modeling 25

2.1.5 Summary 26

2.2 Real Options Valuation in Power System Analysis 26
2.2.1 Methods for Real Options Valuation 29
2.2.2 Summary 32
2.3 Integrated Financial Modelling for DER Investments in Low-Voltage Networks 32
2.3.1 Bus Injection Model 32
2.3.2 Branch Flow Model 33
2.3.3 Optimal Power Flow for Unbalanced Distribution Networks 34
2.3.4 Optimal Sizing and Placement of Energy Storage Systems 35
2.3.5 Control Strategies for Energy Storage Systems 37
2.3.6 Summary 38
2.4 PV Investment Game 38
2.4.1 Game Theoretic Analysis in Distribution Network Investments 38
2.4.2 Inverter Volt/Var Control Functions 40
2.4.3 Summary 41

3 Probabilistic Impact Assessment Framework 43
3.1 Framework Overview 45
3.2 Demand and PV Trace Models 45
3.2.1 Data Preparation 46
3.2.2 Estimating the Dirichlet Distribution 46
3.2.3 Markov Chain Process 47
3.3 Home Energy Management 47
3.3.1 Scheduling Problem 48
3.3.2 Policy Function Approximation 50
3.4 Probabilistic Impact Assessment Framework 51
3.4.1 Sampling Process 51
3.4.2 Power Flow Analysis 53
3.5 Results and Evaluation 54
3.5.1 Computational Performance 54
3.5.2 Test Networks 55
3.5.3 HEM Formulation 55
3.5.4 Voltage Problems 56
3.5.5 Thermal Problems 59
3.5.6 Phase Unbalance 61
3.5.7 Real-World Applications 61

3.6 Summary 62

4 Multi-Stage Compound Real Options Framework 65
4.1 Real Options Valuation 66
4.1.1 ROV with the LSMC method 67
4.1.2 ROV Instruction Manual 69
4.2 Costs and Benefits Analysis 73
4.2.1 NPV Calculation 73
4.2.2 Modelling of Future Uncertainties 75
4.3 Results and Evaluation 78
4.3.1 Diesel Generator Cash Flow Analysis 79
4.3.2 PV-Battery Cash Flow Analysis 79
4.3.3 PV-Battery Investment: ROV Analysis 81
4.3.4 Sensitivity Analysis 83
4.4 Summary 85

5 A Novel Real Options Framework to Value Residential Energy Storage Investment 89
5.1 Impact Assessment framework 90
5.1.1 PV and Demand Synthesis 90
5.1.2 Home Energy Management 91
5.1.3 Policy Function Approximation 91
5.1.4 Power Flow Analysis 92
5.2 Integrated ROV Framework 93
5.2.1 Costs and Benefits Analysis 94
5.2.2 Modelling of Future Uncertainties 95
5.3 Results and Evaluation 96
5.3.1 Computational Performance 96
5.3.2 Test Networks 97
5.3.3 Thermal Loading Reduction 97
5.3.4 Battery Storage Cash Flow Analysis 98
5.3.5 Residential ESS Investment: ROV Analysis 99
5.4 Summary 101

6 A Novel Real Options Framework to Value Grid-Scale Energy Storage Investment 103
6.1 Energy Storage Modelling 104

6.2 Optimal Power Flow Formulation . . . 105
6.2.1 Objective Function . . . 105
6.2.2 Branch Flow Constraints . . . 105
6.2.3 Modified Objective Function . . . 107
6.3 Valuation of Grid-Scale ESS . . . 108
6.4 Results and Evaluation . . . 109
6.4.1 Computational Performance . . . 111
6.4.2 Performance Indices . . . 111
6.4.3 Community ESS . . . 113
6.4.4 Distributed ESS . . . 114
6.4.5 Comparisons of Community and Distributed ESS . . . 117
6.4.6 Community ESS Investment: ROV Analysis . . . 117
6.5 Summary . . . 120

7 PV Investment Game **123**
7.1 Preliminaries . . . 124
7.1.1 Concave Potential Games . . . 124
7.2 Optimal Power Flow Formulation . . . 126
7.2.1 Objective Function . . . 127
7.2.2 Branch flow Constraints . . . 127
7.3 Methodology . . . 129
7.3.1 Payoff Calculation . . . 129
7.3.2 Computing the Nash Equilibrium . . . 130
7.4 Results and Evaluation . . . 131
7.4.1 Test Networks . . . 131
7.4.2 Impact of the VVC function . . . 132
7.4.3 PV Investment Game . . . 133
7.5 Summary . . . 136

8 Conclusion **139**
8.1 Summary of Results . . . 139
8.2 Future Research . . . 141

Bibliography **143**

List of Figures

1.1 Overview of the structure and the connections between the chapters. 7

3.1 Overview of framework used to conduct the probabilistic MC power flow study to assess the impact of PV-battery on distribution networks. 44

3.2 The PFA model. 50

3.3 Example scheduling estimates from PFA ($p_{\mathrm{b}}^{\mathrm{PFA}}$), the calculated schedules from DP ($p_{\mathrm{b}}^{\mathrm{DP}}$), and the corresponding PV generation (p_{PV}), demand (p_{d}), grid powers, $p_{\mathrm{g}}^{\mathrm{PFA}}$ and $p_{\mathrm{g}}^{\mathrm{DP}}$, from PFA and DP, respectively. 52

3.4 Percentage of customers with voltage problems, transformer loading level and phase unbalance. Pink, green and blue bars represent 0%, 50% and 100% ESS penetration levels, respectively. Each bar from top to bottom shows the maximum, 75 percentile, median, 25 percentile and minimum value. 55

3.5 Voltage profiles (top), grid power (p_{g} and $\hat{p}_{\mathrm{g}}$ denote grid power with and without ESS, respectively) (middle), ESS scheduling (p_{b}), PV (p_{PV}), demand (p_{d}), and the SOC (bottom) of a customer with 5.5kW PV and 9.8kWh ESS on AUS 2 on a particular winter day, with 100% P_{PV}. 57

3.6 Voltage profiles (top), grid power profiles (middle), ESS scheduling, PV, demand and the SOC (bottom) of a customer with 3kW PV and 6.5kWh ESS installed on AUS 2 on a particular summer day, assuming 100% P_{PV}. 58

3.7 Voltage profiles (top), grid power profiles (middle), ESS scheduling, PV, demand and the SOC (bottom) of a customer with 7kW PV and 14kWh ESS installed on AUS 2 on a particular summer day, assuming 100% P_{PV}. 59

3.8 Comparisons between HEM under ToU and SCM on AUS 2. 60

4.1 Least square regression in Year 5. 71

4.2 Architecture of the LSMC approach. The top figure shows the forward MC model which captures the variations of state variables, and each decision node is given an option value $F_{t_n,\omega}$. The bottom figure uses Years 1 and 2 as an example to demonstrate how backward induction is used, where $\Pi_{t_n,\omega}$ is the payoff and $\Phi_{t_n,\omega}$ is the continuation value. In the Least square regression box, the best-fitting curve is found based on $\Pi_{t_{n+1},\omega}$, this curve is used to estimate the continuation value at t_n. . 72
4.3 Distribution of simulated average monthly growth in future peak demand that is over the transformer thermal limit via GBM (drift = 1.5% and volatility = 9.8%) 76
4.4 Distribution of simulated future diesel price via a mean reverting process (speed of reversion = 5%, reversion level = 2.6, volatility = 4.7%). 77
4.5 Distribution of simulated future cost of PV-battery system via risk neutral valuation (risk-free rate = 0.06, volatility = 9%) 78
4.6 Costs for executing the diesel generator investment (left) and the PV-battery investment in Year 1 (right). 80
4.7 Payoffs for executing the PV-battery investment in each of the decision years (left), and for expanding the investment in each of the decision years (right). 80
4.8 Frequency distribution of optimal investment timing for the option to defer the investment in the first decision period, and the option to expand the investment in the second decision period (benchmark). 81
4.9 Impact on optimal investment timing with respect to changing drift parameter and volatility of the state variables. 86

5.1 The PFA model. 93
5.2 Transformer loading before/after executing the ESS investment in each decision year (left); Transformer loading before/after the expansion in ESS capacity in each decision year, assuming the investment has been executed (right). P_{b} is the percentage of existing PV installations equipped with ESS in $\mathcal{T}_{\mathrm{inv}}$. P_{b}^{*} is the percentage of new PV installations equipped with an ESS. The increase in the transformer loading is mainly due to the increase in PV penetration levels. Specifically, Fig. 3.1 in Chapter 3 shows the impact of ESS under different PV penetration levels on the same network as the one used in the case study in this Chapter. It shows that the transformer loading level is at 40% when there is no PV, this percentage decreases initially at low PV penetration levels but quickly comes back to just under 50% when PV penetration reaches 50%. Continue increasing the PV capacity would further increase this loading level as more power is flowing back to the transformer. 98

5.3 Length of overloaded distribution lines with/without ESS. The ESS investment is executed in $\mathcal{T}_{inv}$ (left), and expanded in $\mathcal{T}_{exp}$ (right). 98
5.4 Cash flows of ESS investment executed in each decision year in $\mathcal{T}_{inv}$ (left) and expansion executed in each decision year in $\mathcal{T}_{exp}$ (right). 99
5.5 Cash flows of network augmentation for the same amount of network capacity increase from ESS systems throughout $\mathcal{T}_{inv}$ (left) and $\mathcal{T}_{exp}$ (right). 100
5.6 Payoff cash flows of the ESS investment executed in each decision year in $\mathcal{T}_{inv}$ (left) and expansion in $\mathcal{T}_{exp}$ (right), considering the cost of network augmentation as monetary savings. 100

6.1 The unbalanced LV network, the black and red circles denote the substation transformer (bus 1) and CESS (bus 702), while the three green squares represent DESS (buses 153, 676 and 1786) [1]. The purple and yellow circles indicate the locations for bus 2266 and 1940, respectively. 111
6.2 Charging and discharging rates on a typical day in each season, given that the maximum charging and discharging rates are 90kW. 113
6.3 State of Charge on a typical day in each season 114
6.4 Annual energy losses (left) and hosting capacity (right) wrt number of ESSs 115
6.5 This figure shows the payoff for investing in grid-scale ESS in each year (top-left), the cost for investing in grid-scale ESS in each year (top-right), the cost for network augmentation (bottom-left), and the cost for grid supply that is above the transformer limit (bottom-right). 118
6.6 NPV distribution with and without flexibility for the deferral option 119

7.1 Payoff curves for three network customers who have a different payoff trajectory with respect to their PV investment size. Each player's payoff regression curve is approximated by increasing its own investment size, while others remain fixed. . . 125
7.2 The Volt/Var control curve. 128
7.3 Voltage profiles on a randomly selected day for a consumer with 2kW PV system with (blue) and without (red) the VVC function. 131
7.4 Demand, PV generation, reactive power output and PV curtailment on a randomly selected day for a consumer with 2kW PV system. 132
7.5 Payoff curves with respect to the number of iterations for all 39 players. 133
7.6 PV investment size curves with respect to the number of iterations for all 39 players. 134
7.7 PV investment sizes from the game and the centrally-coordinated solution. 135

7.8 Investment payoffs from the game and the centrally-coordinated solution. 136
7.9 Annual PV generation from the game and the centrally-coordinated solution. 137
7.10 Annual Energy cost from the game and the centrally-coordinated solution. 138

List of Tables

3.1 Energy storage system specifications 52
3.2 LV test feeders 54

4.1 Cost specifications. 74
4.2 ROV results under different scenarios - part I. 81
4.3 ROV results under different scenarios - part II. 82

5.1 Energy storage system specifications 93
5.2 Drift and volatility of state variables. 96
5.3 Frequency distribution of optimal strategy 100

6.1 Improvement in energy losses and the hosting capacity wrt different numbers of ESSs 116
6.2 Max and average VUFs wrt numbers of ESSs 117
6.3 Frequency distribution of optimal strategy 120

List of Abbreviations

ADP	Approximated Dynamic Programming
AEMO	Australian Energy Market Operator
AMPL	A Mathematical Programming Language
ANN	Artificial Neural Network
BTM	Behind-the-meter
CESS	Centralized Energy Storage System
DER	Distributed Energy Resources
DG	Distributed Generation
DNSP	Distribution Network Service Provider
DP	Dynamic Programming
DESS	Distributed Energy Storage System
ENWL	Electricity North West Limited
ESS	Energy Storage System
EV	Electric Vehicles
FiT	Feed-in Tariff
HEM	Home Energy Management
LSMC	Least Square Monte Carlo
LV	Low Voltage
MC	Monte Carlo
MDP	Markov Decision Process
MILP	Mixed Integer Linear Programming
NEM	National Electricity Market
NPV	Net Present Value
PDE	Partial Differential Equations
PFA	Policy Function Approximation

PV	Photo-Voltaic System
RNN	Recurrent Neural Network
SCM	Self-consumption Maximization
SOC	State of Charge
ToU	Time-of-Use
VUF	Voltage Unbalance Factor

List of Symbols

Sets

$\mathcal{K}$	Set of total network buses, b
$\mathcal{E}$	Set of potential network buses for an ESS installation
$\mathcal{L}$	Set of distribution lines, l
$\mathcal{D}$	Set of days in one year
$\mathcal{F}$	Set of network phases A, B and C
$\mathcal{O}$	Set of Observed customers, o
$\mathcal{M}$	Set of Unobserved customers, m
Γ	Set of features γ for observed customers
$\mathcal{T}$	Set of time-steps, t in a day, $\mathcal{T} = \{1, ..., 48\}$
$\mathcal{S}$	Set of state variables, s
$\mathcal{X}$	Set of control variables, x
$\mathcal{W}$	Set of random variables, w
$\mathcal{D}_{\text{load}}$	Set of load assignments
$\mathcal{D}_{\text{pv}}$	Set of PV system assignments
$\mathcal{D}_{\text{b}}$	Set of battery storage assignments
$\mathcal{B}$	Set of network features β
$\mathcal{T}_{\text{inv}}$	Set of investment years from t_0 to T_{inv}
$\mathcal{T}_{\text{exp}}$	Set of years for expanding the investment from t_0 to T_{exp}
$\mathcal{N}$	Investment period is divided in to $n \in \mathcal{N}$ intervals, whose length is 1 year
$\mathcal{S}_{\zeta}$	Set of state variables from electricity network
$\mathcal{S}_{\upsilon}$	Set of state variables from electricity market
$s^{\mathbf{M}}$	Set of constraints for all state and control variables
$\mathcal{H}$	Set of options h in an investment
Υ	Set of actions υ in a game

Ψ	Set of iterations ψ of a game
$\mathcal{I}$	Set of players ι in a game
Ξ	Set of payoff functions ξ_ι for players $\iota \in \mathcal{I}$
Ω	Set of Monte Carlo paths, ω

Parameters

$\mathbf{p}$	Parameters of a categorical distribution
$\bar{Q}_i$	Maximum inverter reactive power capacity at bus i
$\bar{S}_i$	PV inverter's maximum capacity at bus i
$\bar{v}$	Maximum phase voltage for all buses
$\underline{v}$	Minimum phase voltage for all buses
R_{ij}	Single phase resistance between buses i and j
X_{ij}	Single phase reactance between buses i and j
η^+	Energy storage charging efficiency
η^-	Energy storage discharging efficiency
η^{i}	Inverter efficiency
γ^c	Maximum charging rate
γ^d	Maximum discharging rate
$s^{\mathrm{b}}_{\max}$	Maximum battery state of charge
$s^{\mathrm{b}}_{\min}$	Minimum battery state of charge
e^{com}	Capacity of a community energy storage system
N_{b}	Number of storage systems in the network
c^{line}	Cost of line reconductoring per unit length
c^{trans}	Cost per 1kVA transformer capacity upgrade
c^{DG}	Capital cost of diesel generator per 1kW
e_0	initial state of charge
e_Ω	Initial state of charge for the next cycle
μ	Drift parameter
σ	Volatility

Variables

S_{m}	Random variable assigning a cluster to each customer
α^{b}_t	Energy storage charging status (0: discharging, 1: charging)
s^{b}_t	State variable for battery state-of-charge at time t

s_t^{p}	State variable for electricity tariff at time t
s_t^{g}	State variable for grid power at time t
s_t^{d}	State variable for household electricity demand at time t
s_t^{pv}	State variable for household PV generation at time t
x_t^{b}	Control variable for battery at time t
w_t^{d}	Perturbation information in demand at time t
w_t^{pv}	Perturbation information in PV generation at time t
$p_{\mathrm{b}}^{\mathrm{PFA}}$	Battery scheduling estimates from policy function approximation
$p_{\mathrm{b}}^{\mathrm{DP}}$	Battery scheduling estimates from dynamic programming
$p_{\mathrm{g}}^{\mathrm{PFA}}$	Grid power estimates from policy function approximation
$p_{\mathrm{b}}^{\mathrm{DP}}$	Battery scheduling estimates from dynamic programming
$p_{t,i}^{\mathrm{d}}$	Active load at time t, bus i
$q_{t,i}^{\mathrm{d}}$	reactive load at time t, bus i
$p_{t,i}^{\mathrm{pv}}$	Active PV generation at time t, bus i
$q_{t,i}^{\mathrm{pv}}$	Reactive generation from PV inverter at time t, bus i
$p_{t,i}^{\mathrm{c}}$	Active power curtailment at time t, bus i
$p_{f,t,ij}$	Single phase active power at time t between buses i and j
$q_{f,t,ij}$	Single phase reactive power at time t between buses i and j
$p_{f,t,ij}^{\mathrm{loss}}$	Single phase active power losses at time t, between buses i and j
$\hat{p}^{\mathrm{c}}$	Maximum inverter active power curtailment in a network
$v_{f,t,i}$	Phase voltage at time t, bus i
v_{sub}	Transformer secondary winding phase voltage
$v_{t,i}^{+}$	Positive sequence voltage at time t, bus i
$v_{t,i}^{-}$	Negative sequence voltage at time t, bus i
$x_t^{\mathrm{b}+}$	Charging rate for one phase at time t
$x_t^{\mathrm{b}-}$	Discharging rate for on phase at time t
$B_{t,i}^{\mathrm{loc}}$	Binary variable to locate an energy storage at bus i
e_j^{dist}	Capacity of distributed energy storage system j
$c_{t_n,\omega}^{\mathrm{pv}}$	Cost of PV system per 1kW in year t_n, ω^{th} simulation path
$c_{t_n,\omega}^{\mathrm{b}}$	Cost of battery per 1kWh in year t_n, ω^{th} simulation path
$c_{t_n,\omega}^{\mathrm{f}}$	Cost of diesel price per litre in year t_n, ω^{th} simulation path
$c_{t_n,\omega}^{\mathrm{aug}}$	Cost of network augmentation in year t_n, ω^{th} simulation path
$c_{t_n,\omega}^{\mathrm{g}}$	Cost of energy over the thermal limit in year t_n, ω^{th} simulation path
$c_{t_n,\omega}^{\mathrm{delay}}$	Cost for overloading the network in year t_n, ω^{th} simulation path

$c^{\mathrm{OM}}_{t_n,\omega}$	Cost of maintenance and operation in year t_n, ω^{th} simulation path
c^{inv}_{n}	Cost of rooftop PV procurement and installation for customer n
c^{r}_{n}	Revenue from exporting to the grid for customer n
$\hat{c}^{\mathrm{e}}_{n}$	Electricity cost with PV system for customer n
c^{e}_{n}	Electricity cost without PV system for customer n
$\Delta p^{\mathrm{max}}_{t_n,\omega}$	Capacity increase in transformer in year t_n, ω^{th} simulation path
$\Delta l_{t_n,\omega}$	Line loading reduction in year t_n, ω^{th} simulation path
$\Delta E^{\mathrm{Cap}}_{t_n,\omega}$	Installed capacity for PV systems in year t_n, ω^{th} simulation path
$p^{\mathrm{d}}_{t_n,\omega}$	Aggregated growth in power demand in year t_n, ω^{th} path
$p^{\mathrm{pv}}_{t_n,\omega}$	PV uptake in year t_n, ω^{th} path
P_{pv}	PV penetration level
P_{b}	Battery penetration level
P^{*}_{pv}	Increase in PV penetration in the period of investment expansion
P^{*}_{b}	Increase in battery penetration from investment expansion
L_j	Orthonormal basis of j^{th} state variable
$\hat{\phi}_j$	Group of optimal coefficients ϕ_j for the basis function of j^{th} state variable
π	Optimal policy
τ_ω	Optimal investment timing in ω^{th} simulation path
$\Pi_{h,t_n,\omega}$	Investment payoff for option h in year t_n, ω^{th} simulation path
$F_{h,t_n,\omega}$	Value of option h in year t_n, ω^{th} simulation path
r	Risk neutral discount rate
$\Phi_{t_n,\omega}$	Continuation value in year t_n, ω^{th} simulation path

Matrices and Vectors

$\mathbf{M}_t$	State transition matrices for observed customers
$\boldsymbol{\alpha}$	Vector of cluster counts

Chapter 1

Introduction

Power systems are currently undergoing a transformation aided by advanced communication technologies and infrastructure. In the future, they are envisaged to comprise increasing amounts of distributed energy resources (DER) connected in low-voltage (LV) distribution networks. DER is a common term taken to describe the combination of flexible energy resources like distributed generation, battery energy storage systems (ESS) and electric vehicles (EV). Distributed generation includes low capacity renewable power generation, which is usually connected to a low voltage (LV) distribution network, and often located near the point of use.

In this context, photovoltaic (PV) systems are becoming an increasingly important part of the electricity supply mix. Rooftop PV investments have been made by businesses and households as they take on a more active role in managing their energy use. According to the International Energy Agency (IEA), the installed capacity of rooftop PV systems has grown from 8GW in 2007 to over 400GW in 2017 [2]. In Australia, the annual installed capacity of small-scale PV systems has grown from less than 200MW in 2009 to 1.1GW in 2017, with the average installation size rising from 1.5kW to 5.5kW [3]. Following this trend, projections by the Australian Energy Market Operator (AEMO) see the installed capacity of rooftop PV reaching 21GW in 2030 [4]. The rise of PV generation is motivated by the steady decline in the cost of technology, as well as customers' initiative to reduce their electricity bills and become less dependent on the electricity grid in the future. Specifically, AEMO predicts an annual cost decline of 1.5% for all PV system sizes until 2040 [3].

However, rooftop PV penetration levels have in many jurisdictions reached levels where network issues have started to emerge; these include over-voltages, reverse power flows, and phase unbalance [5]. However, PV systems alone are ineffective at solving this problem because they do not usually generate power during peak demand periods. The presence of these issues

indicates the need for an urgent solution, especially in Australia, where the uptake of DER is expected to be high in the future.

One solution for distribution network service providers (DNSP) to mitigate the problems caused by high PV generation is to apply network augmentation which in this context involves upgrading transformers and applying line reconductoring to eliminate the technical issues and accommodate the increasing levels of renewable generation [6]. In general, the costs to mitigate voltage violations by using advanced inverters, line voltage regulators or capacitors and adjusting the set points of existing voltage regulating equipment are relatively low [7]. However, a substation load tap changer, if not already present and must be installed, will post a substantial cost, which ranges from $105k to $1350k [7]. Moreover, line reconductoring and/or upgrades in transformer capacity that are required for mitigation of thermal overloading issues also come with high expenses. The cost of reconductoring varies by circuit, i.e. it depends on the size and type of the distribution lines as well as the amount/distance of the lines that must be replaced[1] [7].

To avoid the need for expensive and time-consuming network augmentation, DNSP have shifted its investment focus to flexible DER[2] with storage capability. Examples include grid-scale ESS and residential ESS that are built in conjunction with rooftop PV systems[3]. They are becoming an increasingly appealing alternative because (i) the cost of technology has been falling [8]; and (ii) they are capable of managing power flows in distribution networks and increasing network capacity to accommodate more renewable generation [9].

In fact, battery ESS has gradually become an increasingly popular DER in countries with high PV penetration. In Australia, 12% of the 172,000 residential solar installations in 2017 included an ESS, while this proportion was only 5% in 2016 [10]. Given this, a total of 28,000 ESS had been installed by the end of 2017 [10]. In addition, projections by AEMO see residential ESS capacity reaching 6.6GW by 2035, with 3.8GW expected to be installed as part of PV-battery systems [11]. A key driver to these trends is the falling cost of the technology, predictions by AEMO see the cost of small-scale ESS dropping by greater than 50% from 650$/kWh in 2017 to 300$/kWh in 2037 [12].

Driven by this declining cost, ESS will become economically viable in the near future and therefore a more appealing solution than network augmentation. Current literature and practice

[1] In practice, DNSP will apply reconductoring only to the overloaded part of the network.

[2] In this context, flexible DER refer to any resource that provides flexibility in electricity demand and production. Examples include ESS (electric vehicles) that can charge with excess PV generation and discharge for peak demand support and loads that use thermal inertial to maintain the temperature in an acceptable range.

[3] In Australia and some other jurisdictions, asset ring-fencing regulations mean that PV-battery systems must be owned by network customers. However, to promote the use of this technology, DNSP must provide incentives to cover a large proportion of ESS procurement and installation cost.

use heuristic rules such as self-consumption maximisation to determine ESS operational profiles. However, it is expected that in the future a large proportion of the ESS installations will be equipped by HEM to optimally facilitate energy use within each household to save electricity bills, given that they exist now (e.g. Reposit) and the move to more fog and edge computing, driven by the Internet of things (IoT), will likely to push this further. Within this context, limited research has studied how uncoordinated PV-battery systems, whose operational profiles are determined by HEM optimisation, can benefit our networks [13].

Specifically, ESS and other flexible DER pose significant challenges in power system planning and operation, due to two reasons. First, including flexible DER into a probabilistic analysis considering uncertainties such as load behaviour, operations of DER, as well as sizing and location of DER is challenging. This is because properly capturing these uncertainties considering a range of PV and battery penetration levels requires thousands of simulation runs, typically by using Monte Carlo (MC) approaches. However, the operational profiles of DER are determined by computationally intensive optimisation. Solving optimisation for thousands of MC simulation runs is therefore impractical. Second, MC analysis requires a large pool of statistically-representative demand and PV profiles to sample from such that it can capture the uncertainties involved with customers' energy use, sizing and placement in DER. However, in many jurisdictions smart metering data are scarce.

To fill these gaps, this thesis develops a toolchain to enable DNSP to study the techno-economic performance of flexible DER investments. First, a novel probabilistic impact assessment framework is proposed to investigate the technical benefits of DER deployments in distribution networks. This framework enables DNSP to evaluate the applications that require optimisation for resource scheduling, such as probabilistic studies on impact of DER scheduling on distribution networks.

Second, this thesis develops a financial framework to enable DNSP to determine efficient and well-timed strategy for a DER investment to maximise its value and reduce any downside risks. In this regard, the probabilistic impact assessment framework provides two key ingredients to conduct the financial assessment including (i) quantitative evaluation of technical impacts of DER on distribution networks; and (ii) network uncertainties including load behaviour, operation of DER, as well as sizing and placement of DER.

Even though, DNSPs still face increasing challenges in designing optimal strategy in DER investments, because of (i) the existence of *real options* that add opportunity values to the investment; and (ii) the need to consider the uncertainties that come from various sources including both the network planning & operation and electricity market. Failing to systematically

capture the value of *real options* and their associated uncertainties can lead to decisions that undervalue the investment.

A tool fit for purpose in this context is *real options valuations* (ROV) because of its ability to flexibly execute *real options* during the life time of an investment. Whereas traditional cash flow analysis commits to making future decisions at the present time, an investor may have the options to alter the investment decisions in the future, based on the realisation of uncertainty. For example, an investor can delay the investment, or invest with a lower capital budget and expend the investment if the market condition turns more favourable in the future. These options are called *real options* which exist due to uncertainties. Example options in a distribution network investment include options to *defer*, *expand*, *contract* and *abandon*. Each of these options is a contingent decision that the investor has the flexibility to make based on the realisation of future uncertainties, typically captured by MC simulations. Following the optimal strategy designed by ROV to execute the options reduces the exposure to risk and increases the investment value, assuming that it is management's right, but not obligation, to make contingent decisions [14].

The concept of ROV highlights the importance of managerial flexibility, which is not captured in standard cash flow assessments. Typically, standard cash flow approaches often undervalue the investments by ignoring the possibility of flexibly executing the real options presented by uncertainty. The decision rule of these approaches is to undertake the investment immediately if the net present value (NPV) is positive and reject those with a negative NPV, regardless of how future uncertainties will unfold [15]. The future decisions are made at the present time, and therefore ignoring the managerial flexibility in executing the options in an irreversible distribution network investment.

However, it is difficult to apply ROV to distribution network investments because (i) the cash flows for these distribution network investments are usually negative and not close to zero[4]; and (ii) it is difficult to identify and include all uncertainties that can be coming from multiple sources such as the network and electricity market, and typically when there are more than one investment involved. Specifically, capturing network uncertainties including load behaviour, operation of DER, as well as sizing and placement of DER requires explicit and integrated modelling of the distribution network within MC-based financial frameworks. Failing to overcome these challenges renders these investments an suitable candidate for the application of ROV.

Moreover, there are generally several interacting options embedded in an investment. The most common interaction happens when a subsequent option becomes available after the pre-requisite option is executed. In this case, the subsequent option provides additional future

[4]For projects with a very high or low NPV, ROV tends to be less useful because the decision is already clear from the standard cash flow analysis.

contingency that affects the investor's decisions. Examples of such options include system expansion, relocation, re-contracting and abandonment which often appear only after the option to invest has been executed. Properly incorporating these subsequent options into the valuation of the prerequisite option may lead to a different investment strategy, and therefore provide additional value to the investment. Nonetheless, there is currently limited literature that presents a valuation framework to explicitly consider the inter-dependency among the options available in a distribution network investment.

Against this background, this thesis tackles the above challenges in using ROV to assess the economic performance of a DER investment. As a result, the proposed ROV framework executes multiple interacting options to increase the investment value and mitigate the risk of financial losses in the presence of future uncertainties from electricity market.

Based on the ROV framework, this thesis develops an integrated financial assessment framework that is able to incorporate appropriate DER models for specific investment applications. By doing so, the integrated framework enables to capture uncertainties in:

- Distribution network including:
  - Operation of DER;
  - Sizing and location of DER;
  - Customer load behaviour; and
- Electricity market including:
  - Future cost of DER;
  - Varying electricity price.

Two models are used in this thesis to showcase the efficacy of the integrated ROV framework, including (i) the probabilistic impact assessment framework to value the investment in residential ESS[5]; and (ii) an AC optimal power flow model to value the investment in a grid-scale ESS.

Overall, the integrated ROV framework is able to: (i) include power flow simulations and thus the uncertainties from both the network and electricity market; (ii) efficiently incorporate DER scheduling optimisation including HEM based residential DER and AC OPF based grid-scale DER investments in the MC financial study underpinned by the ROV, (iii) identify and value the relations among the available interacting options, and make contingent decisions upon the

[5]This thesis assumes that DNSP is to support the residential ESS investments by subsidising a proportion of the investment cost.

realization of future uncertainty, and (iv) derive an optimal strategy to maximise the value of a DER investment for DNSP.

Finally, this thesis evaluates the policies and regulations from DNSP to manage distribution networks and prevent the detrimental impacts caused by the increasing DER penetration. In this thesis, the efficiency of rooftop PV investments under DNSP's restriction on investment capacity in certain network areas is examined. This restriction aims to prevent the hosting capacity from exceeding its network limit. Specifically, any additional PV installations in places where the network hosting capacity is already fully exploited will trigger some detrimental impacts on the network operation and/or other customers, including over-voltages, reverse power flows with congestion, and phase unbalance [9].

In this regard, a quantitative tool is developed to evaluate policies and regulations for improving network resource allocation and coordination for PV hosting capacity (and that of other DER). A game theoretic model is proposed to simulate the natural uncoordinated process where network customers independently invest in PV systems to maximise their investment payoff. The game follows the policy where if the network hosting capacity is exceeded in a local region, the investment in the surrounding neighbourhood will be prohibited to prevent any network issues from happening. To evaluate the efficiency of the investments under such policy, the natural uncoordinated investment process simulated using game theory is compared to an optimal PV sizing problem that optimises each customer's investment size to maximise the overall network profit; i.e. the sum of electricity bills saved by the network customers who have equipped a PV system.

In summary, the methods and tools developed in this thesis enable DNSP to:

- Assess the network technical benefits of DER using a probabilistic impact assessment framework;

- Design strategic plans to increase the value and mitigate downside risks of DER investments, considering uncertainties from both the distribution network and electricity market using a ROV framework; and

- Evaluate the policies and regulations by DNSP for improving network resource allocation and coordination for PV hosting capacity (and that of other DER) for increased DER penetration using a game theoretic model.

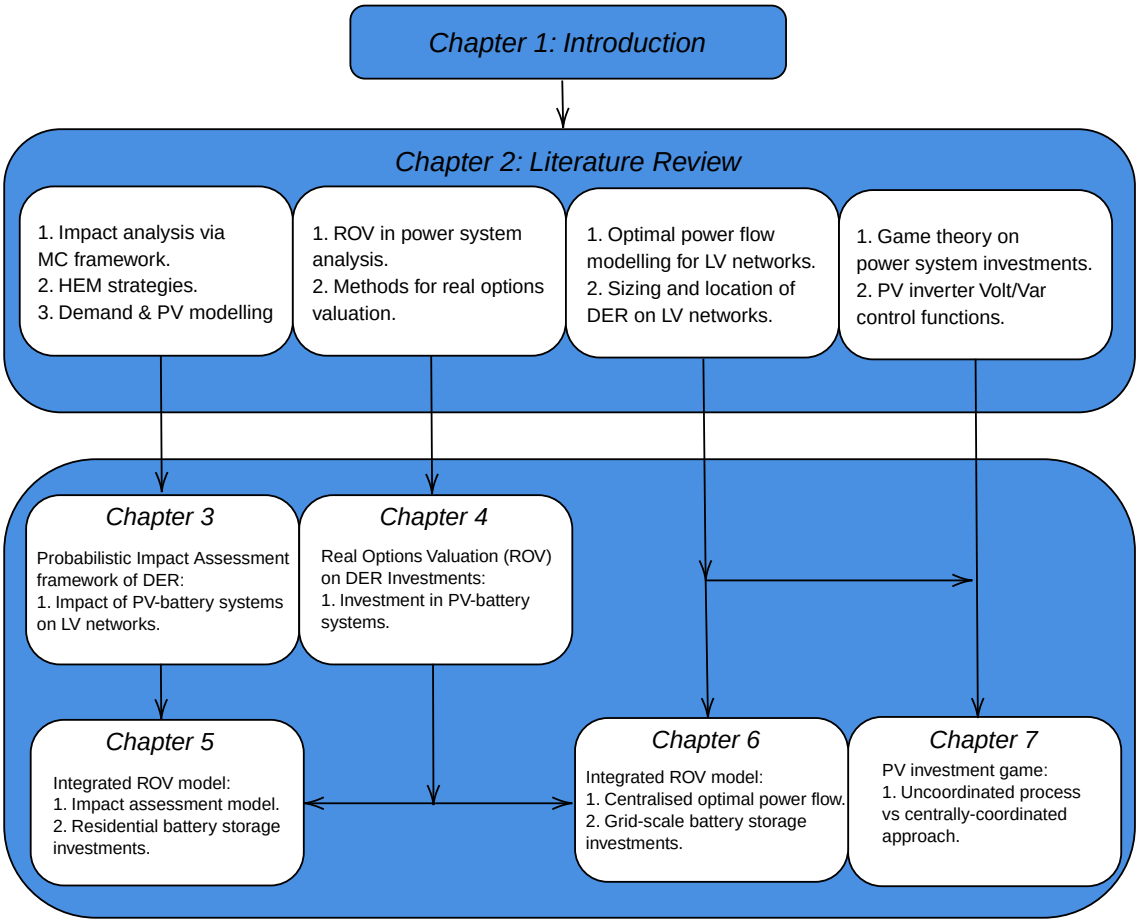

Figure 1.1: Overview of the structure and the connections between the chapters.

1.1 Thesis Structure

The thesis is structured as follows:

- Chapter 2 performs a detailed review on the existing literature related to the topics in this thesis.

- Chapter 3 proposes a novel probabilistic assessment framework to study the impact of DER on distribution networks. The probabilistic impact assessment model has a broad application appeal in the power system context; it can be used in applications that require optimisation for resource scheduling, such as probabilistic studies of the impact of DER scheduling on distribution networks, economic appraisal of DER investments in network

planning using real options analysis (Another key focus of this thesis), and probabilistic estimation of DER capacity available for power system frequency and voltage services.

- Chapter 4 develops a novel multi-stage ROV framework to (i) value multiple interacting real options embedded in future uncertainties; and (ii) determine the optimal strategy to flexibly execute these options to maximise the investment payoff. The case study used to demonstrate the efficacy of the framework is to strategically design an incentive scheme for DNSPs to support residential PV-battery investments for additional grid supply during peak demand periods.

- Chapters 5 and 6 integrate the ROV framework with two separate network models, subject to two different DER investments. The integrated framework enables DNSPs to capture both the network and electricity market uncertainties. Specifically, Chapter 5 incorporates the probabilistic impact assessment framework with ROV to value the options for DNSPs to incentivise residential ESS investments. In regards to large grid-scale DER, Chapter 6 proposes a AC OPF model to perform technical assessments on a grid-scale ESS investment by calculating the overall reduction on network loading. Then, the OPF model is integrated with the ROV framework to increase the value and reduce the downside risks of the investment.

- Chapter 7 proposes a game theoretic approach that simulates the natural uncoordinated process where customers independently invest in rooftop PV systems to maximise their own investment payoffs. Then, a centrally-coordinated approach is formulated to compute the optimal PV sizing for each customer to maximise the overall network profit. The results are compared to test the efficiency loss of residential PV investments in the recent PV inverter standards from AS4777. This framework is useful for DNSP to assess the impact of the policies and regulations for improving network resource allocation on DER investments.

1.2 Background

This section describes the background, motivation and contributions for each chapter of the thesis in detail. Fig. 1.1 overviews the links between the chapters in this thesis.

1.2.1 Probabilistic Impact Assessment Framework

The first technical contribution in this thesis, incorporated in Chapter 3, is on the 'Probabilistic impact assessment of DER on distribution networks'. The efficacy of the framework has been demonstrated using rooftop PV-battery systems. The work presented in this section of the Introduction has also been detailed in the following publication:

---

[9] **Yiju Ma**, Donald Azuatalam, Thomas Power, Archie C. Chapman and Gregor Verbič, A Novel Probabilistic Framework to Study the Impact of Photovoltaic-battery Systems on Low-Voltage Distribution Networks, *Applied Energy* Issue 254, Number 113669, 2019.

Background and Motivation

In the recent decade, it has been widely conjectured that battery ESS will largely mitigate the problems of excessive PV generation [13]. However, ESS and other flexible resources[6] pose a challenge in power system planning and operation. This is because in the future a large proportion of ESS will be equipped by optimisation-based HEM to better facilitate energy use within each household, and solving the scheduling optimisation is time-consuming. To capture the impact of DER on distribution networks under varying system conditions, it is required to solve the HEM optimisation problem for a large group of customers. This is computationally prohibitive because the optimisation problems are sufficiently hard, due in part to a decision horizon of one day or more being required. Thus, including flexible resources in the existing MC approaches, commonly used in probabilistic power flow system analysis, becomes infeasible.

Very little work has been done so far to address the issue of how to include optimization in MC simulation. A possible solution is to reformulate the problem, for example by using a two-point estimate method as in [16], but this requires some strong assumptions, such as modeling random variables by well-behaved probability distributions. Using such assumptions to properly capture the stochastic behavior of residential users with PV-battery systems is overly simplistic; in fact, it requires the use of more sophisticated modelling techniques, such as Bayesian nonparametric models.

Furthermore, no existing research has investigated the extent to which hybrid PV-battery systems, equipped by optimisation-based HEM, can benefit distribution networks with high PV penetration, due to the infeasibility of the resulting MC simulation, as discussed above.

[6] In this context, flexible resources refer to any resource that provides flexibility in electricity demand and production. Examples include ESS (electric vehicles) that can charge with excess PV generation and discharge for peak demand support and loads that use thermal inertial to maintain the temperature in an acceptable range.

Because grid integration of large populations of behind-the-meter distributed energy resources has become a hot topic in Australia [17], methods and tools to study the impact of PV-battery systems on low-voltage (LV) distribution networks are desperately needed.

Contributions

Within this background, this thesis fills this important knowledge gap by proposing a novel probabilistic framework that overcomes the shortcoming of existing MC power flow studies, which fail to explicitly include battery scheduling optimization due to its excessive computational burden. Thus, for the first time, this work provides a MC framework that explicitly includes the DER scheduling used to manage customers' behind-the-meter energy use. In addition, the proposed framework provides a principled statistical way that allows MC power flow analysis to be conducted with exiguous smart meter data. Smart-meter roll-out is ongoing, but there are still many jurisdictions where coverage is still patchy, e.g. NSW in Australia [18]. Thus, it examines the conjecture that using existing strategies to schedule batteries, include HEM under *time-of-use* tariffs or *self-consumption maximization*, can serendipitously reduce the technical problems caused by excessive PV generation. Specifically:

- I use a Markov chain approach to synthesize large numbers of statistically similar, but independent demand and PV profiles using smart meter data;
- I incorporate ESS scheduling optimization within the MC analysis by training a policy function approximation (PFA) using an artificial neural network (ANN) to estimate the near-optimal ESS schedules for a large pool of customers, which reduces the computational time required to solve the HEM problem by more than 95%;
- I complete a comprehensive PV hosting capacity assessment using a probabilistic time-series power flow analysis for several real-world representative LV feeders to show that uncoordinated ESS scheduling has a limited beneficial impact on the reduction in over-voltages, transformer loading and phase balancing in LV networks; this disproves the conjecture that ESS will serendipitously mitigate the technical problems induced by PV generation.

By overcoming the existing gaps, the proposed framework provides a tool-chain for technically and financially evaluating future DER deployment and investment, as demonstrated in a rooftop PV hosting capacity assessment. Moreover, this framework can be used to develop other

types of future network assessments and investigations, including real options valuation (ROV) of staged DER deployment and probabilistic DER power system service capacity estimation.

1.2.2 Real Options Valuation

The second technical contribution in this thesis is on the 'Development of a novel multi-stage ROV framework to assess the DER investments'. The proposed ROV framework can be used to perform strategic valuation of efficient and well-timed network investments. The framework is described and shown effective using three different case studies in Chapters 4 to 6, respectively. The background and motivation for each of these case studies are described in this section.

Multi-Stage ROV in Residential PV-Battery Investments

The work described in Chapter 4 and has been published by the following journal:

---

[19] **Yiju Ma**, Kevin Swandi, Archie C. Chapman and Gregor Verbič, Multi-Stage Compound Real Options Valuation in Residential PV-Battery Investment, *Energy* Issue 191, Number 116537, 2019.

Background and Motivation

Peak demand is the time when consumer demand for electricity is at its highest. In distribution systems, the installed power transfer capacity must be greater than the expected annual peak demand. However, in reality, it has become common for forecast electricity demand to exceed the distribution network's supply capacity in the near future, as peak demand continues to increase [20].

Network augmentations including upgrading transformers and conductors are an expensive solution, and therefore DNSPs sometimes also consider non-network solutions including investing in local generation sources. Examples include a new diesel generator that injects power into the substation for peak demand support and residential PV-battery systems.

Investing in a new diesel generator at the substation is an uncommon approach, but it makes sense for very 'peaky' peaks, i.e. seasonal/weather-driven, characterized by high peak-to-average load profiles. However, this is an expensive method considering that the diesel costs are uncertain due to the relatively high capital cost and price uncertainty of liquid fuels.

Alternatively, residential PV-battery systems can be effective at providing peak demand support and reducing the risk of supply falling short of demand. Although the technology is currently expensive to implement, the continuous cost reduction has made it increasingly

attractive for reducing conventional generation [21], and thus providing opportunities to replace the costly diesel generator investment, as well as to defer expensive network augmentations [8, 22].

However, the valuation methods used by DNSPs for assessing the non-network solutions require investors to commit to deterministic decisions made at present, which often undervalue the investment. In response to this, this thesis proposes a ROV framework that captures the option values generated by making contingent decisions under uncertainties.

In Chapter 4, the use of the proposed ROV framework is demonstrated by capturing the option values created by investing in PV-battery systems to replace the need for a new diesel generator. The diesel generator investment is considered because (i) it is also a method for providing peak demand support; (ii) the investment cost can be used as monetary savings as it is being replaced, which reduces the overall investment cost for PV-battery systems and makes the deferral option valuable for the analysis of ROV.

Contributions

The proposed ROV framework needs to overcome two main challenges that have not been addressed in the existing literature. Specifically, ROV is often not particularly useful in distribution network investments because the NPV of these investments is generally negative and not close to zero; i.e. for projects with very high or low NPV, ROV tends to be less useful because the decision is already clear from the standard cash flow analysis. The main contributions from this chapter are therefore summarised as follows:

- The economic benefits of the PV-battery investment are calculated as the cost saving from replacing the expensive diesel generation investment to enable the application of ROV;
- ROV is used to determine the optimal investment plan that subjects to multiple interacting options available in the application of PV-battery system investment; and
- By combining the investments in diesel generator and PV-battery systems, the uncertainties involved in both investments are integrated within one valuation process to provide a greater investment value.

Given that ROV is a well-known concept. The main contributions of the chapter therefore are within the investment application (rooftop PV-battery systems). First, using ROV to value the investments in PV-battery systems and diesel generation individually and compare the results for the optimal investment decisions is not applicable in the first place, because the cash flows

for both investments are negative and not close to zero. In this case, since PV-battery investment replaces the conventional diesel generator investment, the cost of latter is therefore used as monetary savings to increase the cash flows of the PV-battery investment to a level where ROV can be enabled.

Therefore, the framework not only enables the use of ROV to determine the optimal investment strategy, but also integrates the uncertainties from two investments within one valuation process to provide greater opportunity values. In addition, with the benefits given by considering the multiple interacting options, the results suggest to delay the PV-battery investment to a later year instead of abandoning it or investing in diesel generator immediately.

1.2.3 Integrated ROV Framework considering Network Constraints

Building on from ROV framework developed in Chapter 4, Chapters 5 and 6 propose a novel ROV framework that integrates network constraints for valuing DER investments. By doing so, the framework is able to include the network uncertainties, including (i) operation of DER; (ii) sizing and location of DER; and (iii) customer load behaviour, on top of the uncertainties in electricity market including (i) the future cost of DER; and (ii) varying electricity price. The additional uncertainties added in from explicitly modelling the network can bring great option values to the DER investments.

The use of the integrated ROV framework is demonstrated using two case studies including (i) investigating whether equipping ESS to existing PV systems can be used to delay network augmentation for the purpose to increase network capacity in Chapter 5; and (ii) studying the investment in grid-scale battery storage for deferring the costly network augmentation in Chapter 6. These case studies are designed for networks where PV penetration has reached a level that issues including over-voltage and network overloading have risen.

In addition, specific to each case study, different models are integrated in the ROV framework. Chapter 5, the operation of residential ESS is modelled using the network impact assessment framework described in Chapter 3. On the other hand, in Chapter 6 an AC optimal power flow (OPF) model is used to calculate the operational profiles for the grid-scale ESS. The background and contribution of these case studies are detailed in this section.

Integration of network Impact Assessment Framework

The following paper has been incorporated in this subsection and in Chapter 5:

[23] **Yiju Ma**, Archie C. Chapman and Gregor Verbič, Strategic Valuation of Compound Options for the Investment in Residential Battery Systems, *submitted to IEEE Transactions on Power systems*, 2020.

Rooftop PV generation is predicted to continue to increase worldwide in the near future. In order to accommodate this growth, expensive and time-consuming network augmentation is required in places, especially in Australia, where excessive PV generation has caused voltage and loading excursions on distribution level [5]. Small-scale ESS installed in conjunction with PV systems have been proposed to defer network augmentation as they can mitigate the network issues to some extent [13]. However, the NPV of ESS deployment is often negative due to its high cost, which renders them infeasible as an immediate investment. However, predictions by Australian Energy Market Operator see the technology cost decreasing by more than 30% in the next decade. Considering these predictions together with the cost savings from implementing network augmentation makes it a rational conjecture that the investment[7] will become economically viable in the near future [12]. Given this context, strategically carrying out investments in residential ESS may delay or even avoid the expensive network augmentation.

However, determining efficient and well-timed investments in residential ESS using MC based financial assessment such as ROV poses significant challenges, because of the need to capture increasing network uncertainties in the associated investments in both ESS and network augmentation. This is aggravated by the fact that ESS operational profiles are determined by time-consuming optimisation, assuming that a large proportion of the ESS installations will be equipped by optimisation-based HEM in the near future. Solving the HEM optimisation for thousands of MC runs is therefore computationally impractical. Within this context, no literature has evaluated the investment in residential ESS deployment which involves designing and solving a distribution planning problem in coordination with the MC analysis underpinned by ROV.

Contributions

In response to the technical challenges, Chapter 5 proposes an integrated ROV framework based on the network impact assessment framework that incorporates ESS scheduling optimisation problem within a MC study to capture network uncertainties. By doing so, the framework enables DNSPs to overcome the above challenges and thoroughly evaluate the investment to subsidise

[7] In Australia and some other jurisdictions, asset ring-fencing regulations mean that these ESS must be owned by network customers. However, to promote the use of this technology, DNSP must provide incentives to cover a large proportion of ESS procurement and installation cost.

residential ESS installations. Therefore, the main contributions of this work are highlighted as follows:

- A novel integrated ROV framework is formulated which combines a forward looking MC model to incorporate stochastic power flow simulation presented in Chapter 3, and a recursive backward induction model over all MC paths to value compound options;
- Using the PFA approach proposed in Chapter 3 to reduce computation time by more than 95%; and
- The interactions among options, if systematically examined in an uncertain setting, are demonstrated to provide benefits beyond valuing the options independently.

Integration of AC Optimal Power Flow Model

The following publications have been incorporated in this subsection and in Chapter 6:

---

1. [24] **Yiju Ma**, Mohammad Seydali Seyf Abad, Donald Azuatalam, Gregor Verbič, Archie Chapman, Impacts of Community and Distributed Energy Storage Systems on Unbalanced Low Voltage Networks, *Australiasian Universities Power Engineering Conference (AUPEC)*, Melbourne, 2017.
2. [25] **Yiju Ma**, Gregor Verbič and Archie C. Chapman, Estimating the Option Value of Grid-Scale Battery Systems to Distribution Network Service Providers, *PowerTech*, Milan, 2019.
3. [26] **Yiju Ma**, Gregor Verbič and Archie C. Chapman, Optimal Investment Strategy in Grid-Scale Energy Storage Systems, *Asia-Pacific Solar Research Conference*, 2018.

Grid-scale ESS can be an appealing technology to DNSPs due to several reasons. First, they can better utilize intermittent renewable generation, reduce peak loading and remove line congestion. Second, they provide enhancement to grid flexibility and ensure a higher security of energy supply during undesired weather conditions [27]. Third, they can mitigate over voltages by absorbing excessive renewable generation in LV networks, and release the stored energy whenever it is needed [28]. In addition, the main advantage of a grid-scale ESS over residential ESS is that it is simpler to optimally schedule the ESS to maximise the above benefits.

Taking into account these benefits, the value of ESS has risen significantly, especially in Australia, where PV penetration is significantly higher than the rest of the world [29]. However, there is still considerable debate as to whether a community ESS (CESS) or distribution ESS (DESS) is more valuable to our networks, and currently few studies have compared their benefits and drawbacks. Further, there are still open questions regarding the values that a grid-scale ESS

can bring to DNSPs and distribution networks [30], consdering increasing uncertainties in ESS prices, the fluctuations of power demands, and the intermittency of DER.

Contributions

Chapter 6 integrates an AC OPF model within the ROV framework to solve above problems. First, an AC OPF model is developed to study the impacts of different sizing and configuration of grid-scale ESS in power losses, the hosting capacity and network unbalance in LV networks. Then, the benefit from reducing network loading is calculated and included within ROV to help DNSPs make contingent decisions and determine an optimal investment plan to carry out the ESS investment.

1.2.4 PV Investment Game

The final section of this thesis simulates the natural uncoordinated process in residential DER investments carried out by network customers via game theory, and compare the results to a centrally-coordinated approach. This framework can be used to evaluate the policies and regulations designed for improving network resource allocation and coordination for PV hosting capacity (and that of other DER). Rooftop PV investment was employed as a case study to demonstrate the efficacy of the framework. The work presented in this section has been detailed in Chapter 7 and the following publication:

---

[31] **Yiju Ma**, Daniel Gebbran, Archie C. Chapman and Gregor Verbič, A Photovoltaic System Investment Game for Assessing Network Hosting Capacity Allocation, *in the Eleventh ACM International Conference on Future Energy Systems* (*e'Energy*), June 2020, pp. 1-9

Background and Motivation

The rapid rise of PV installations in distribution networks means that they are likely to exceed the network's *hosting capacity*[8]. Any additional PV installations in places where the network

[8] In our study, the hosting capacity is defined as the total amount of PV installed capacity that can be connected to the grid while keeping the voltage profile within 0.94pu and 1.1pu for 95% of the time within a week according to AS 61000 [32].

hosting capacity is already fully exploited will trigger some detrimental impacts on the network operation and/or other customers, including over-voltages, reverse power flows with congestion, and phase unbalance [9].

For this reason, DNSP have begun to place restrictions on installations of residential PV systems. Specifically, if a local network has large systems that have fully used, or possibly exceeded, the available hosting capacity, any additional installations in the same part of the network may be prohibited or limited to a small size. This is clearly unfair for those who are willing to install PV systems, but have not yet done so.

Another approach used by DNSP is demonstrated in the evolution of PV inverter connection codes, which in Australia now contain a requirement for inverters to contribute to network voltage management by either curtailing their active power output, or by absorbing reactive power, at higher voltages. Example specifications of these inverter functions can be found in recent standards in AS4777 [33]. In this regard, as more PV is installed nearby, existing PV investment may become inefficient as it is curtailed more often.

Given that renewable power generation is a key way to transform of our future power grid, it is useful to understand how such policies and regulations, and the information on hosting capacity and investment value available to customers, contribute to the economic value of renewable installations. To this end, the model and methods developed in this work allow DNSP to explore the inefficiencies that arise when customers are permitted to decide their investment size under a natural uncoordinated process.

Contributions

Specifically, I first propose a novel game-theoretic model that simulates the natural uncoordinated process of customers that independently invest to maximise their own welfare under limited network hosting capacity. The Nash equilibrium of this game is used as a prediction of the pattern of PV investment. To compute the Nash equilibrium, an adaptive learning process is employed, which converges in *concave games*, even if a player initially knows nothing about the game they are playing and cannot observe the actions of other players. Later, the model shows that the annual benefits for different sized investments are concave (making the game concave), and therefore the convergence is possible in this game, as demonstrated in Section 7.4.

However, investments under this natural uncoordinated process can be inefficient since each customer independently maximises their own payoff. For example, it is possible that one customer, by increasing its PV capacity, limits the capacity or curtails the output of others to the point where more is imported from the grid overall. This leads to a reduced investment payoff.

To determine this inefficiency, the socially-optimal solution is computed by solving a centrally-coordinated approach, which is formulated as an optimal power flow study that includes the Volt/Var control (VVC) function and active power curtailment (APC) function in each PV inverter to regulate voltage. This solution provides the optimal investment size for each customer so that the sum of all customers' annual investment payoffs is maximised. Recent standards in AS4777 has provided several modes of operation, which require explicit models to reflect their proper functioning [33]. The inverter reactive power output depends on VVC curve and the voltage measured at the connection point. The VVC function has a direct impact on the voltages of the system and therefore, needs to be explicitly modelled within the OPF study. On top of this, APC is used to curtail all PV systems by the same amount until all over-voltages are completely eliminated, so this function should be applied after VVC. Most existing literature either has considered the VVC function as a decentralised approach [34, 35], or do not explicitly model the the VVC curve when working with a centralised OPF [36–38].

To this end, this work extends the model from [36] by including the VVC and APC functions within a centralised OPF with an objective to maximise each customer's investment payoff. To the best of our knowledge, this is the first time that the natural uncoordinated process that customers undertake to invest in PV systems is modelled using game theory. Our work shows that this uncoordinated process, which happens in real world, leads to significant inefficiencies in investment compared to a centrally-coordinated approach. Thus, this model provides a quantitative tool for evaluating policies and regulations for improving coordination and allocation of PV hosting capacity (and that of other DER investments) between customers on LV feeders.

Chapter 2

Literature Review

This chapter presents a detailed literature review relevant to the topics covered in this thesis along the following related headings:

- Probabilistic impact analysis of PV and energy storage systems on distribution networks (Section 2.1):
  - Residential PV-battery impact analysis;
  - Monte Carlo Approaches;
  - Home energy management with PV-battery systems;
  - Residential solar and demand modelling;
- Real options valuation in power system analysis (Section 2.2):
  - Methods for real options valuation;
  - Integrated financial modelling for distributed energy resources investments in low-voltage networks;
  - Integration of probabilistic impact assessment framework;
  - Integration of AC optimal power flow model;
- PV investment game (Section 2.3):
  - Game theoretic analysis in distribution network investments;
  - Modelling of PV inverter Volt/Var Control Function.

2.1 Probabilistic Impact Analysis of PV and Energy Storage Systems on Distribution Networks

This section reviews the existing literature on methods and tools involved in assessing the impact of behind-the-meter (BTM) distributed energy resources (DER) on low-voltage (LV) distribution networks.

2.1.1 Residential PV-battery Impact Analysis

Existing literature has mainly focused on (i) single grid-scale energy storage systems (ESS) or a small number of distributed ESS; and (ii) heuristic methods such as self-consumption maximization to schedule the ESS. These works have shown that ESS can effectively mitigate technical problems including over-voltages, thermal over-loading and phase unbalance on LV networks. In the near future, a large proportion of the ESS installations is expected to be equipped by HEM to optimally facilitate energy use within each household to save electricity bills. However, it is still a conjecture that residential ESS, equipped by optimisation-based HEM, can largely mitigate the technical problems of excessive PV generation.

For example, the study in [39] proposed a heuristic strategy to schedule a grid-scale ESS to achieve several desired purposes including peak shaving, valley filling and load balancing. The authors in [40] combined genetic algorithm with linear programming to determine the optimal number, placement, sizing and scheduling of the ESS that removes all network voltage problems and prevents reverse power flows. The study in [41] proposed a probabilistic network reinforcement approach using ESS and the reactive power capability from PV inverters to achieve effective voltage control. The study in [42] assesses the limitations in residential ESS in distribution networks, the battery ESS are controlled under self-consumption maximization. This study finds that residential storage is limited in the ability to mitigate voltage and thermal issues. The study in [43] investigates the network impacts of residential ESS controlled by a decentralised approach. The proposed control strategy overcomes the main limitation that ESS does not generally fully discharge overnight which reduces the ability to store surplus PV generation the following day by adapting the charging power proportionally to the PV generation. The authors demonstrated that the proposed control method can be as effective as an ideal optimisation-based approach, and the method is able to manage all technical issues without significantly affecting customers.

Looking deeper, the study in [44] designed a centralised coordination controller for distributed ESS and on-load tap changer transformers to solve over-voltage problems. Similarly, the authors

in [45] presented a two-stage centralised control scheme for distributed ESS to reduce voltage violations and thermal over-loading. These studies showed that ESS under proper coordinated control can solve the problems caused by excessive PV generation.

The above literature review shows that none of these studies evaluates to what extent that uncoordinated residential ESS, equipped by optimisation-based HEM, can benefit the network, given that self-owned ESS installations have been rapidly increasing on distribution level.

2.1.2 Monte Carlo Approaches

Monte Carlo (MC) analysis has been employed in many studies to capture uncertainties in the location and size of DER when assessing their impacts on voltage profiles and peak loading in LV networks. In particular, the study in [46] applied a probabilistic approach to evaluate the impacts of distributed generation with different penetration levels on voltage profiles. The authors in [47] proposed a probabilistic methodology based on MC analysis to investigate the impact of electric heat pumps on LV networks, with a focus on voltage and thermal limits. A similar approach was used in [48] to probabilistically allocate PV, combined heat and power systems, electric heat pumps and electric vehicles (EVs), to investigate the prevalence of voltage problems on LV feeders with different penetration levels of these *low carbon technologies*. The authors in [49] studied the impact of PV generation and electric heat pumps on LV networks using MC analysis that captures uncertainties in building characteristics (geometry and insulation quality), feeder size, cable type and heat pump and PV penetration levels. In addition, the study in [50] proposed a probabilistic approach using MC analysis to investigate the maximum PV penetration level that can be tolerated by an LV network without voltage problems. Furthermore, they assume that schedules of flexible devices are independent of PV generation, which might not be true in practice. Charging of EVs, for example, should preferably coincide with co-located PV generation to minimise grid in-feed. Additionally, flexible technologies with thermal inertia can serve as ”solar sponges” to maximise self-consumption [51].

However, none of these studies includes ESS scheduling, as solving the HEM problem inside MC simulations is impractical due to the excessive computational burden. In fact, very little work in the existing literature has provided a approach that is computationally feasible to include optimisation, commonly needed in the modelling of DER, in MC analysis. Given that grid integration of large populations of DER has become a hot topic in countries such as Australia [17], methods and tools to study the impact of DER on LV networks are desperately needed.

2.1.3 Home Energy Management with PV-Battery Systems

The fast deployment of DER in the residential sector has provided the network customers more control over their electricity usage. It is expected that DER in the future will be equipped and managed by a home energy management (HEM) system that uses optimisation to schedule DER to minimise energy cost. In this regard, this section reviews the existing literature on how the HEM system minimises this cost by facilitating PV-battery systems.

Specifically, ESS scheduling refers to the charging and discharging profile, i.e. the ”behavior” of the ESS. This scheduling problem is typically formulated as an optimisation problem and solved using a HEM system. The objective can vary, but it is usually to minimise energy expenditure for the user [52]. In jurisdictions where the PV feed-in (or buyback) tariff is less than the electricity tariff (e.g. in Australia), energy expenditure minimization coincides with self-consumption maximization (SCM).

In fact, SCM (and many other similar heuristic methods) has been frequently used by the existing literature because it is simple to implement yet quite effective at saving electricity cost [53–57]. In particular, this scheduling approach can help saving up to 30% of the electricity bill per day in summer, when PV generation is usually higher [54]. Moreover, the study in [56] shows that matching the size of the ESS with customer's daily energy consumption helps the ESS perform best under SCM. In addition, a 13-24% increase in the ratio between the consumed energy and PV generation is observed when the size of the ESS is 0.5-1kWh per kW PV installed [56], while installations with a large or smaller size would cause the benefits to become marginal [58]. Heuristic methods such as SCM offers advantages in computational speed and simplicity, but they are only able to achieve sub-optimal solutions as compared to principled optimisation methods.

Principled optimisation approaches that have been employed in the existing literature include mixed integer linear programming [59–63], mixed integer quadratic programming [64], dynamic programming (DP) [65, 66] and approximate dynamic programming [65, 66]. A common feature of these methods is their relatively high computational burden, which hinders a direct implementation in MC studies. This high computational burden is usually led by the consideration of the non-linear operating characteristics of the device [67].

Examples can be found in dynamic programming (DP), where the solutions have high-quality as the non-linear operating characteristics of the ESS are captured in the formulation. Mixed integer linear programming (MILP) addresses the computational challenge by linearising the ESS operating characteristics, but the trade-off is the reduction in the solution quality. In additional, the study in [66] shows that approximating the uncertainties in demand and PV can significantly

reduce the computational burden. On the other hand, the study in [68] uses temporal difference learning to approximate DP (ADP), which leads to a high computational speed with very little reduction in quality. Moreover, policy function approximation (PFA) is shown effective at obtaining close-to-optimal solutions [69]. This approach uses machine learning techniques to train neural networks on the training data computed using high-quality solution approach, such as DP. Then, the neural networks can be used to generate close-to-optimal ESS operational decision given a series of inputs including demand, PV generation, tariffs and etc. This approach reduces the computational burden by reducing the total number of times needed for solving the ESS scheduling optimisation problem, since only a small pool of training data is required to train the neural networks.

In our thesis, the choice of the HEM optimisation formulation is arbitrary; none of the existing solution techniques is computationally efficient enough to be directly used in MC analysis, as reviewed above. Thus, DP[1] is used in conjunction with PFA [69] to emulate DER scheduling policies for the large pool of customers, allowing the HEM operational decisions to be feasibly included within the MC power flow analysis within the probabilistic impact assessment framework.

2.1.4 Residential Solar and Demand Modeling

For synthesizing stochastic demand and PV profiles, Markov chains using a bottom-up approach starting at the appliance level are typically used. Examples include the simulation of building occupancy profiles for the purposes of generating lighting demand [70] and residential energy demand profiles [71–73]. However, such bottom-up approaches that start from the smallest possible units of a system and aggregate these units to reach higher system levels, are computationally expensive, especially with high time resolution and high spatial resolution that involve large amount of data. Therefore, it is difficult to model energy usage at the appliance level in a way that represents the diversity of customer behavior.

Given these shortcomings, the study in [74] proposed a methodology for generating residential demand and solar profiles using a Markov process specific to the features of the existing *smart meter* data. Instead of working up from the appliance level, the method generates the synthetic profiles by clustering a set of observed profiles using a Dirichlet process, and then generating transition matrices used in the Markov process from these clusters.

[1]DP is notorious for the curse of dimensionality, but in this study deterministic DP is considered with only one schedulable device, so the computational performance is comparable to mixed-integer linear programming.

This thesis extends the work from [74] on synthesis of demand and solar PV generation within the probabilistic impact assessment framework that requires a large pool of synthetic demand and PV traces to sample from. In many jurisdictions smart metering data are scarce, so we need to be able to generate statistically representative samples when only a limited number of demand and PV traces is available [18].

2.1.5 Summary

Against the above literature review, Chapter 3 proposes novel probabilistic impact assessment framework that embeds the ESS scheduling optimisation problem in the MC analysis to assess the effects of ESS scheduling on LV networks. First, using available smart meter data, a Bayesian nonparametric model is used to generate statistically-representative synthetic demand and PV traces. Second, a policy function approximation that emulates ESS scheduling decisions is used to make the simulation of optimisation-based HEM feasible for the large pool of demand and PV traces within a MC framework. Finally, the results from the PFA are included within a probabilistic MC power flow analysis to form a toolchain to determine the impact of PV-battery systems on distribution networks. More technical details are described in Chapter 3.

2.2 Real Options Valuation in Power System Analysis

Traditional discounted cash flow (DCF) is known to be a useful and practical model for calculating the value of an investment. It generates reasonable investment estimations in the form of net present value (NPV) [14]. Usually, a positive NPV indicates that an investment should be undertaken immediately, whereas a negative NPV means otherwise. Specifically, DNSP are often exposed to increasing uncertainties in (i) electricity market such as power demand and electricity price; and (ii) distribution networks including load behaviour, sizing and location of DER. The existing methods for modelling uncertainties are described in [75] and [76] which employ a probabilistic framework and a possibilistic framework, respectively. These methods calculate NPV under various scenarios, and they help investors make decisions at the present time in response to future uncertainty. After the project life cycle begins, the investors will not be able to adjust the decisions regardless how future uncertainty unfolds.

In this regard, DCF often underestimates the managerial flexibility of a project, and fails to capture uncertainty due to the lack of future information. In more detail, the DCF analysis requires investors to make all decisions at the beginning of a project, and after this, it implicitly assumes a passive role of the management. The future decisions are made based on a set

of deterministic input values without allowing any decisions to be made in response to any contingent events [14].

However, managerial flexibility generally exists in a project, which allows the investor to make contingent decisions based on the realisation of future uncertainty. These decisions are interpreted as the real options in the concept of real options valuation (ROV) [77]. Specifically, ROV uses the NPV as its building block and allows the integration of decision tree to provide more meaningful analyses [14]. It was firstly introduced by Stewart C. Myers in 1977 [78]. The concept of real options emphasises the importance of time waiting, making a recommendation regarding whether to invest in the project at each time step throughout the entire project life cycle. During the waiting stage, the investor can gather more information regarding the expected investment value in the future. More specifically, if sufficient evidence suggest that the investment value is to become worse than expected, the investor has the option not to proceed or abandon the investment activity at this point of time [79].

In more detail, the concept of ROV is to value the flexibility from management, given that the investors have the right, but not the obligation to undertake an investment decision. In this way, it changes the focus from ”whether to invest or not”, to ”when to invest to maximise the profit”. Usually, investments involve many contingent decisions which are usually continuously revised following the changes in the market. For example, an investment can be deferred (option to defer) and expanded (option to expand) in a later date if the market environment turns favourable. With the flexibility to deal with these options, the investors can increase the investment value significantly. In more detail, ROV evaluates contingent decisions based on realizations of future uncertainties, thereby taking strategic decisions in order to increase the investment value. The options have the potential to be more valuable when high uncertainty presents. Thus, ROV is used to simulate the flexible decision-making process, with the aim of mitigating downside risks, or exploiting upside potential under the realization of uncertainty. The most common real options include:

- Option to invest in certain assets;
- Option to defer an investment until market environment turns favourable;
- Option to abandon an investment permanently if market conditions turn unfavourable; and
- Option to expand or extend the life cycle of an investment.

ROV introduces a new insight regarding the effects of uncertainties, which contradicts the conventional method. Surprisingly, it turns out that in the ROV, the higher the risk of an

investment, the larger the chance for higher profits. High volatility market increases the profit potential, and limits the downside losses due to the flexibility in management which can decide an option to exercise [79]. Real options offers numerous options in addition to the option to defer, embedded behind every investment, including the option to expand, the option to abandon and compound option [14], [79]. The presence of any of these options may exceptionally increase the economic value of an investment.

Nonetheless, there are generally multiple interacting options in the investment in power systems, and models for effective valuation of compound options within an ESS investment have not appeared in the existing literature, because the NPV is usually negative and not close to zero, which renders the investment a suitable candidate for the application in ROV. Below is a review on a list of works that have used ROV to study the investment in transmission and distribution networks.

In recent years, ROV has been widely accepted by academics as a tool for capital budgeting and investment appraisal, and frequently applied for valuation of distribution and transmission network investments, including transmission network expansion [80–82], thermal power plants [83, 84], distributed generation [85], and renewable generation including hydro-power [86], wind generation [87–91], solar generation [92–96] and large scale ESS [25]. A common feature of these studies is that they determine the value to execute one or several *independent* options embedded in a network investment in the presence of uncertain electricity market conditions or regulatory policies, and hence the optimal investment timing. However, in practice, a distribution network investment often involves multiple *interacting* (i.e. not independent) options which actively engage with each other to produce a greater investment value. For this setting, the authors in [97] determine the value of multiple options, including the option to invest, followed by the subsequent options (expand, re-power, contract and abandon), in a wind farm investment. However, the investment timing for the subsequent options are fixed (i.e. a European call option) to reduce the size of the problem. Currently, the method to properly value American compound options, with flexible execution timing, has not been presented in the existing literature. More importantly, it is found that the topic of addressing investment in hybrid renewable generation systems, such as PV-battery, using ROV has not been presented, which drives our research direction.

In the context of residential DER investments in distribution networks, DNSPs often provide subsidy to cover part of the investment cost of each system, and that customers own and contribute the balance of the cost, for two reasons. First, customers are willing to cover part of the investment cost because that reduces their electricity bills. Second, in fully-deregulated

power systems like Australia, residential DER need to be owned by customers (or a third-party) because of regulations that prohibit monopoly networks owning and operating assets that straddle the regulated and contestable parts of the system. Specifically, in Australia, DNSPs are permitted to subsidise customer-owned equipment if they are also used for supplying energy and services to contestable markets to provide network support services. Given this, to promote the use of this technology, DNSPs may provide incentives to cover a large proportion of PV-battery procurement and installation cost, and in this way, they can effectively invest in these assets. In general, the size of the subsidy is a free variable in this type of investment decision, which means DNSPs are free to decide these figures as they feel appropriate in practice and context.

2.2.1 Methods for Real Options Valuation

This subsection reviews a list of approaches that can be used to address the problems above. These approaches can be divided into two categories: (i) analytical solutions such as *partial differential equations* that are based on exact equations; and (ii) numerical solutions such as *binomial trees*, *binomial lattice* and *MC simulations* that are based on approximation provided by simulations [6]. Specifically, numerical methods approximate stochastic processes within discrete time intervals.

Partial Differential Equations

The *partial differential equations* (PDE) approach is based on the research of Black, Scholes and Merton, and it is an analytical method [98–103]. It is the best approach when applicable, because it is extremely fast to compute and generate exact solutions. In the application in power system analysis, such approach was first applied to the produce financial assessments for large-scale energy projects [104], followed by the valuation of the investments in petroleum development [105] and natural resource planning [106]. More recently, PDE has been used to value the real options in renewable investments, including the value to delay the investment in renewable power plants [107] and demand response projects [108].

However, this solution approach for ROV is not recommended for investments in power systems due to three reasons. First, the PDE approach can be used to incorporate only one uncertainty, or at most two correlated ones. This is not the case in the electricity market where multiple uncertainties exist. Meanwhile, the uncertainty needs to be modelled using geometric Brownian motion, which follows a lognormal distribution. However, many uncertainties, such as commodity price, follow a mean-reversion process, with spikes due to unforeseen events such as a drone attack [109]. This has a significant impact on the valuation results because the

investment span usually can go for years or even decades. Second, the simulation of uncertainty follows constant mean and volatility. This is a strong assumption when the investment period is long. Third, PDE is best suited for valuing the decisions on a specific time, i.e. European-type of option analysis in which the option is either at the start or the expiry date of the option's life. However, options (American options) can often be executed at any time during the investment period, which provides a greater value of flexibility [110].

Binomial Lattice

When there is no analytical solution, numerical approaches must be applied. In this regard, *binomial lattice* can make a good replacement for finding the optimal time for executing an American option. This model was developed in [111]. During each discrete investment time-interval, the value of executing the option immediately is compared with the value to defer, to make the investment decision. Examples of application of the lattice model include the valuation of the investment in wind power projects [112].

The lattice model is based on the assumption that the state variables have only a finite number of values. The binomial tree model uses a probabilistic framework and a decision tree model to decide whether to take an action or wait for more information to unfold. For instance, the value of a state variable can either move up or down based on a certain probability. Thus, including more sources of uncertainty will make the model increasingly complex. In addition, the lattice model uses backward induction, and the prior path of the underlying variable is unknown at the time computations are made, making it impossible to incorporate multiple interacting options with numerous state variables [110]. However, there usually exist multiple interacting options in the investment in power systems, and the inter-dependencies can greatly affect the option value. Overall, *binomial lattice* are not suitable for investments where there are multiple sources of uncertainty and interacting options.

Binomial Tree

In contrast, *binomial trees* [89, 91, 96] have been widely applied to include more sources of uncertainty by adding additional decision nodes, and the model allows to consider the interactions between options made during different stages of the investment period [97, 113]. Unlike the lattice model, the tree model allows for different probabilities and weights at each decision node. However, this feature also means that the computation complexity grows exponentially with the increasing number of decision nodes, constraining their use to complex but smaller-sized problems.

Monte Carlo Simulations

Based on the The investments in power system planning and operation often involve many uncertainties from both the system and electricity market. In this regard, MC simulations are a better choice in capturing many sources of uncertainty and they have the advantage in incorporating stochastic processes with different probability distribution to value multiple investment options. In addition, this approach can capture simulation results from both mean-reversion process for commodity price and conventional geometric Brownian motion, it has become a primary tool value the investment in power system [114].

Despite the strong adaptability of MC simulations in real world applications, this approach cannot value American-type options. Specifically, it can only determine the option value if the option is to be executed immediately, but not the optimal timing for the option executed in the future. This is because the model is forward-looking, while the optimal timing can only be determined by backward induction [115].

Least Squares Monte Carlo

In light of this, the *least square Monte Carlo* (LSMC) method [116] is developed by combining a forward-looking MC model with backward induction to consider many sources of uncertainty while determining the optimal investment timing. Due to these advantages, the LSMC approach has been applied to many power system investments [81, 85–87, 93, 95, 117].

For example, the authors in [117] applied this method to value flexible AC transmission systems devices in transmission networks, by modeling both demand and fuel costs as stochastic processes, and providing the optimal timing for the option to install, locate and remove the asset. The results from this strategy indicate that the presence of uncertainties can significantly increase the risks involved in large-scale irreversible investments. The managerial flexibility in having the options to defer, abandon and relocate such investments in light of unfolding information is highly valuable. Authors in [85] proposed a real options framework for deciding the optimal timing to invest in distributed generation (DG) in a distribution network. The flexibility of management and uncertainties are modelled using an extended LSMC. Within the framework, the benefits from investing in DG are compared with a no-DG investment over a certain period. This study captures the stochastic nature of future power demands and electricity prices using the Geometric Brownian Motion and MC Simulation.

After reviewing the existing literature, the LSMC approach is selected because it presents high-level performance in valuating real options with the least computational complexity comparing with the other methods [85].

2.2.2 Summary

Given this background, Chapter 4 proposes a multi-stage valuation framework that uses ROV to evaluate an investment with compound options under multiple future uncertainties, via the least squares Monte Carlo approach reviewed previously. As a case study, the economic benefits and costs accrued to a DNSP for providing incentives to network customers to purchase PV-battery systems have been investigated to demonstrate the characteristics of the framework. By financially supporting PV-battery investments, DNSP removes the need to install additional substation diesel generators. More details are included in Chapter 4.

2.3 Integrated Financial Modelling for DER Investments in Low-Voltage Networks

The most important contribution of this thesis is to develop a complete financial appraisal that incorporates power flow models to capture both the uncertainties from the network and electricity market. To this end, Chapter 5 develops an integrated ROV framework that combines the probabilistic impact assessment model in Chapter 3 and the ROV model in Chapter 4 to form an integrated ROV framework to value the DNSP's project that incentivises residential energy storage system (ESS) investments. Following this, Chapter 6 includes AC optimal power flow (OPF) analysis within the ROV model to value the investment in grid-scale ESS. In this regard, this sections takes a look at the technical details covered by the existing literature.

2.3.1 Bus Injection Model

Authors in [118] used a DC OPF model to decide the optimal ESS sizing and placement. In this model, all non-linear contraints of AC OPF are linearised, and the overall problem is reduced to a linear program. This significantly reduces the computational complexity, however, DC OPF is often applied in practice for transmission networks over distribution networks.

A full AC OPF can assist in achieving accurate results for distribution networks, but the problem often becomes intractable due to its non-convexity. In order to reduce the computational burden, various methods have been developed. The study in [119] uses trust-region based method incorporated with interior point method to solve non-linear OPF problems. The authors illustrated that the model presents high-level performance in terms of the accuracy of the results and computation speed. Authors in [120] applied Lagrangian Newton method to solve large-scale power flow problems. Similar to the previous method, this model determines a trust region and

finds the local optima within this region. Although these methods can effectively determine the local optima, the optimality is not guarranteed as the results can be highly suboptimal. Moreover, the model often fails to converge when complicated systems are involved.

The computational difficulties can also be overcome by adopting convex relaxation, suggested in [121]. Relaxations are widely used for relaxing higher-order terms in objective functions and constraints to achieve a more efficient program in solving the OPF. Authors in [122] illustrated that the AC OPF model can be relaxed to quadratically constrained semidefinite programming (SDP). If the SDP relaxation converges successfully, the global optima can be determined. This method has also been employed in [122] and [123], both of which indicated noticeable increase in computation speed. However, whether the convergence of the problem is exact has not been well-justified. In addition, the limitation of the SDP has been investigated in [124], it is shown that as a line-flow constraint is tightened, the duality gap becomes non-zero and the solutions produced by the SDP become meanless.

A different convexation approach has been described in [125], in this case, the authors replaced the non-linear terms in the power balance equations with inequality constraints, this process is known as conic convexation. By doing so, the model is recast as a second order cone problem (SOCP), in which some buses become unbounded and are able to draw infinite power from the network. This is also referred to as load over-satisfaction in [126], which shows that the successful convergence of the problem requires some buses to draw more power than needed. Comparing with the SDP method, the SOCP reduces computational burden further. However, this method is exact only if the SDP relaxation is exact. The study in [127] compares a linear OPF to a quadratically-constrained OPF. The results show that the linear OPF offers speed advantages, while the quadratically-constrained OPF can achieve better accuracy but slower in computation speed.

2.3.2 Branch Flow Model

The branch flow model was first introduced in [128]. The authors from this literature demonstrated that the phase angles of currents and voltages can be relaxed. The results indicated an obvious reduction in computational burden, and surprisingly, the problem remains exact for radial distribution networks. The model was properly defined and shown effective in power flow analysis in radial distribution networks in [129]. More recently, authors in [130] and [36] employed this model and rewrote the quadratic expressions, representing power losses, in the power balance equations as inequality constraints to explore the optimal inverter VAR control and optimal capacity placement, respectively. By doing so, the original model is recast as a

SOCP and the upper bounds on the loads are eliminated, as reviewed previously. These studies also show that the conic relaxation in branch flow models is exact for radial distribution networks. This model provides accurate results, however, the computation speed can be high when dealing with complex networks.

Authors in [38] applied the branch flow model in their study to determine a coordinated Volt/Var control (VVC) scheme for distribution networks. Instead of applying conic relaxation, they simply neglected the quadratic terms in the power balance equations to retain a linear model. The power loss is re-calculated in a separate equality contraint after solving the branch flow equations. This method has been applied in multiple literatures, with the effectiveness and accuracy being extensively justified [131], [132]. It is shown in these literatures that the impacts of eliminating the quadratic terms from the power balance equations is insignificant because the amount of power losses is negligible when comparing with the main power flows. Moreover, the computation speed experiences noticeable drops, which can be helpful when a more complicated system is involved. However, the method becomes unreliable when system losses are high.

Different branch flow models have been studied in [133] and [134]. Opposite to the models introduced previously in [130] and [36], [133] sets powers from receiving-end branches as variables, it is shown that the exact solution can be obtained with phase angles being eliminated. Moreover, authors in [134] defined the real and imaginary components of sending and receiving bus voltages, $V_i V_j^*$, as new variables and hence, eliminating voltage angles. However, non of these models has shown its optimality, therefore, will not be considered in our research. In addition, all of the above studies assume the distribution network is balanced while distribution networks are typically multi-phase and unbalanced.

2.3.3 Optimal Power Flow for Unbalanced Distribution Networks

Earlier studies propose various distributed algorithms for solving the OPF problem in unbalanced distribution networks [135], [136]. Although these studies overlook the existence of non-convexity, they illustrated that the methods for single-phase networks can be applied to model a three-phase unbalanced network, specifically, each bus-phase pair in the multi-phase network can be represented by a single bus in the equivalent model. In addition, it is shown in [137] that the multi-phase unbalanced OPF can be solved using both bus injection model and branch flow model. More specifically, the study develops two SDPs based on the bus injection model and branch flow model, respectively, as well as a linearly approximated model of the OPF. It is shown that both of the SDP methods are effective in modelling three-phase distribution networks, and the SDP developed from the branch flow model is numerically more stable. The linear OPF

is accurate when power losses are small and the network is nearly balanced. Moreover, the SDP from the branch flow model is exact only if certain conditions are satisfied by the linear approximation of the OPF.

Most of the methods for solving multi-phase OPF problems are based on existing SDP solvers, which can be computationally intensive when dealing with large-scale networks. A more recent study developes an algorithm to decompose the OPF problem into sub-problems based on alternating direction method of multiplier (ADMM) [138]. The branch flow model discussed in [130], [36] and [128] were employed and the sub-problems were solved via a closed form expression. This method is able to eliminate the use of SDP and further decrease the computation speed. However, the accuracy of this method has not been justified.

After balancing the advantages and disadvantages of different techniques detailed above. The branch flow model introduced in [128] is considered as an effective tool in the multi-phase OPF modelling because the results are more stable than bus injection models. In addition, the computation speed can be escalated by recasting the problem as a SOCP.

2.3.4 Optimal Sizing and Placement of Energy Storage Systems

Grid-scale ESS have been widely recognised as a technically viable alternative to network augmentation in integrating growing renewable penetration in distribution networks. Specifically, the capacity of PV systems connected to the distribution system has increased consistently over the past decade in Australia. The annual installed capacity of small-scale PV systems has grown from less than 200MW in 2009 to 1.1GW in 2017, with the average installation size rising from 1.5kW to 5.5kW [12]. The increasing deployment of PV generation can lead to reverse power flows with congestion problems, over-voltages and phase unbalance, which impact the operations at distribution level [5]. Network augmentation that involves transformer and line capacity upgrades are required to mitigate these negative impacts and accommodate the increasing PV penetration, however, this method is time-consuming and overly expensive [7].

Alternatively, grid-scale ESS that consumes surplus PV generation, and utilises the stored energy in the evening for the peak-load support are recommended to the DNSP [5]. By doing so, it helps manage the power flows in distribution networks, and mitigates the technical problems caused by excess PV generation [9]. Although the technology is currently expensive to implement, it has already shown its potential to become an economically viable alternative to the costly network augmentation in the near future [8], [22].

Given this background, the primary objective of Chapter 6 is to conduct fair comparisons between the CESS, DESS and BTM ESS, therefore, it is necessary to determine the optimal

sizing and placement for both community and distributed ESS. However, determining the optimal sizing and location of an ESS simultaneously is a non-deterministic polynomial-time (NP) hard problem, and currently, limited methods can effectively solve this problem [139]. The methodologies which have been employed to solve this problem can be clustered in three groups, namely, mathematical programming, exhaustive search and heuristic methods. This subsection provides a comprehensive review over each of these three methodologies.

Mathematical programming includes all numerical methods which can discover the optimal solution of an optimisation model. Numerous studies have presented their optimisation models and have shown the potential in achieving this task under different circumstances. Authors in [118] use a DC OPF model for deciding the optimal ESS sizing and placement. This model is based on the linearization of AC OPF and it presents limited computational complexity. However, this model is only suitable for transmission networks as discussed in the previous section. In [140], a MILP model is applied to explore the optimal sizing of a large-scale ESS for islanded wind-diesel gneration. More specifically, it investigated the impacts of different levels wind penetration on ESS sizing. Similarly, the study in [27] develops an MILP to determine the optimal sizing of ESS in a wind generation farm, the objective of the model is to minimise system power losses. Both [140] and [27] applied linearised OPF to determine the optimal sizing of a large-scale ESS, which presents limited computational burden, however, these studies are not conducted in distribution networks. [141] described a linearised AC OPF model for optimal ESS sizing and location on a LV feeder based on cost minimisation. It demonstrated the great potential of utility-scale ESS in boosting the hosting capacity with the aid from active power curtailment (APC). However, this study does not consider power loss minimization, and the network is assumed to be balanced.

As previously described, a full AC OPF can assist in producing accurate results for distribution networks, but the problem is generally non-convex and computationally intensive. Convex relaxation is often applied in this case to reduce the computational complexity. In [142], the authors applied conic relaxation to the AC OPF model to illustrate the effectiveness of ESS in voltage regulation, congestion elimination and power loss reduction, with the objective being minimising the ESS investment cost and the weighted operational cost. Similar method was adopted in [143], which aimed to investigate the impacts of ESS on energy arbitrage and power losses in a distribution network. These goals can be accomplished by optimally placing and sizing ESS. Both studies show that using conic relaxation significantly reduces the computational complexity. However, these studies assume the networks applied are balanced, which is usually not the case for distribution networks. In addition, the study in [144] uses a two-stage AC OPF

model to determine the minimum sizing for ESS in wind power-rich networks. The first stage uses AC OPF to find the initial size, while the second stage adopts a high granular control driven by bi-level AC OPF to tune the storage sizes determine in the first stage.

The method involves exhaustive search guarantees finding an optimal solution, however, it is nearly impossible to solve both location and sizing problems simultaneously because they are generally NP hard and requires significant amount of computation time [139]. Heuristic methods include all methods in which experience and knowledge are incorporated. Unlike exhaustive search, this method does not guarantee finding an optimal solution, and additionally, it requires more computation time than all methods introduced previously to converge to an acceptable solution. Multiple studies have applied this method to determine the optimal location and sizing of ESS simultaneously. A decoupled AC OPF incorporated with genetic algorithm (GA) is applied to determine the optimal sizing of ESS in, with the objective being minimising the electricity provision cost for network operators [145]. In [146], the authors applied particle swarm optimisation (PSO) to determine the size of ESS in a smart household, the objective is to minimise operational cost. Both of these studies employ small-scale systems, while the computation speed will be reduced significantly when the system complexity increases.

Recently, [147] studied the differences between a centralised ESS and multiple distributed ESS in a LV network. A forward-backward sweep linearised AC optimal power flow model was proposed for determining the optimal location and sizing for the DESS. However, this study was conducted on a balanced network, and it failed to investigate the benefits of an optimally placed and sized centralised ESS. None of the papers above have explored the differences between various ESS configurations when considering their values to unbalanced distribution networks and electric utilities as a whole.

2.3.5 Control Strategies for Energy Storage Systems

Many studies do not consider optimal sizing and location, and instead, they propose a range of heuristic control strategies to maximise the benefits of ESS. For instance, [148] illustrated that ESS with the proposed coordinated control strategy can effectively mitigate over votlages when exposed to high PV generation. Authors in [**?**] proposed a decentralised storage control strategy based on voltage sensitivity analysis in LV networks with high PV penetration. The results showed that high PV generation can lead to over sizing of ESS, which is uneconomical to operators. These studies do not optimally place and size the ESS, while the results can be significantly different otherwise.

2.3.6 Summary

After reviewing the existing literauture, the branch flow model with conic relaxation is used when determining the optimal sizing and location of utility-scale ESS, because it shows significant reduction in computational burden with minimum sacrifice in accuracy among all. Then, Chapter 6 incorporates the AC OPF model to form an integrated ROV framework to determine the optimal strategy to carry out a grid-scale ESS investment.

2.4 PV Investment Game

This reminder of this section performs a detailed literature review on topics including (i) applications of game-theoretic analysis on planning and operations in power systems; (ii) existing methods for solving a game with unknown payoff functions and continuous action sets; and (iii) recent literature on modelling of the inverter VVC functions.

2.4.1 Game Theoretic Analysis in Distribution Network Investments

The modern electricity network allows more decisions to be made locally and directly by the end consumers. In this regard, game theory has taken more relevance in providing a framework to evaluate the impact of distributed actions on the network, since it naturally models interactions in distributed decision making processes. For instance, the study in [149] proposes a game-theoretic approach to the operation and control of individual components including loads and generation in small-scale power systems. In [150], the authors proposed a cooperative game in the context of a grid-connected hybrid power system where the three players are wind generation, PV generation and ESS. By playing this game, the players maximise their own profits by choosing their individual optimal capacity. However, in this model, the players are aware of their opponents' actions after each round of play. In [151], game theory is used to design attractive demand response contracts that engage more consumers to actively manage their demand for peak shaving. The game is played between the utility and the customers. A list of contracts is designed to encourage customers to voluntarily sign up for the contract that best suits their needs. The study in [152] proposes a distributed load management strategy to control power demand at peak hours. This method is formulated as a network congestion game which is shown to converge to a pure Nash equilibrium (NE). In the above studies, game theoretic analysis has been employed in the context of power system planning and operation. However, none of the

existing literature has investigated the allocation of available network capacity for residential PV investments.

In our study, we formulate a congestion game where players only observe their own payoff from the current investment profile. The players decide each action based on their own payoff history. This is a simple learning process. In this regard, the learning literature has essentially focused on finite action games. One of the most widely-explored adaptive process is *fictitious play*. In each iteration of this process, players play a best response to the frequency of their opponents actions. This method converges to a Nash equilibrium in 2-player zero-sum games [153] and potential games[2] [154]. However, our study assumes that players do not observe their opponents' actions.

Reinforcement learning processes can be used when players have no knowledge of their opponents' actions [155]. In [156], a log-linear learning algorithm is shown to converge in potential games when players adapt learning only from payoffs. Similarly, the study in [157] investigates the effects when players adjust their actions based on the cumulative payoffs over time. Reinforcement learning has been widely applied in different contexts including transmission power control in cognitive radio networks [158]. However, in contrast to these works, our learning process occurs in a continuous action space.

Bringing the two lines of system design and algorithm convergence together, an optimal wind farm control design was derived using a potential game framework and solved using a learning algorithm in [159]. A similar problem was tackled in [160] for an ad-hoc sensor network problem where rewards are initially unknown and have to be learned from experience, using result on learning in noisy unknown games from [161]. However, both of these approaches apply to games with discrete action sets.

In the context of learning with continuous actions space and unknown payoff functions, simple learning processes have been used in strictly concave games [162]. Under such processes, players only observe their own payoffs after each iteration of play, and they choose actions based on the difference of the payoff from the previous iteration. More recently, *dual averaging* has been shown as an efficient learning method in finite games [163]. This method requires players to take small steps along their individual payoff gradients and then "mirror" the output back to their action space to choose an action for the next round. We make use of this algorithm in Chapter 7 to compute the equilibrium PV investment profile of independent electricity customers.

[2]Congestion games of the type investigated here are subset of potential games.

2.4.2 Inverter Volt/Var Control Functions

Recent studies in the existing literature fall into two categories. One considers centralised optimisation, where computations are done by a single central authority which is assumed to have full observability of the system. Such a system requires two-way communications between the central authority and at least all of controlled inverters. The study in [164] formulates an OPF problem to control the reactive power function from PV inverters and simultaneously improve voltage profiles, minimise network losses and generation costs. These objectives are aggregated into one using the weighted-sum method, which is then solved by the global sequential quadratic programming. On the other hand, [36] and [37] solve the OPF problem by relaxing it into a SOCP. The study in [38] proposes a multi-timescale centralised approach that coordinates capacitor banks (CBs), on-load tap changers (OLTCs) and PV inverters to regulate network voltage in the presence of uncertainties in load dand PV generation. Specifically, the PV inverters are operated in a 15-min timescale to respond to transient PV cloud movements, while the CBs and OLTCs are operated in a longer timescale. Nonetheless, all centralised approaches would require high-quality communication of the measurements and control signals, which is not yet a reality for most distribution systems. In addition, potential communication delays would challenge their optimality and stability for real-time implementations.

To tackle this, the existing literature have investigated in decentralised methods that typically require no communications. These inherently sub-optimal methods rely only on node-local measurements as inputs to a policy that converts the measurements into a control action. Specifically, in [165], a local droop controller is designed for the inverters to absorb/generate reactive power for mitigating voltage rise. In [166], an adaptive proportional-integral controller is designed for multiple inverters to achieve plug-and-play VVC. In [35], two droop control methods that are inherited from the standard $\cos\gamma(P)$ and $Q(U)$ strategies are combined to a $\cos\gamma(P,U)$ method, which works effectively to fairly employ all inverters. Although being fast and simple, the decentralised methods prohibit system-wide coordination and optimisation.

Different approaches have been proposed to address the problems raised above. The study in [167] solves the Var control optimisation problem using a distributed alternating direction method of multipliers (ADMM). The model uses only local measurements augmented with limited information from the neighboring nodes through cyber channels. On the other hand, [34] formulates a decentralised reactive power optimisation problem that reduces voltage deviations using only local measurements. With the measurements being tuned up by a stability analysis, the optimal solutions are attained to a surrogate centralised optimisation problem. The study in [132] proposes an adaptive control algorithm to improve the performance of reactive power control,

while minimising power losses and voltage mismatch on each network node. However, as a common drawback in the above studies, the uncertainties in load and PV generation are generally not considered. In response to this, a three-stage robust inverter-based Volt/Var control approach is proposed in [168]. This approach systematically coordinates centralised and decentralised approaches for voltage regulation and power loss minimization. Specifically, in the first stage, the CBs and an OLTC are scheduled to minimise power losses and track regular voltage variations; the second stage dispatches PV inverters in a short period for voltage regulation; local droop controllers are used to respond to real-time voltage violations caused by varying load and PV generation in the third stage. By reviewing the existing literature, no one has implemented the droop control function within centralised optimisation model due to the following reasons: (i) communication delays that would challenge the optimality, and (ii) the non-convexity introduced by the feasibility sets drawn by the droop control curves.

2.4.3 Summary

Against the literature review, Chapter 7 develops a novel game theoretic model to simulate the uncoordinated process where residential customers independently invest in PV systems to maximise their own welfare. Then, this chapter formulates an optimal PV sizing problem, considering inverter VVC and APC functions. Solving this optimisation problem provides the socially-optimal solution, which is compared to the NE solution from the game to determine the efficiency loss of the investments under the natural uncoordinated process.

Chapter 3

Probabilistic Impact Assessment Framework

Rising photovoltaic (PV) penetrations can impose numerous technical problems on networks including over-voltages, reverse power flows with congestion problems, and phase unbalance. Energy storage systems (ESS), particularly residential ESS coupled with rooftop PV, is emerging as an essential component of the smart grid technology mix. It is widely believed that ESS will largely mitigate these problems [5], [24]. However, including ESS and other flexible resources like electric vehicles and loads with thermal inertia into a probabilistic analysis based on Monte Carlo (MC) simulation is challenging, because their operational profiles are determined by computationally intensive optimization[1]. Additionally, MC analysis requires a large pool of statistically-representative demand profiles to sample from. As a result, the analysis of the network impact of PV-battery systems[2] has attracted little attention in the existing literature.

To fill these knowledge gaps, Chapter 3 develops a probabilistic MC framework to study the impact of PV-battery systems on low-voltage distribution networks. Specifically, the framework embeds the ESS scheduling optimization problem in the MC analysis to assess the effects of ESS scheduling on low-voltage (LV) networks. By doing so, the framework tests the conjecture that using existing strategies to schedule batteries, include HEM under *time-of-use* tariffs or *self-consumption maximization*, can serendipitously reduce the technical problems caused by excessive PV generation.

The remainder of this chapter is organised as follows. Section 3.1 provides an overview of the

[1]It is expected that ESS will be equipped by HEM in the future to optimally facilitate energy use within a household.

[2]In this thesis, PV systems that are coupled with an ESS are called PV-battery systems

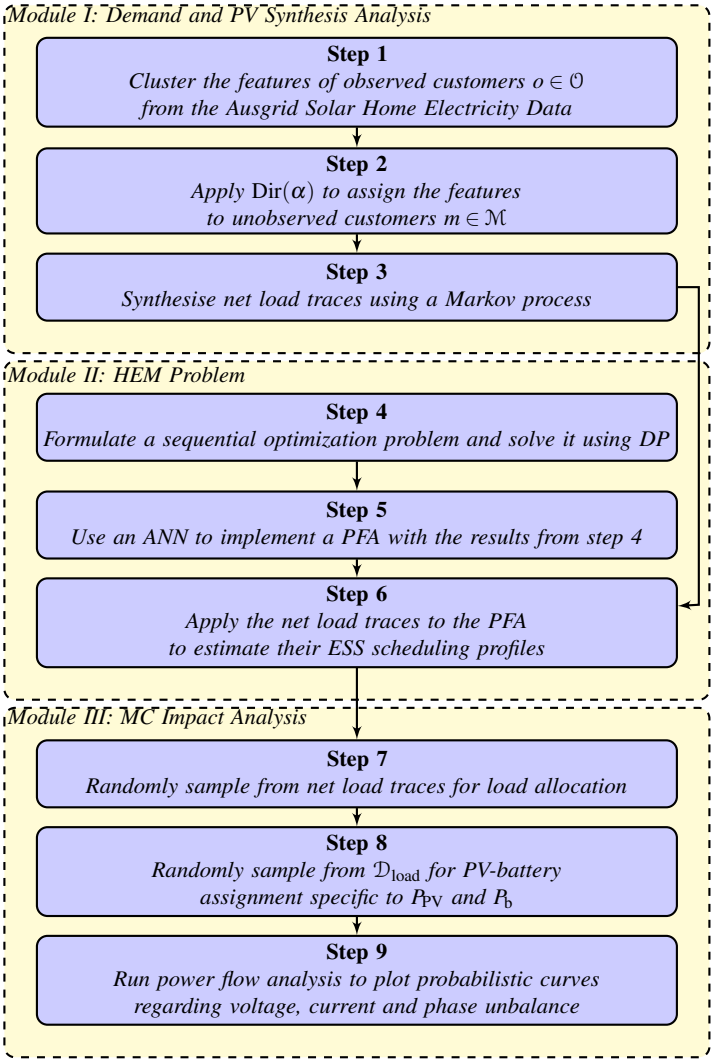

Figure 3.1: Overview of framework used to conduct the probabilistic MC power flow study to assess the impact of PV-battery on distribution networks.

proposed framework. Section 3.2 describes the module that synthesises large pools of demand and PV profiles. Section 3.3 presents the HEM system used to compute the ESS schedules for each customer from the large data pool. The probabilistic power flow study via MC analysis is described in Section 3.4. The three modules described in Sections 3.2, 3.3 and 3.4 are used to form the probabilistic impact assessment framework, as shown in Fig. 3.1. The results are discussed in Section 3.5. Section 3.6 draws conclusions.

3.1 Framework Overview

The proposed framework integrates three modules, as shown in Fig. 3.1, to conduct the probabilistic MC power flow study to assess the impact of PV-battery systems on distribution networks. This section summarises the purpose of each module and demonstrate how they interact within the toolchain.

First, to capture the varying load behaviours in a distribution system using a MC study, a large pool of demand and PV traces is required for sampling. Thus, the purpose of Module 1 is to synthesise this large pool of traces using a small amount of existing data provided by Ausgrid Solar Home electricity data, which has smart meter and PV generation data with a 30-minute resolution for 150 customers for a period of three years [169]. The steps of this module are discussed with more details in Section 3.2.

Second, following this, Module 2 formulates the ESS scheduling optimization as a home energy management (HEM) problem, which is solved for all customers from the Ausgrid dataset to provide a training dataset. Then, a policy function approximation (PFA) is trained to emulate near-optimal ESS schedules for the large data pool synthesised in Module 1. This module is used to provide fast solutions to the ESS scheduling problem. The mathematical formulation of the HEM scheduling system and the construction of PFA are detailed in Section 3.3.

Third, Module 3 randomly samples from the large pool of demand, PV and ESS profiles obtained from the previous modules, and allocate them to the network according to varying PV and ESS penetration levels (percentage of customers owning a PV system, or a PV-battery system). Power flow analysis is performed to determine the impact of ESS schedules on distribution networks specific to different PV and ESS penetration levels. This step is repeated within the MC study to capture the varying system conditions related to load behaviours, sizing and placement of PV and ESS. The detailed procedure is covered in Section 3.4.

3.2 Demand and PV Trace Models

Probabilistic assessment of the impact of distributed energy resources (DER) on distribution networks requires a large pool of synthetic demand and PV traces to sample from. In many jurisdictions smart metering data are scarce, so the framework needs to be able to generate statistically representative samples when only a limited number of demand and PV traces is available [18]. This is the purpose of Module 1 in Fig. 3.1; to use an existing dataset to generate a larger pool of demand and PV profiles (net load traces). Module 1 works by assigning Markov processes according to a Dirichlet distribution identified via clustering, as explained below.

3.2.1 Data Preparation

This work extends the non-parametric Bayesian model [170] to generate net load traces that are statistically similar to historical demand and PV generation of observed customers. The observed data was collected from the Augrid dataset [169].

Let $o \in \mathcal{O}$ and $m \in \mathcal{M}$ denote the set of observed and unobserved customers, respectively. The module first applies a clustering technique, namely *maximum a-posteriori Dirichlet process mixtures* [171], to cluster $o \in \mathcal{O}$ customers into representative sets $\beta \in \mathcal{B}$ according to their features. This technique is useful for instances in which the number of clusters cannot be easily determined. The features of demand are the day types (weekday or weekend) and number of residents, while those for PV include the PV capacity, panel orientation and weather information. Clustering is important because (i) considering each customer as a single category is computationally expensive, and (ii) it provides generalizable statistical information as the demand and PV generation in each set are correlated with their features.

3.2.2 Estimating the Dirichlet Distribution

After clustering, the next step is to compute the frequencies, $\{p_\gamma\}_{\gamma\in\Gamma}$, of each $\gamma \in \Gamma$ in the population $\mathcal{O}$. These frequencies can be interpreted as the probability of an unobserved customer having certain features. However, they are only an estimate across the observed customers, and directly using them to allocate features fails to properly consider the error in this estimate, which can be significant where the fraction of customers observed is small. Thus, a Bayesian estimation approach is employed.

Specifically, in Step 2 in Module 1, the model uses the count of each $\gamma \in \Gamma$ in the observed $\mathcal{O}$ as a hyperparameter of a Dirichlet distribution, which itself is sampled to yield a *categorical* probability distribution over the features for unobserved customers, $m \in \mathcal{M}$. Formally, this is given by:

$$\begin{aligned} \boldsymbol{\alpha} &\quad \text{Vector of cluster counts} \\ \mathbf{p} \mid \boldsymbol{\alpha} &\sim \text{Dir}(\boldsymbol{\alpha}) \\ S_m \mid \mathbf{p} &\sim \text{Cat}(\mathbf{p}) \end{aligned}$$

In more detail, $\boldsymbol{\alpha}$ is a vector of *concentration hyper-parameters* given by the number (c.f. frequency) of observed customers within each $\gamma \in \Gamma$. Sampling from $\text{Dir}(\boldsymbol{\alpha})$ yields the parameters, $\mathbf{p}$ of a categorical probability distribution, $\text{Cat}(\mathbf{p})$ over the features for unobserved customers, $m \in \mathcal{M}$. Finally, S_m is the random variable assigning a cluster to each unobserved customer o, which is drawn from $\text{Cat}(\mathbf{p})$. This Bayesian approach to assigning clusters to unobserved cus-

tomers ensures that the error in the estimate previously discussed is probabilistically accounted for.

3.2.3 Markov Chain Process

Step 3 in Module 1 involves synthesizing a large number of net load traces based on the feature assignments, by (i) generating Markov transition matrices and then (ii) sampling a trace, as follows.

First, a conditional Markov process is identified by constructing a set of observed state transition matrices, defined as:

$$\mathbf{M}_t = [\mathbf{M}_1, \mathbf{M}_2, ..., \mathbf{M}_{48}]. \tag{3.1}$$

In each matrix $\mathbf{M}_t$, the states are used to represent the amount of electricity used by one observed customer for one time-step. Following this, a matrix of transition frequencies that records all observed state transitions is constructed for each $\mathbf{M}_t$. One time-step is 30 minutes, which means it is needed to sample from 48 transition frequency matrices to construct one unobserved profile.

In more detail, to sample from the transition frequency matrices, the first step is to calculate the conditional distribution of the initial state. Specifically, the process sums up each row of the first transition matrix, and run Gaussian kernel density estimation over these sums to give a probability measure; the initial state is then sampled from a conditional distribution defined by this measure. Gaussian kernel density estimation ensures that unobserved state transitions are attainable (i.e. a nonzero transition probability is provided to latent states conditional on the observed data). Given this, kernel estimation is run over each row of each transition matrix to provide the probability measures for the rest of the states. This process is continued for each remaining time-step to construct one net load trace for one year. The net load traces serve as the inputs to the HEM problem in Module 2 for fast ESS scheduling estimation. For more details regarding the non-parametric Bayesian model, please see [170].

3.3 Home Energy Management

The choice of the HEM optimization formulation is arbitrary; none of the existing solution techniques is computationally efficient enough to be directly used in MC analysis. Module 2 uses dynamic programming (DP)[3] in conjunction with PFA [69] to emulate ESS scheduling policies

[3]DP is notorious for the curse of dimensionality, but in this study I consider deterministic DP with only one schedulable device, so the computational performance is comparable to mixed-integer linear programming.

for the large pool of customers synthesised in Module 1, allowing the HEM operational decisions to be feasibly included within the MC analysis. Specifically, the process first formulates a *Markov decision process* (MDP) for each observed customer, $o \in \mathcal{O}$. The objective is to minimise the energy costs for each customer, with costs and benefits given by time-of-use tariffs and feed-in-tariffs. The decision variables of this algorithm include the optimal scheduling policies for each ESS over a year. Next, using the observed dataset and the outputs from solving the HEM problem, an artificial neural network (ANN) is trained as a PFA algorithm, which is then used to compute fast solutions to the ESS scheduling problem for the net load traces synthesised in Module 1. The details of Module 2 are discussed below.

3.3.1 Scheduling Problem

The general formulation of the scheduling problem for each HEM system follows [68]. In brief, the ESS scheduling problem comprises a sequence of time-steps, $\mathcal{T} = \{1...t...T\}$, where T and t represent the total number of time-steps and a particular time-step in a decision horizon, respectively. The historical data provided by Ausgrid has a 30-minute resolution. Therefore, the decision horizon is one day (24 hours) with 48 time-steps. Given that each HEM system has one controllable ESS, the MDP consists of the following:

- A set of state variables, $s_t \in \mathcal{S}$ to represent electricity demand (s_t^{d}), PV output (s_t^{pv}), electricity tariff (s_t^{p}), grid power (s_t^{g}) and ESS state of charge (SOC, s_t^{b});
- A decision variable, $x_t^{\mathrm{b}} \in \mathcal{X}$ to describe each control action for the ESS, including charging and discharging rates;
- Constraints for all control and state variables, denoted as $\mathbf{s}^{\mathrm{M}}$; and
- A random variable, $w_t \in \mathcal{W}$ to capture the perturbation information given by non-controllable inputs, such as demand (w_t^{d}) and PV generation (w_t^{pv}).

Thus, the state transition function for describing the evolution of a state from t to $t+1$ is:

$$s_{t+1} = \mathbf{s}^{M}(s_t, x_t, w_t). \tag{3.2}$$

Each state contains the information that is necessary and sufficient to make decisions and compute rewards, costs and transitions. An optimal control action is taken to minimise the electricity cost for each observed customer. The problem is solved using DP, which computes the value function that provides the expected future discounted electricity cost for each state.

An optimal policy, π is extracted from the value function by selecting the state transitions that follow a minimum value function path, such action minimises the expected sum of future costs over the decision horizon; that is:

$$F = \min_{\pi} \mathbb{E}\left(\sum_{t=0}^{T} C_t(s_t, x_t, w_t)\right), \tag{3.3}$$

where $C_t(s_t, x_t, w_t) = s_t^{\mathrm{p}}(s_t^{\mathrm{d}} + w_t^{\mathrm{d}} - \eta^{\mathrm{i}} x_t^{\mathrm{i}})$ is the cost of energy incurred at time-step t, which accumulates over time. η^{i} is the inverter efficiency, and x_t^{i} is the inverter power, which is formulated as:

$$x_t^{\mathrm{i}} = s_t^{\mathrm{pv}} + w_t^{\mathrm{pv}} - \eta^{\mathrm{b}} x_t^{\mathrm{b}}. \tag{3.4}$$

where $\eta^{\mathrm{b}+/-}$ is the ESS charging/discharging efficiency. The energy balance constraint (3.5), and ESS operation constraints (3.6) to (3.9) are shown as follows:

$$s_t^{\mathrm{d}} + w_t^{\mathrm{d}} = \eta^{\mathrm{i}} x_t^{\mathrm{i}} + s_t^{\mathrm{g}}. \tag{3.5}$$

$$s_{t+1}^{\mathrm{b}} = s_t^{\mathrm{b}} + \left(\eta^{+} x_t^{\mathrm{b}+} - \frac{1}{\eta^{-}} x_t^{\mathrm{b}-}\right). \tag{3.6}$$

$$0 \leq x_t^{\mathrm{b}+} \leq \gamma^{\mathrm{c}} * \alpha_t^{\mathrm{b}}. \tag{3.7}$$

$$0 \leq x_t^{\mathrm{b}-} \leq \gamma^{\mathrm{d}} * (1 - \alpha_t^{\mathrm{b}}). \tag{3.8}$$

$$s_{\min}^{\mathrm{b}} \leq s_t^{\mathrm{b}} \leq s_{\max}^{\mathrm{b}}. \tag{3.9}$$

The state-of-charge (SOC) at time-step $t+1$ of an ESS (s_t^{b}) is a function of the SOC at time-step t, and the charging ($x_t^{\mathrm{b}+}$) and discharging ($x_t^{\mathrm{b}-}$) rates for this time interval, given by (3.6). The charging and discharging rates are constrained by the maximum charging and discharging rates, denoted γ^{c} and γ^{d}, respectively, given by (3.7) and (3.8). In addition, the state of charge cannot exceed the minimum and maximum SOC at all times, as described in (3.9). The minimum SOC is 20% of the ESS capacity specified by the manufacturers listed in Table 1. This limitation is set to protect batteries from quick degradation. For more details regarding the HEM formulation, please visit [68].

Solving this HEM problem using DP for each customer for one year requires 3 hours. This is time-consuming, and therefore impractical within MC analysis.

Algorithm 1 PFA Algorithm

1: Obtain ESS scheduling policies by solving the HEM problem for $o \in \mathcal{O}$ over one year.
2: Train an ANN with the population $\mathcal{O}$ by iterating through Steps 3 to 7.
3: **for** $o \in \mathcal{O}$ **do**
4: **for** $t \in \mathcal{T}$ **do**
5: Train an ANN using s^{b}_{t-1}, s^{d}_t, s^{pv}_t and s^{p}_t as inputs, and s^{b}_t as target.
6: **end for**
7: **end for**
8: Use the trained ANN to compute optimal ESS schedules for sythesised customers by iterating through Steps 9 to 15.
9: **for** $m \in \mathcal{M}$ **do**
10: **for** $t \in \mathcal{T}$ **do**
11: Compute s^{b}_t from the ANN.
12: Modify x^{b}_t and s^{b}_t so that they are within the constraints (3.7) to (3.9).
13: $s^{\mathrm{b}}_t = s^{\mathrm{b}}_{t+1}$.
14: **end for**
15: **end for**

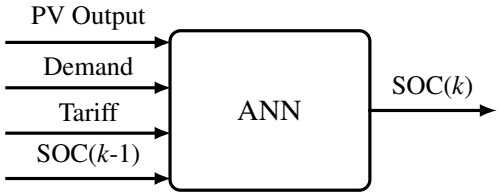

Figure 3.2: The PFA model.

3.3.2 Policy Function Approximation

MC analysis requires thousands of runs, so solving the HEM problem exactly is computationally prohibitive. Instead a PFA implemented in Step 5 in Module 2 is used. The PFA, illustrated in Fig. 3.2, refers to a lookup table that returns an ESS schedule for a given set of inputs, including PV output, demand, electricity tariff and SOC at the previous time-step. The ESS scheduling decisions generated in Step 4 in Module 2 are used to train the ANN. Similar to the HEM problem, the choice of the ANN is arbitrary. The authors showed in [69] that several machine learning techniques could be used with similar performance. In this work, a *recurrent neural network* (RNN) is used because it has been shown to provide close-to-optimal performance when executing ESS schedules trained on similar data [69]. The PFA algorithm is shown in Algorithm 1, and explained in more details below.

The training process requires a training dataset, which includes historical demand (s^{d}_t), PV generation (s^{pv}_t), electricity tariff (s^{p}_t), and the calculated SOC with a delay of 1 time-step (s^{b}_{t-1}), while the SOC at the current time-step (s^{b}_t) is the target. The ANN learns to use the present and

the most recent information to predict the output (target) for each time-step. I use the trained ANN as the PFA to emulate the outputs from the ESS scheduling optimization.

Specifically, the net load traces synthesised in Module 2 is fed into the PFA to compute s_t^{b}. To prevent the outputs from violating the ESS operation constraints, a control strategy is implemented. This strategy compares the outputs of the PFA at t and $t-1$, and adjust s_t^{b} so that both s_t^{b} and x_t^{b} satisfy the boundaries set by (3.7) to (3.9), before feeding back to the PFA. By doing so, the constraints on both ESS operation and capacity are included within the PFA algorithm.

A set of generated demand and PV profiles were used to verify the accuracy of the PFA before feeding the net load traces to the ANN (Step 6 in Module 3). Fig. 3.3 illustrates the difference between the calculated and estimated ESS schedules from DP and the PFA, respectively, for one particular day. Observe that the results from DP and PFA are acceptably close. Specifically, the ESS is set to charge with the excess PV generation during the middle of the day. However, due to the limited ESS capacity, observe that additional PV generation is fed into the grid, as indicated by $p_{\mathrm{g}}^{\mathrm{PFA}}$ and $p_{\mathrm{g}}^{\mathrm{DP}}$. Following this, as PV generation drops, the ESS starts to discharge at around 5pm for peak demand support. Moreover, the energy costs for the same customer are \$2.24 and \$2.29, using the calculated and estimated ESS schedules, respectively. These results are acceptably close, hence, it is reasonable to consider the loss in performance of the PFA to be fit for purpose. This result corroborates those in [69] that the PFA provides close-to-optimal ESS schedules.

3.4 Probabilistic Impact Assessment Framework

To probabilistically assess the impact of residential batteries on distribution networks, Module 3 incorporates the HEM problem within the MC analysis, summarised in Algorithm 2. The MC simulation is run 100 times for 11 PV and 3 ESS penetration levels, resulting in 3300 yearly power flow simulations with a half hourly resolution. The results provide insights regarding the probabilities for a technical issue to occur based on different PV and ESS penetration levels, which define the percentage of customers that have a PV system alone, or a PV-battery system.

3.4.1 Sampling Process

The size of individual PV systems from the Ausgrid dataset is increased to better represent the average residential PV size, which was around 5.5kW in Australia in 2017. The ESS size is decided based on the size of each PV system. In Australia, 2kWh of ESS is typically used per

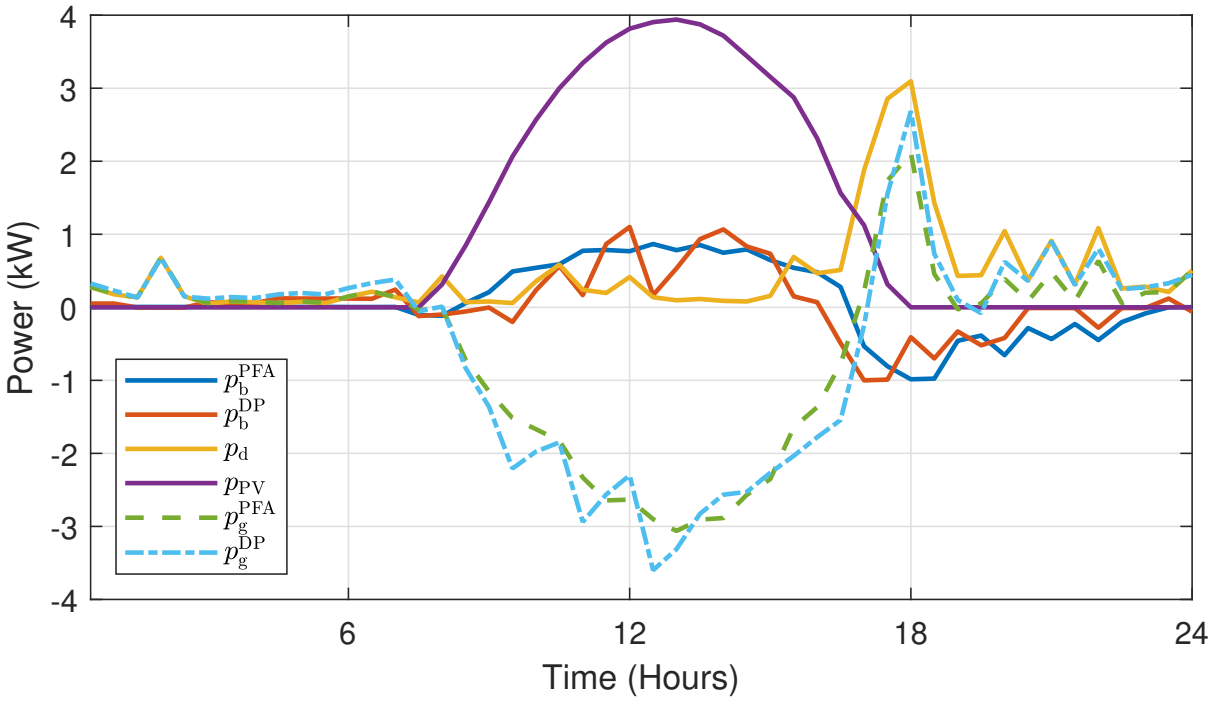

Figure 3.3: Example scheduling estimates from PFA (p_b^{PFA}), the calculated schedules from DP (p_b^{DP}), and the corresponding PV generation (p_{PV}), demand (p_d), grid powers, p_g^{PFA} and p_g^{DP}, from PFA and DP, respectively.

Table 3.1: Energy storage system specifications

Attached PV size (kW)	≤ 4	5-6	7-10
ESS Capacity (kWh)	6.5	9.8	14.0
ESS Power (kW)	4.2	5.0	5.0
Manufacturer	LG	LG	Tesla

1kW of PV installed. The batteries used are from LG and Tesla, which provide three ESS sizes to match the PV size ranges. The detailed allocation is summarised in Table 3.1.

For each customer obtained from the Ausgrid smart meter dataset, the ESS scheduling policies are calculated for the whole year using DP, which are then used to train the ANN in the PFA. The PFA was then used to provide ESS scheduling policies for the 3000 synthetic demand and PV traces generated in Module 1. The uncertainties in the power flow study are captured by probabilistically sampling from this pool of synthetic net load traces for random allocation of loads, PV and ESS. In more detail, each load assignment accounts for eleven levels of PV penetration, denoted P_{PV}, ranging from 0% to 100%. Specific to each P_{PV}, a set of load traces with a PV system $\mathcal{D}_{PV}$ is randomly sampled from the set of load traces $\mathcal{D}_{load}$. Following this,

Algorithm 2 Probabilistic Impact Assessment

```
for i = 1:100 do
    Randomly sample net load traces from D_load.
    for P_PV = 0%:10%:100% do
        Randomly sample from D_load a set of PV assignments D_PV.
        for P_b = 0%:50%:100% do
            Randomly sample from D_PV a set of ESS assignments D_b.
            Run power flow analysis.
        end for
    end for
end for
```

three ESS penetration levels P_b (0%, 50%, 100%) are implemented for each P_{PV}. A set of traces with an ESS $\mathcal{D}_b$ is randomly drawn from $\mathcal{D}_{PV}$. This process covers both Steps 7 and 8 in Module 3.

3.4.2 Power Flow Analysis

The sampled data are used to run yearly power flow simulations for all MC realization paths (Step 9 in Module 3)[4]. Yearly voltage profiles for each customer and feeder head loading are used to determine the probabilities of a technical problem, namely over-voltage and/or congestion problem, according to the specific metrics defined below.

Voltage Problem

The maximum and minimum phase voltage thresholds at each busbar are 241.5 (1.05 pu) and 218.5 (0.95 pu) phase-to-neutral, respectively. This provides room for voltage rise and drop when peak load or high PV penetration occurs. Comparing to the real set points at 0.94 pu and 1.1 pu, a narrower voltage band is selected so that voltage issues can occur at a lower PV penetration level. This is useful to show the efficacy of the methodology and demonstrate the impact of uncoordinated PV-battery systems on distribution networks. The daily voltage profile is calculated for each customer and checked for compliance with the modified standard BS EN 50160 [173], which states that customers' voltages must be between the predefined set points during 95% of the time within each week.

[4]In this work, OpenDSS [172] is used for power flow analysis.

Table 3.2: LV test feeders

Feeder Name	Length (m)	No. of customers on Phase A, B and C	Feeder head ampacity (A)
AUS 1	10235	103, 108 and 91	1155
AUS 2	5656	73, 69 and 81	1200
UK	5656	73, 69 and 81	400

Thermal Loading Problem

The thermal loading level is defined by the ratio of the half-hourly maximum current to the transformer capacity. Specifically, if the ratio is greater than 1, the network has a thermal problem.

Phase unbalance

This study also investigates the effects of PV-battery systems on the voltage unbalance factor, which is a measure of the phase unbalance [174]. It is calculated as the maximum deviation from the average phase voltage during each 30-minute time interval.

3.5 Results and Evaluation

The probabilistic impact assessment framework is applied to two typical Australian LV networks and one UK LV network. The results are analysed by running yearly power flow analysis. The magnitude of a technical problem (over-voltage, transformer loading level and phase unbalance) is recorded at different levels of P_{PV} and P_{b}.

3.5.1 Computational Performance

The improvements in computational performance is the linchpin of the proposed framework. Solving the scheduling problem for each net load trace for one year using DP requires 3 hours. Given the 3300 yearly power flow simulations (100 MC runs for 11 PV penetration levels each with three ESS penetration levels), this is clearly impractical. Thus, instead of using DP in the MC assessment directly, a PFA is trained using ANN to emulate the ESS scheduling policies, which is akin to referring to a lookup table with a given set of inputs. By doing so, I was able to reduce the computational time to five minutes for each customer, which is more than a 95% reduction. Training the ANN only takes 30 minutes, which is negligible. Thus, the use of PFAs is essential to making the entire MC process computationally feasible.

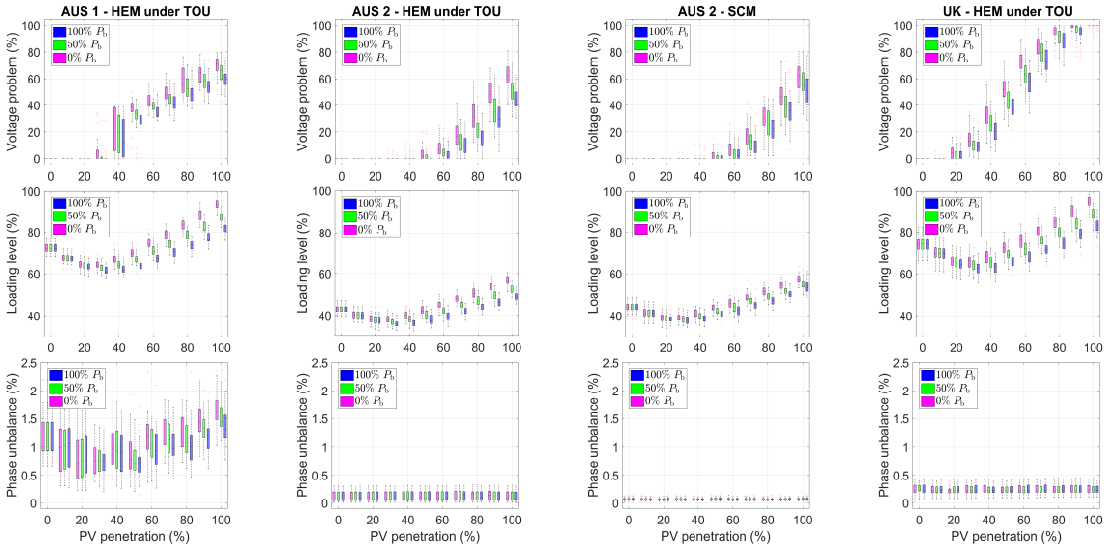

Figure 3.4: Percentage of customers with voltage problems, transformer loading level and phase unbalance. Pink, green and blue bars represent 0%, 50% and 100% ESS penetration levels, respectively. Each bar from top to bottom shows the maximum, 75 percentile, median, 25 percentile and minimum value.

3.5.2 Test Networks

In order to evaluate the method, two four-wire three-phase unbalanced LV test networks with different lengths are adopted from Electricity North West Limited (ENWL), a British network operator [1]. Typically, Australian LV networks are designed to have higher capacity than the UK ones, mainly due to much larger air-conditioning loads. To match this design, the UK test networks are transformed into Australian-type LV networks by tripling the transformer and line capacity[5]. These test feeders are denoted as AUS 1 and AUS 2, respectively. Each feeder is supplied by a 2250kVA 11kV/0.4kV 3-phase transformer. In addition, one of the selected UK feeders is supplied as the third test case, denoted UK, with a lower feeder head ampacity for comparison. The details of the test networks are summarised in Table 3.2 [1]. The framework samples from the pool of net load traces synthesised in Module 1 of our method for allocation to load points.

3.5.3 HEM Formulation

The HEM objective is to minimise energy expenditure under a *time-of-use* (ToU) tariff with the peak demand period from 2pm–8pm. The PV buy-back rate (the "feed-in tariff") is much

[5]For transformers, I reduced the impedance, while for transmission lines I only reduced the resistance. The reactance mainly depends on the distance between the conductors, so I left it unchanged.

lower than the electricity tariff so there is no incentive for the HEM to export power to the grid. As a benchmark, *self-consumption maximization* (SCM) heuristic scheduling strategy is used, whereby the energy from the solar PV is first used to meet the demand, and then any excess PV generation is used to charge the ESS, or exported to the grid if the ESS is full. For brevity, the SCM is applied only to AUS 2 which has a larger potential for greater technical problems, and the results are compared with the HEM under ToU tariff.

3.5.4 Voltage Problems

The frequency of voltage problems with respect to increasing P_{PV} and P_{b} on the LV feeders is shown in Fig. 3.4, row one. The percentage of customers with a voltage problem follows an increasing trend across all test feeders with respect to rising P_{PV}. Specifically, the voltage problem appears on the UK network from only 20% P_{PV}, followed by 30% on AUS 1, and 40% on AUS 2. This is because the UK network has a higher line impedance, and thus greater voltage problems across all penetration levels. AUS 1, on the other hand, has a larger size that allows PV installations to be concentrated in particular parts of the network. Thus, greater variability in the voltage metric at low P_{PV} is observed (Fig. 3.4).

Voltage problems can be reduced by 10-20% across all test feeders using HEM under ToU (Fig. 3.4). This scheduling strategy encourages batteries to charge when electricity price is low, and discharge when the price is high (during peak hours). Fig. 3.5 illustrates the voltage and power profiles of a customer before and after the network is equipped with ESS on a particular winter day. In this case, the ESS charges with excess PV generation, and discharges during peak demand, because peak demand occurs after PV generation drops. As a result, peak voltages are reduced throughout the period when excess PV generation presents.

However, ESS scheduled by HEM under TOU do not always perform up to the standard shown in Fig. 3.5 for voltage reduction. In fact, it depends on the customer's energy consumption pattern. For instance, ESS scheduling becomes less effective when excess PV generation overlaps with the peak demand, which often occurs in summer. This is illustrated for some specific case in Fig. 3.6, in which the peak demand occurs between 4 and 6pm, causing the ESS to discharge during high PV output. This reduces the grid power supply (p_{g}), when compared to the case without the ESS ($\hat{p_{\mathrm{g}}}$). As a result, p_{g} and $\hat{p_{\mathrm{g}}}$ cross at around 4:30pm, where the voltages become the same (as highlighted in the black boxes). Furthermore, at 4:30pm, rising demand causes the ESS to decrease its charging power at high PV output, which keeps the voltage at a high level. In these scenarios, HEM under ToU is less effective at reducing over-voltage problems. It should be also realised that the SOC reaches the peak at 5pm while the ESS is still charging. This is

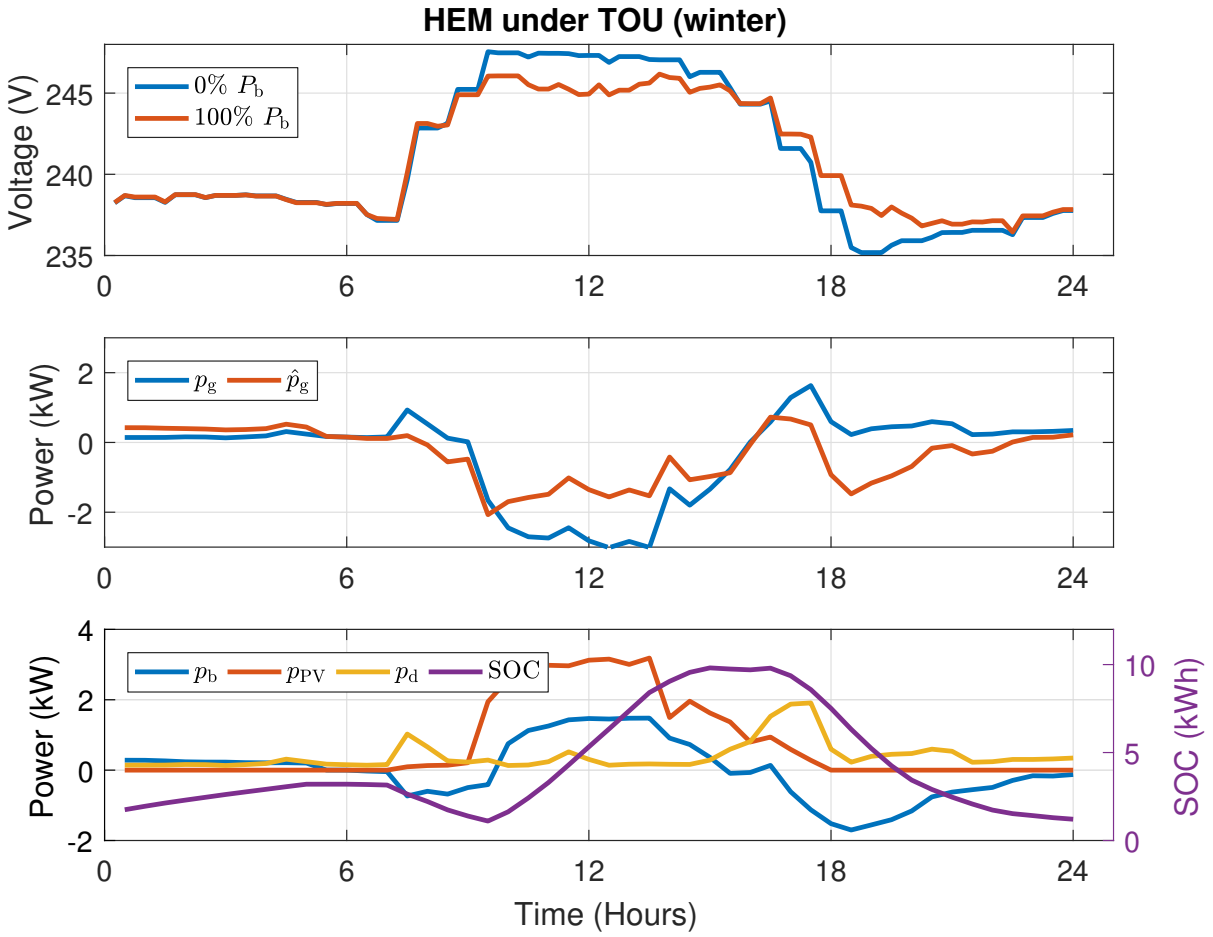

Figure 3.5: Voltage profiles (top), grid power (p_g and $\hat{p}_g$ denote grid power with and without ESS, respectively) (middle), ESS scheduling (p_b), PV (p_{PV}), demand (p_d), and the SOC (bottom) of a customer with 5.5kW PV and 9.8kWh ESS on AUS 2 on a particular winter day, with 100% P_{PV}.

because the ESS switches to discharging at 5:30pm, which leads to a decreasing SOC from 5 to 5:30pm.

In addition, longer feeders (AUS 1) experience larger voltage drops, and hence, the rate of increase in frequency of voltage problems with respect to P_{PV} is lower when compared with the smaller feeders (AUS 2 and UK). This is illustrated in Fig. 3.4, where the voltage problems increase at a slower rate towards high P_{PV} for AUS 1.

Compared to the SCM benchmark, HEM under ToU is more effective in mitigating over-voltage problems (Fig. 3.8). The SCM forces batteries to charge with excess PV output to reach the ESS's full capacity, which usually occurs before the end of the high solar generation time period. Due to this, batteries fail to consistently reduce voltage problems across the entire PV

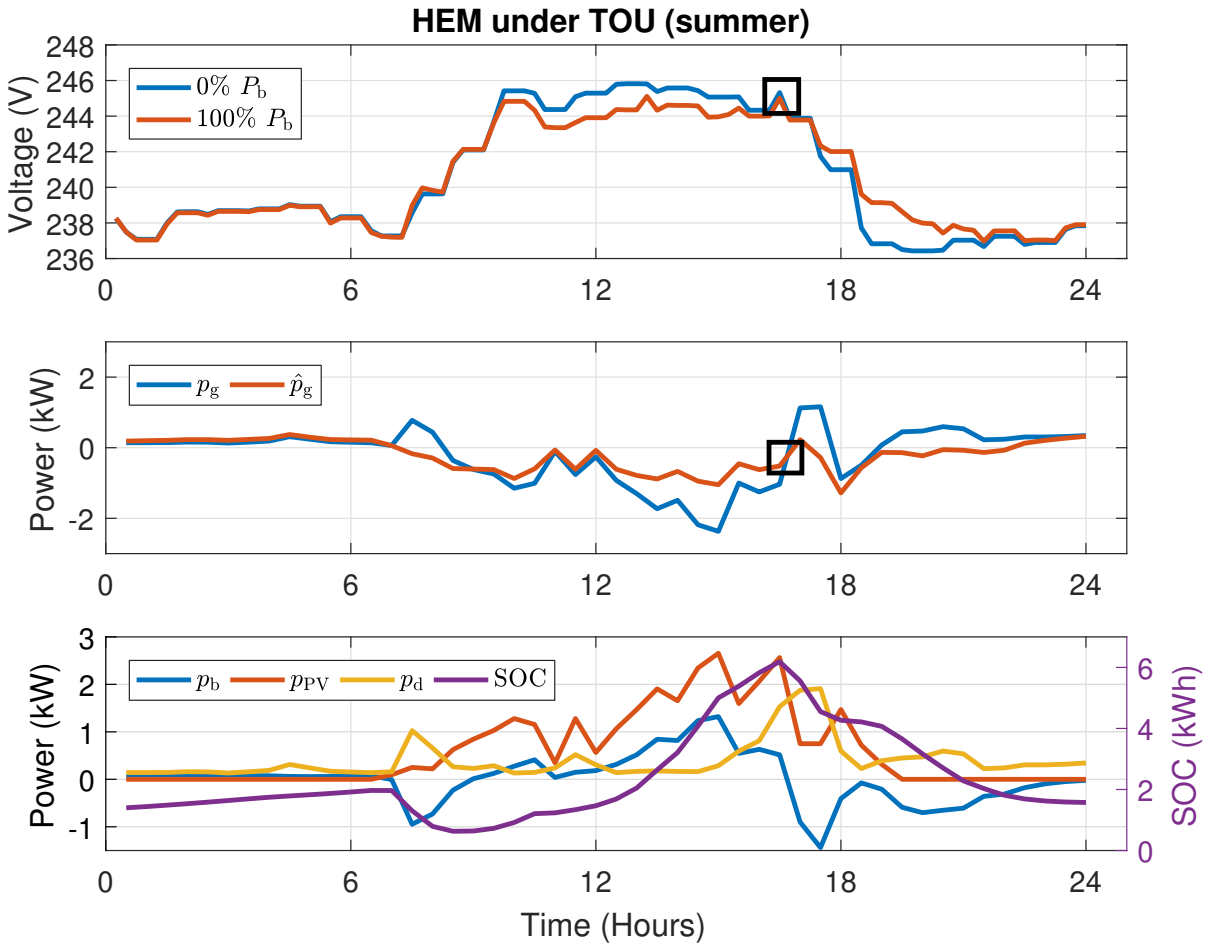

Figure 3.6: Voltage profiles (top), grid power profiles (middle), ESS scheduling, PV, demand and the SOC (bottom) of a customer with 3kW PV and 6.5kWh ESS installed on AUS 2 on a particular summer day, assuming 100% P_{PV}.

generation period. This can be seen in Fig. 3.7, where the ESS reaches its full capacity at 3pm (purple curve). As a result, all excess solar generation after 3pm is exported to the grid, as illustrated by the section where $\hat{p}_g$ overlaps p_g, keeping the voltage at a high level between 3 and 6pm. On the other hand, the HEM under ToU considers the price of electricity, which is an indication of the timely demand and PV generation. In this method (Fig. 3.6), the charging profile (blue curve in the bottom plot) is more evenly distributed throughout the PV generation period, hence a more consistent reduction of the problems is expected. Overall, ESS operation via HEM under TOU is noticeably more effective than SCM. However, both strategies, when applied under an uncoordinated setting, are far from a panacea for voltage problems on distribution feeders.

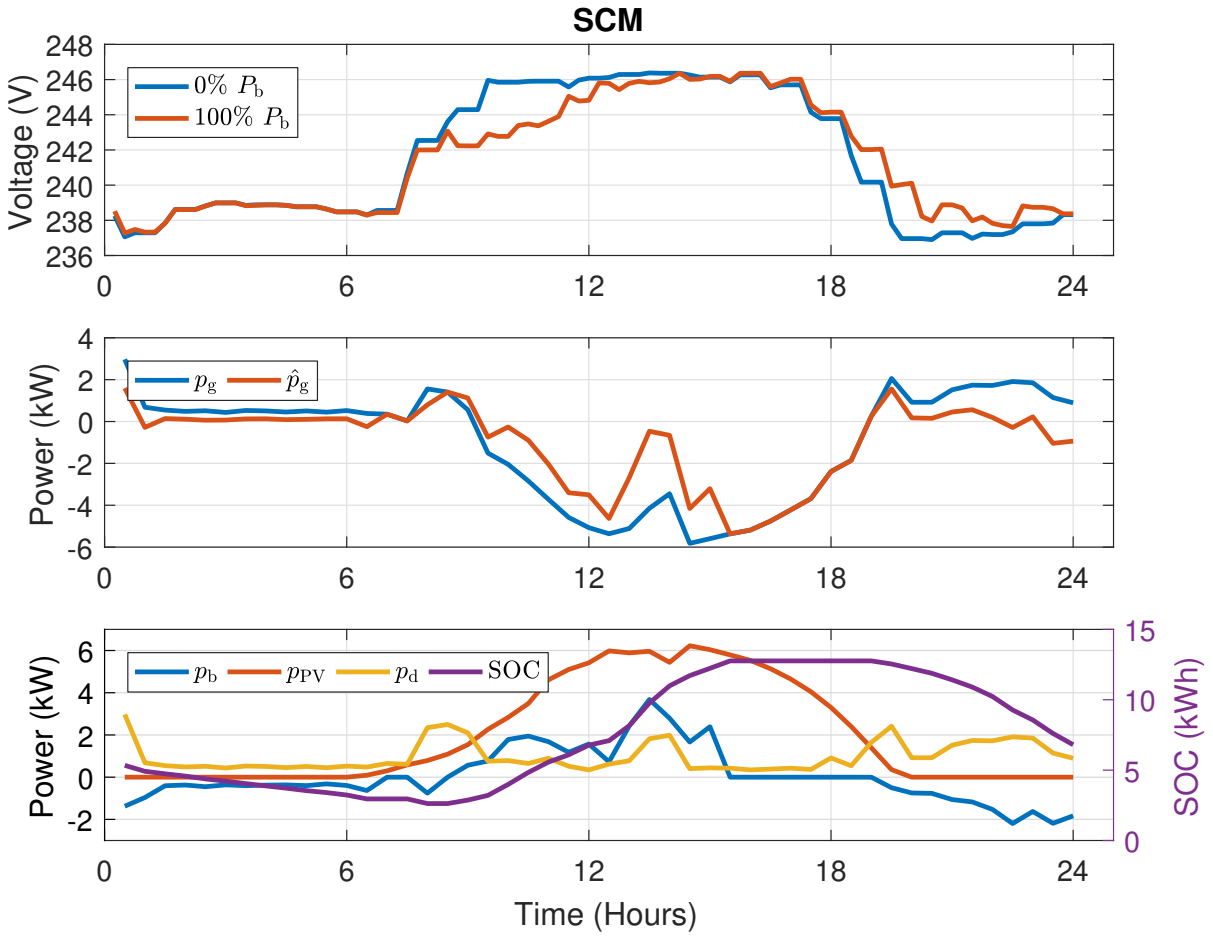

Figure 3.7: Voltage profiles (top), grid power profiles (middle), ESS scheduling, PV, demand and the SOC (bottom) of a customer with 7kW PV and 14kWh ESS installed on AUS 2 on a particular summer day, assuming 100% P_{PV}.

3.5.5 Thermal Problems

This subsection evaluates the occurrence of thermal problems across all test feeders. The transformer loading drops between 0% and 40% P_{PV} for all test feeders, as illustrated by Fig. 3.4, row two. Within this interval, all solar generation is consumed by demand. However, with greater P_{PV} (more than 40%), excess solar generation is exported to the grid, accumulating at the feeder head and increasing the transformer loading level. All test feeders follow these trends with the turning point at roughly 40%. Before this point, PV systems alone helps in transformer loading reduction. Additionally, the loading levels are higher for longer feeders (AUS 1), as well as the feeders with lower transformer capacity (UK).

Batteries reduce the transformer loading levels by charging with solar generation, and then

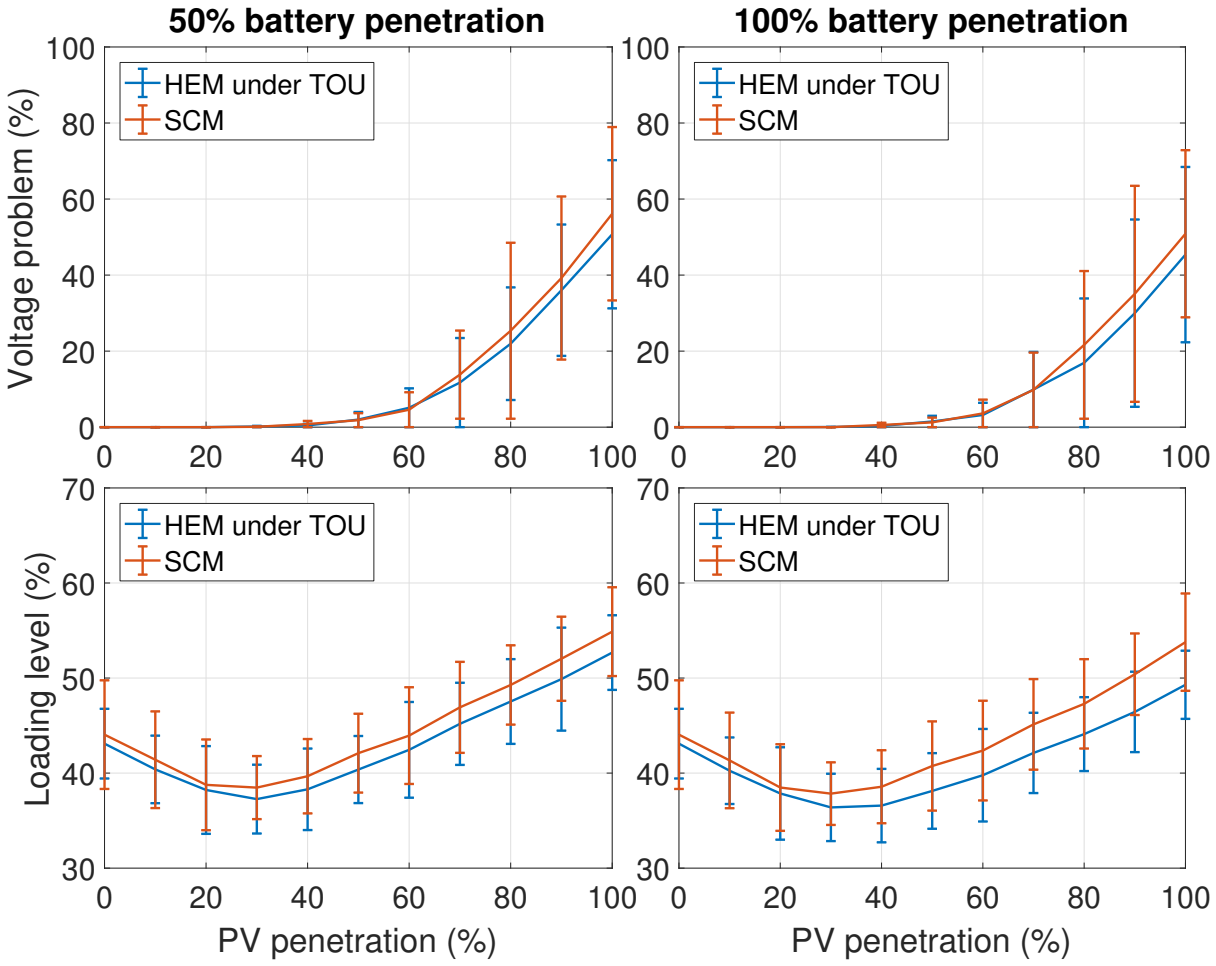

Figure 3.8: Comparisons between HEM under ToU and SCM on AUS 2.

discharge during peak periods. They become more effective as both PV and ESS capacities increase after 40% P_{PV}. For example, in AUS 1 (Fig. 3.4, row two), a 5% reduction in thermal loading is achieved at 40% P_{PV}, this proportion increases to 20% at 100% P_{PV}. In contrast to voltage problem reduction, HEM under ToU is more effective on longer feeders (AUS 1) that have higher ESS capacities for charging with excess PV generation. Compared to the benchmark, the HEM under ToU is more effective in thermal loading reduction, as seen in Fig. 3.8. This is because the SCM forces the ESS to charge to its full capacity before the end of the PV generation period, as explained previously for voltage problem reduction.

3.5.6 Phase Unbalance

This subsection presents the impacts on the voltage unbalance factor, with the results shown in Fig. 3.4, row three. Increasing P_{PV} can amplify phase unbalance. Using AUS 1 as an example, when P_{PV} on the feeder is low, typically between 0% and 40%, solar generation alone helps reduce the phase unbalance. When P_{PV} is greater than 40%, unused solar generation is exported to the grid, and hence, increasing the phase unbalance. In this case, the unbalance is improved by charging the ESS with excess solar generation. Specifically, the voltage unbalance factor for AUS 1 is reduced from 1.6% to 1.2% at 100% P_{PV}. PV and ESS are shown to mitigate cases of high unbalance, as on AUS 1; while the impacts are less pronounced for the other test feeders (AUS 2 and UK) as they are rather balanced to begin with. Overall, the improvement on phase unbalance for either the HEM under ToU or the SCM is limited.

3.5.7 Real-World Applications

In real-world applications of DER deployments and investments, MC analysis is typically required to capture the network uncertainties, including load behaviour, sizing and placement of DER. Such probabilistic assessments, especially for flexible resources including ESS, electric vehicles and loads with thermal inertia often require solving optimization within each MC run to determine their operational profiles, as demonstrated in this work for the deployment of residential PV-battery systems. This is clearly computationally prohibitive. In addition, MC analysis requires a large pool of statistically-representative demand and PV profiles to sample from. These data are generally not available on distribution level and thus, requires to be synthesised. The proposed framework overcomes these knowledge gaps and enables these applications by significantly reducing the computation time required for running MC optimal power flow analysis.

Using PV-battery systems as an example, the proposed framework used to determine the reduction in transformer loading level and over-loading cables can be fitted in the MC simulations underpinned by a financial assessment, such as real options valuation.

Finally, it should be noted that the voltage used at the transformer bus is fixed at 11kV because the upstream network has not been included in the model. The level of this voltage depends on what is happening on the primary side of the transformer, which can affect the voltage on the distribution network. Specifically, MV-LV integrated networks should be considered to study the impact of PV generation on both voltage levels and to understand the extent to which residential ESS can mitigate technical problems across LV and MV networks.

3.6 Summary

In LV distribution networks, behind-the-meter DER have the potential to either mitigate or exacerbate existing network issues like thermal and voltage problems. This is however, dependent on how customers schedule their DER and in general, on the DER penetration level. This chapter demonstrated the efficacy of the probabilistic impact assessment model by studying the impact of PV-battery system on LV distribution networks. Particularly, the proposed model incorporated HEM operational decisions within the MC time series power flow analysis following a three-step process. First, using available smart meter data, I used a Bayesian nonparametric model to generate statistically-representative synthetic demand and PV profiles. Second, a policy function approximation that emulates ESS scheduling decisions was used to make the simulation of optimization-based HEM feasible within the MC framework. Third, I completed a comprehensive PV hosting capacity assessment using a probabilistic power flow analysis to study the impact of PV-battery systems on distribution networks. The results showed that the PFA reduces the time needed to compute ESS schedules by more than 95%, which made it feasible to incorporate DER scheduling in a MC framework. The results indicated that uncoordinated PV-battery systems have limited beneficial impact on LV networks, which goes against the conjecture that ESS scheduling will serendipitously mitigate the technical problems induced by high PV penetration. Perhaps surprisingly, the inclusion of ToU tariffs in the HEM problem only marginally affects the peak demand compared to SCM, which goes to show that at very high penetration levels, DER scheduling needs to be coordinated by a distribution system operator [175–177].

Chapter 4

Multi-Stage Compound Real Options Framework

After presenting the probabilistic impact assessment framework that evaluates the technical benefits of distribution network resources (DER) on distribution networks in Chapter 3. Chapter 4 develops a novel multi-stage real options valuation (ROV) framework that can be used to evaluate the investments in DER. To showcase the characteristics of this framework, this chapter designs an optimal strategy for distribution network service providers (DNSP) to provide incentives to support the investment in residential PV-battery systems for additional grid supply during peak demand periods. The options considered in this investment include the options to defer and expand, where the option to expand is the preceding option after the option to defer has been executed. The uncertainties associated with these options are the growing peak demand, varying diesel fuel price, and the declining cost of PV-battery technology.

Using this case study, this chapter demonstrates the use of ROV for deriving the optimal strategy for a distribution network investment. Although ROV based on the least square Monte Carlo (LSMC) method has already been used in the evaluation of network investments, this is the first time that the usefulness of these techniques has been shown for assessing the investment value of customer-owned PV-battery systems in particular, and for distribution investments in general.

This study assumes the DNSP to cover 70% of the investment cost for each PV-battery intallation. In Australia and some other jurisdictions, asset ring-fencing regulations mean that these PV-battery systems cannot be owned by (regulated) DNSP if they are also used for supplying energy and services to contestable markets. However, to promote the use of this

technology, DNSPs may provide incentives to cover a large proportion of PV-battery procurement and installation cost, and in this way, they can effectively invest in these assets. Due to these reasons, this work sets a high percentage 70% for this case study to promote the PV-battery investment. Note that these percentages are indicative figures to demonstrate the use of the methodology. DNSPs are free to decide these figures as they feel appropriate in practice and context.

The rest of the chapter is organised as follows. Section 4.1 explains the LSMC approach which is used for valuing the managerial flexibility. Section 4.2 describes the costs and benefits analysis of the PV-battery investment, and presents the stochastic modeling of future uncertainties including power demand growth, varying diesel fuel price, and the declining cost of PV-battery systems. The outcomes are evaluated in Section 4.3. Finally, Section 4.4 draws conclusions.

4.1 Real Options Valuation

The traditional NPV method fails to appraise an investment under uncertainties and in the presence of contingency, as it considers managerial flexibility as a passive factor and attains only deterministic investment decisions. In contrast, ROV recognises the benefits of contingency and includes this as an active entity in its calculation, which potentially changes the value of the investment [14].

In terms of subsidising residential PV-battery investments in distribution networks, the framework identifies two interacting options, which are:

- The option to *defer* the PV-battery investment in the first decision period; and
- The option to *expand* this investment in the second decision period.

The option to expand is a subsequent option, which is only considered after the option to defer is executed. Given this, the value of the deferral option is also dependent on this subsequent option. The proposed framework derives the optimal investment strategy subject to these options by quantitatively taking into account the uncertainties and the flexibility of making decisions contingent to unfolding information.

The uncertainties considered in this work are:

- Growing peak power demand which decides the capacity of the PV-battery investment, as well as diesel generator operational cost;
- Varying diesel price that determines the cost of diesel procurement; and

- The declining cost of PV-battery technology.

These uncertainties are chosen as the state variables to the ROV because their future projections affect the behaviour of the cash flow, and the stochastic variations provide opportunities for a DNSP to increase the investment value by making decisions contingent on their realisations.

For multi-stage compound options valuation, it is needed to determine the value of the subsequent options (the option to expand), and incorporate this value when valuing the deferral option. In this case, the option to defer is to be executed within a 5-year decision period, $\mathcal{T}_{\text{inv}}$, while the option to expand is considered in the next 5-year decision period, $\mathcal{T}_{\text{exp}}$. The optimal investment strategy is extracted from this process. The mathematical formulation for solving compound options via the LSMC method is detailed in this section.

4.1.1 ROV with the LSMC method

To determine the optimal investment strategy subject to the compound options, the first task is to apply the LSMC method to calculate the value of the subsequent option to expand the investment, assuming that the investment has already been carried out. Specifically, this method combines a forward-looking Monte Carlo (MC) analysis for incorporating uncertainties, and a backward recursion (least square regression) for determining the value of an option [110]. The option can be executed any year from the initial year t_0 to the maturity T_{exp}. This time-span is divided in to $n \in \mathcal{N}$ intervals, whose length is 1 year.

This work assumes that there are $h \in \mathcal{H}$ options within an investment, thus, I use h and $h+1$ to represent the options to defer and expand, respectively. Given this, the investment value in year t_n considering the option to expand is denoted as $F_{h+1,t_n,S_{t_n}}$, where S_{t_n} is the state variable of the investment, including the growing power demand, varying diesel fuel price, and the declining PV-battery cost. Hence, the future discounted value of the subsequent investment option can be expressed as follows:

$$F_{h+1,t_0,S_{t_0}} = \max_{\tau \in [t_0, T_{\text{m}}]} \left\{ e^{-r(\tau - t_0)} E^*_{t_0} \left[\Pi_{h+1,\tau,S_\tau} \right] \right\}, \tag{4.1}$$

where τ is the optimal stopping time on each MC path, Π_{h+1,τ,S_τ} is the payoff for expanding the project, $E^*_{t_n}\left[\Pi_{h+1,\tau,S_\tau}\right]$ is the expectation on the information available at t_n, and r is the risk neutral discount rate.

LSMC integrates MC simulations with least square regression to accurately estimate the option value. The dynamic features of state variables are simulated by generating a set, Ω, of MC realisation paths by means of *geometric Brownian motion* (GBM). Then, the continuation

value is estimated, denoted $\Phi_{t_n,\omega,S_{t_n}}$, which is essentially an estimate of the investment value of the next time step, given a realisation $\omega \in \Omega$. This value represents the value of continuing to wait for the realisation of future random variables at each time along the ω^{th} path. By comparing $\Phi_{t_n,\omega,S_{t_n}}$ to the value of investing immediately, the optimal stopping time along each MC path is found. The process for calculating the optimal stopping times is described by the *Bellman's principle of optimality*, which is expressed as follows:

$$F_{h+1,t_n,S_{t_n}} = \max\left\{\Pi_{h+1,t_n,S_{t_n}}, \Phi_{h+1,t_n,S_{t_n}}\right\}, \tag{4.2}$$

where

$$\Phi_{h+1,t_n,S_{t_n}} = E^*_{t_n}\left[\sum_{i=n+1}^{N} e^{-r(t_i-t_n)}\Pi_{h+1,t_n,t_i,\tau}\right]. \tag{4.3}$$

In more detail, the least square regression estimates the continuation value by regressing the discounted future investment values on a linear combination of a group of basis functions of the current state variables. Each group of the basis functions represents the payoff trajectory within a time interval, and they are used to estimate the payoff at t_{n+1} (continuation value). This process has been employed in many recent studies, which generally apply simple powers of the state variable S_{t_n} as basis functions [85], [117]. Given this, the orthonormal basis of the j^{th} state variable is defined as L_j. The optimal coefficients, $\hat{\phi}_j$, for the basis functions are obtained using (4.4).

$$\begin{aligned}\hat{\phi}_{j,t_n} = \underset{\phi_{j,t_n}}{\operatorname{argmin}}\Bigg\{ &\sum_{i=n+1}^{N} e^{-r(t_i-t_n)}\Pi_{h+1,t_i,\omega,S_{t_i}} \\ &- \sum_{j=1}^{J}\phi_{j,t_n}L_{j,\omega,S_{t_n}}\Bigg\}^2.\end{aligned} \tag{4.4}$$

The continuation value for each MC path is thus calculated by feeding the optimal coefficient $\hat{\phi}_j$ into the linear combination of the basis functions, that is:

$$\Phi_{h+1,t_n,\omega,S_{t_n}} = \sum_{j=1}^{J}\hat{\phi}_{j,t_n}L_{j,\omega,S_{t_n}}. \tag{4.5}$$

The option value is maximised along each path if the option is executed as soon as the payoff exceeds the continuation value. The optimal stopping time along each of the in-the-money paths is determined by applying Bellman's principle of optimality, given by (4.2) recursively from maturity T_{exp} to t_0. If the decision rule holds true at t_n, the stopping time τ_ω along the ω^{th} path will be updated to t_n, that is:

$$\text{if } \Phi_{h+1,t_n,\omega,S_{t_n}} \leq \Pi_{h+1,\tau,\omega,S_{t_n}}, \text{ then } \tau_\omega = t_n. \tag{4.6}$$

The optimal stopping time of each MC path τ_ω forms a unique optimal stopping time matrix, which includes the earliest investment timing for all in-the-money MC paths. Using this matrix, the option value at t_0 that considers managerial flexibility and future uncertainty is determined by the following equation:

$$F_{h+1,t_0,S_{t_0}} = \frac{1}{|\Omega|} \sum_{\omega \in \Omega} e^{-r\tau_\omega} \Pi_{h+1,\tau_\omega,S_{\tau_\omega}}. \tag{4.7}$$

Given the value of the subsequent option, to calculate the value of the option to defer the PV-battery investment, the Bellman's principle of optimality described by (4.2) becomes:

$$F_{h,t_n,S_{t_n}} = \max\left\{\Pi_{h,t_n,S_{t_n}} + F_{h+1,t_n,S_{t_n}}, \Phi_{h,t_n,S_{t_n}}\right\}, \tag{4.8}$$

where

$$\Phi_{h,t_n,S_{t_n}} = E^*_{t_n}\left[\sum_{i=n+1}^{N} e^{-r(t_i-t_n)} \sum_{l=h}^{H} \Pi_{h,t_n,t_i,\tau}\right]. \tag{4.9}$$

For the deferral option value, the continuation value, $\Phi_{h,t_n,S_{t_n}}$ is compared to the payoff of the investment, $\Pi_{h,t_n,S_{t_n}}$, plus the value of the option to expand, $F_{h+1,t_n,S_{t_n}}$. Thus, the stopping time τ_ω along the ω^{th} path is updated to t_n, if:

$$\Phi_{h,t_n,\omega,S_{t_n}} \leq \Pi_{h,t_n,\omega,S_{t_n}} + F_{h+1,t_n,\omega,S_{t_n}}. \tag{4.10}$$

ROV uses the updated decision rule in the LSMC method to calculate the deferral option value, and hence the optimal investment strategy. The accuracy of the estimation grows as the number of simulation paths and basis functions increases. The presented method can be applied to multiple subsequent options, where the payoff of the $(h+n)^{\text{th}}$ option needs to be incorporated when calculating the value of the $(h+n-1)^{\text{th}}$ option in (4.8), (4.9) and (4.10) within the LSMC approach.

4.1.2 ROV Instruction Manual

In order to demonstrate the use of the ROV, I decompose the LSMC approach and provide an instruction manual to guide through the mathematical formulations that are used to value the real options created uncertainty. The steps are listed and explained in further detail below.

- Simulate future contingencies using GBM and MC simulation.
- Enable the application of ROV by calculating the path-wise payoff of executing and expanding the investment in the two decision periods.

- Use backward induction and apply Bellman's principle of optimality at each time-step to solve the path-wise optimal stopping problem and determine the value of the subsequent option (expand).
- Incorporate the contingent decisions made for the subsequent option when solving the path-wise optimal stopping problem for the deferral option.
- Given the path-wise decisions for executing both options, calculate the option value at t_0, and hence determine the overall optimal investment strategy.

The first step is to generate Ω realisation paths of the underlying state variables $s \in \mathcal{S}$. Specifically, I incorporate GBM and and mean-reverting process to simulate future power demand, electricity price and the cost of PV-battery technology. The forward-looking MC model is described by the top diagram in Fig. 4.2. The initial node provides the option value F_{t_0} if the investment is made immediately. Following this, the decision nodes along each MC path provide an opportunity for the DNSP to make contingent decisions (delay, invest, abandon or expand), which are made based on the option values $F_{h,t_n,\omega}$ calculated via ROV upon the realisation of uncertainties.

Second, to enable the use of ROV, the future payoff cash flows of the investment is estimated by including the investment cost of additional diesel generation as monetary savings, as described by (4.13). This is because the purpose of implementing PV-battery systems is to delay and/or avoid the expensive generation investments. Meanwhile, by doing so, ROV captures the uncertainties that involve in the cost of generation such as electricity price.

Third, to value the compound options, the first step is to determine the path-wise stopping time and option value $F_{h+1,\omega}$ of the subsequent option (expand) via the LSMC approach. Then, $F_{h+1,\omega}$ is added to the payoff $\Pi_{h,t_n,\omega}$ in $\mathcal{T}_{\text{inv}}$ to calculate the optimal stopping time for the deferral option, as stated in (4.8).

Fourth, the LSMC approach uses backward induction to iterate through all realisation paths of the state variables, and assigns an option value to each decision node. The option values represent the profit given by making a contingent decision to delay or execute the investment in each time-interval. This process is visualised by the tree model shown in Fig. 4.2.

In more detail, each option value $F_{t_n,\omega}$ is the maximum between the continuation value $\Phi_{t_n,\omega}$ and the payoff to invest immediately $\Pi_{t_n,\omega}$. This decision rule is formally expressed by the *Bellman's principal of optimality* in (4.2) and it is recursively applied throughout all realisation paths, as illustrated in the bottom diagram in Fig. 4.2. The path-wise optimal investment timing is decided by the first payoff that is greater than the continuation value. Solving the path-wise

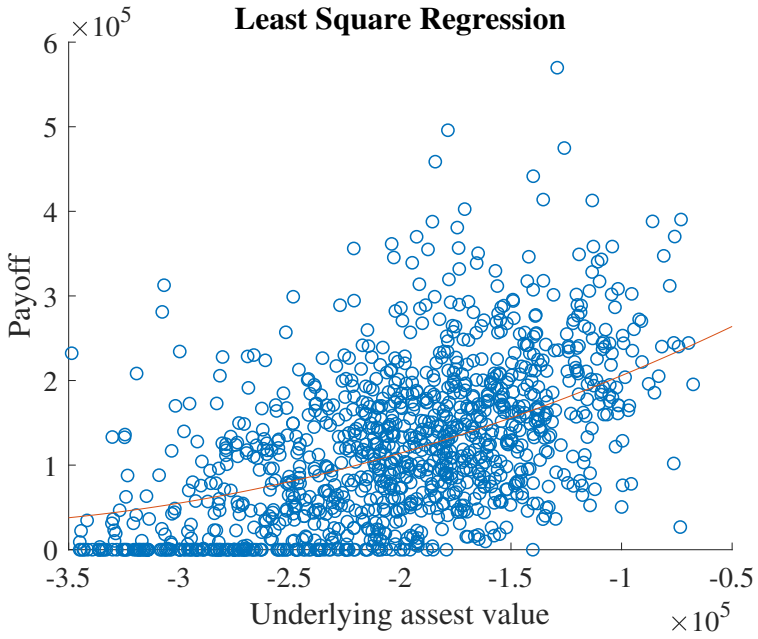

Figure 4.1: Least square regression in Year 5.

optimal stopping problem forms an optimal investment timing matrix that provides the probability of executing the investment in each year. The year with the greatest frequency hints for the most likely investment year.

The continuation value in each node is essentially the expected payoff in the next time-interval. It is estimated using an m^{th} degree polynomial that is formulated as a linear combination of a group of basis functions of the current state variables. Each polynomial function draws the payoff trajectory, which is also the best fitting curve to the current set of state variables. The coefficients ϕ for each trajectory are determined using least square regression stated in (4.4) and (4.5). The degree m of the polynomial is dependent on the nature of the problem, but generally simple powers are applied. This work uses a second degree polynomial function as shown in (4.11), and an example of the trajectory described by this function in Year 5 is illustrated in Fig. 4.1.

$$\Phi_{t_n,\omega,\mathcal{S}} = \phi_2 s^2 + \phi_1 s + \phi_0. \tag{4.11}$$

Finally, the option values calculated in all decision nodes are considered to determine the option value for the current year, F_{t_0} using (4.7). This is essentially an average across all future discounted option values given by the realisation of uncertainty. If F_{t_0} is positive and greater than the investment value in Year 0, the ROV suggests to delay the investment.

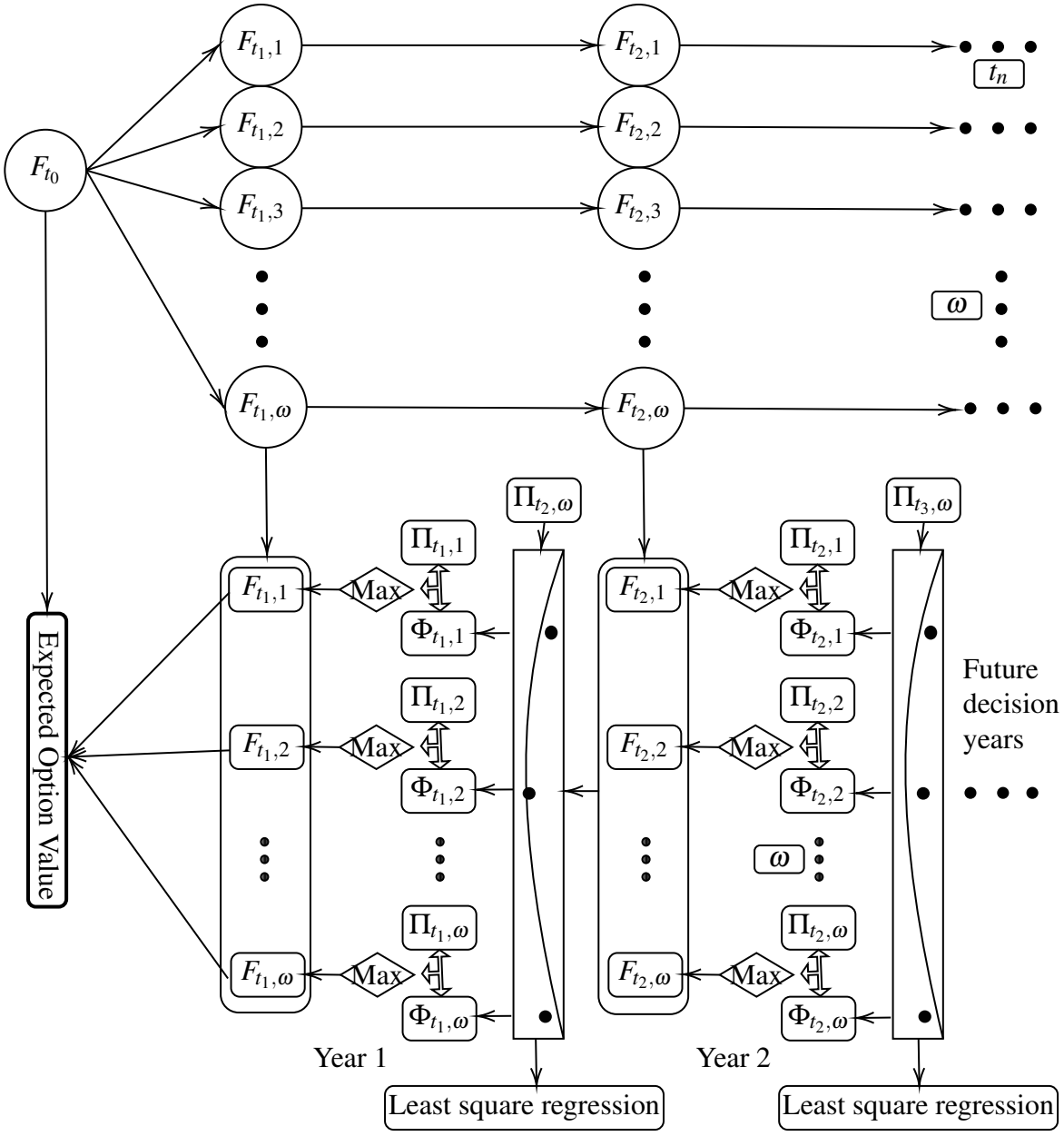

Figure 4.2: Architecture of the LSMC approach. The top figure shows the forward MC model which captures the variations of state variables, and each decision node is given an option value $F_{t_n,\omega}$. The bottom figure uses Years 1 and 2 as an example to demonstrate how backward induction is used, where $\Pi_{t_n,\omega}$ is the payoff and $\Phi_{t_n,\omega}$ is the continuation value. In the Least square regression box, the best-fitting curve is found based on $\Pi_{t_{n+1},\omega}$, this curve is used to estimate the continuation value at t_n.

4.2 Costs and Benefits Analysis

To carry out the financial assessment of the PV-battery investment, it is needed to determine the cost and payoff for carrying out and expanding the investment, respectively. These values are used as the inputs to the ROV to value the compound options, and therefore the corresponding optimal investment strategy. The valuation algorithm is described in Algorithm 3, and discussed in more detail below.

Specifically, the cost of the investment is calculated via the traditional NPV method, and hence the payoff ($\Pi_{h,t_n,\omega}$) from replacing the diesel generator investment with the PV-battery investment during the first 5-year decision period, and the payoff ($\Pi_{h+1,t_n,\omega}$) from expanding this investment in the next 5-year decision period. This period is chosen so that the DNSP can fully capture the benefit of delaying the PV-battery investment, while carrying out the appropriate investment for peak demand support within a relatively short time-span. The detailed formulation is described in this section. Then, I demonstrate the modelling process of future uncertainties including (i) growing power demand, (ii) varying diesel fuel price, and (iii) declining cost of the PV-battery technology.

4.2.1 NPV Calculation

The energy delivered through the transformer that is over the thermal limit for each day between 2014 and 2017 is calculated from the aggregated historical electricity usage data from the Top Ryde substation (132/33), which has a thermal limit of 35MVA. These data, provided by Ausgrid[1], have a 15-minute resolution. The future growth in power demand that is over the thermal limit is then simulated. I take the average across the simulated data for each future decision year, and use it as the aggregated installed capacity for the PV systems and diesel generator, denoted as $E^{\text{Cap}}_{t_n,\omega}$. The size of the battery energy storage system is decided based on the PV size. In Australia, 2kWh of battery is typically used per 1kW of PV installed.

The future costs of the PV-battery investment ($c^{\text{PV}}_{t_n,\omega}$) and diesel generator investment ($c^{\text{G}}_{t_n,\omega}$) need to be discounted via the traditional NPV method as follows before calculating the payoffs:

$$NPV = \sum_{t=1}^{T} \frac{c_t}{(1+r)^t}. \tag{4.12}$$

where r is the risk-free discount rate[2].

[1] a DNSP in New South Wales, Australia; see `https://www.ausgrid.com.au/Industry/Innovation-and-research/Data-to-share/Distribution-zone-substation-data`.

[2] This work assumes that the future costs are risk free. Thus, this value is fixed to a constant (0.06).

Table 4.1: Cost specifications.

Items	Cost
PV-battery system, $c^{\mathrm{PV}}_{t_n,\omega}$	Risk neutral valuation
Peak demand, $E^{\mathrm{Cap}}_{t_n,\omega}$	GBM
Diesel fuel, $c^{\mathrm{f}}_{t_n,\omega}$	Mean-reverting process
Diesel generator cost, c^{G}	\$500k [178]
Operation and maintenance, c^{OM}	\$100k/year [178]
Transformer Step-up	\$85k
Cabling	\$90k
Civil structure for the generator	\$5k
Machinery (Forklifts, Cranes)	\$10k
Control Panels (including breakers)	\$25k
Contingencies	\$100k

In more detail, DNSP is assumed to be responsible for 70% of PV-battery procurement (the rest is paid by the customers), and it is obliged to cover the cost of electricity usage over the thermal limit and is not covered by the additional generation capacity provided by PV-battery systems (denoted as $c^{\mathrm{g}}_{t_n,\omega}$). This cost occurs when the PV-battery investment is delayed or the peak demand exceeds the installed generation capacity. Thus, $\Pi_{h,t_n,\omega}$, including $c^{\mathrm{g}}_{t_n,\omega}$ is given by:

$$\Pi_{h,t_n,\omega} = \left(c^{\mathrm{PV}}_{t_n,\omega} - c^{\mathrm{G}}\right) E^{\mathrm{Cap}}_{t_n,\omega} - c^{\mathrm{OM}} + c^{\mathrm{g}}_{t_n,\omega}, \tag{4.13}$$

where $c^{\mathrm{PV}}_{t_n,\omega}$ and c^{G} are the costs per 1kW for the same aggregated capacity $E^{\mathrm{Cap}}_{t_n,\omega}$, $c^{\mathrm{OM}}_{h,t_n,\omega}$ is the maintenance and operation cost, while $c^{\mathrm{g}}_{t_n,\omega}$ is given by:

$$c^{\mathrm{g}}_{t_n,\omega} = c^{\mathrm{f}}_{t_n,\omega} \Delta E^{\mathrm{g}}_{t_n,\omega}, \tag{4.14}$$

where $c^{\mathrm{f}}_{t_n,\omega}$ is the diesel price, and $\Delta E^{\mathrm{g}}_{t_n,\omega}$ is the electricity usage over the thermal limit and fails to be covered by PV-battery systems.

The aggregated capacity of the PV-battery systems installed in the first decision period does not cover the power demand growth in the future, which leaves an open question as to whether the expansion is necessary. If the option to expand is abandoned, the future power demand growth will be covered by installing an additional diesel generator.

In more detail, the payoff for expanding the PV-battery investment, $\Pi_{h+1,t_n,\omega}$, assuming that the investment has already been executed, is the difference between the cost of installing additional PV-battery systems to cover the peak demand growth after the first decision period, and the cost of expanding the diesel generation investment for the same amount of aggregated generation capacity, $E^{\mathrm{Cap}}_{h+1,t_n,\omega}$; that is:

$$\Pi_{h+1,t_n,\omega} = \left(c^{\mathrm{PV}}_{t_n,\omega} - c^{\mathrm{G}}\right) E^{\mathrm{Cap}}_{h+1,t_n,\omega} - c^{\mathrm{OM}}_{h+1,t_n,\omega} + c^{\mathrm{g}}_{t_n,\omega}. \tag{4.15}$$

Algorithm 3 Real options valuation algorithm

Generate Ω realisation paths of ΔE^{Cap}, c^{f} and c^{PV}.
for ω = 1:Ω **do**
  for year = 6:10 **do**
    Calculate Π_{h+1}.
  end for
end for
for $t = T_{\text{exp}}$:-1:t_0 **do**
  Calculate Φ_{h+1} via LSMC for all in-the-money paths.
  for ω = 1:Ω **do**
    if $\Pi >= \Phi_{h+1}(t, S_t(\omega))$ **then**
      Update τ = t.
    end if
  end for
end for
Calculate the F_{h+1} using (4.7).
Repeat the steps 3 to 6 to calculate Π_h from Years 1 to 5
for $t = T_{\text{inv}}$:-1:t_0 **do**
  Calculate Φ_h via LSMC for all in-the-money paths.
  for ω = 1:Ω **do**
    Update the decision rule to (4.10).
    if $\Pi + F_{h+1} >= \Phi_{\text{h}}(t, S_t(\omega))$ **then**
      Update τ = t.
    end if
  end for
end for
Calculate F_h and extract the optimal investment strategy.

This work assumes that the DNSP is in charge of electricity distribution, network planning, monitoring and maintenance. The primary source of revenue for the DNSP is from delivering the energy produced by the diesel generator. This revenue is given by the network customers as part of their electricity bills. Cash outflows in this investment include system procurement, installation, maintenance and operation costs for the generator.

4.2.2 Modelling of Future Uncertainties

This subsection simulates the random variables used in the payoff calculation, including growing power demand that exceeds the thermal limit ($\Delta E^{\text{Cap}}_{t_n,\omega}$), cost of diesel fuel ($c^{\text{f}}_{t_n,\omega}$), and the declining cost of PV-battery technology ($c^{\text{PV}}_{t_n,\omega}$). Specifically, the growing peak demand that exceeds the thermal limit ($\Delta E^{\text{Cap}}_{t_n,\omega}$) is governed by the GBM and simulated using MC analysis. GBM is used in this case as the stochastic peak demand evolution over time is assumed to be captured by a GBM process. This assumption relies on the fact that the increments of process in the GBM show the Markov property, which assumes that any future change is independent from the previous values, while the variable remains positive throughout the process [107]. The GBM for

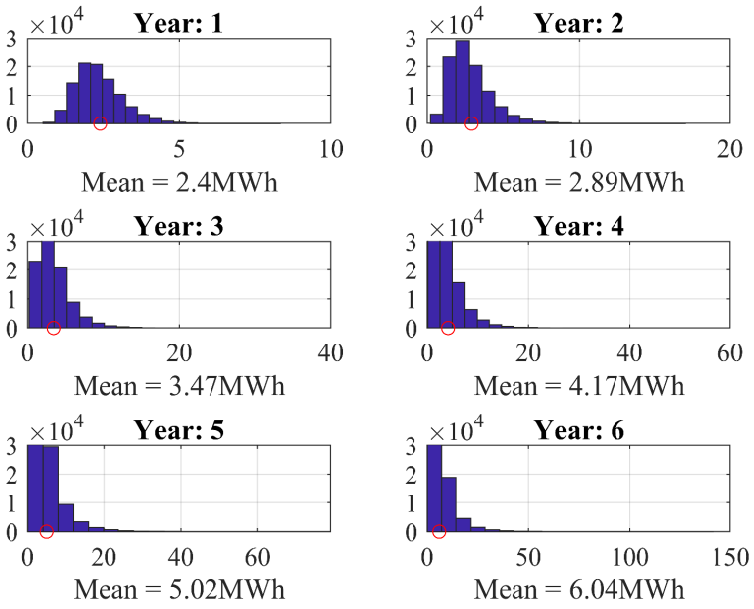

Figure 4.3: Distribution of simulated average monthly growth in future peak demand that is over the transformer thermal limit via GBM (drift = 1.5% and volatility = 9.8%)

the growing peak demand is therefore described mathematically as follows:

$$dS_t^{\mathrm{d}} = \mu S_t^{\mathrm{d}} dt + \sigma S_t^{\mathrm{d}} dW_t, \tag{4.16}$$

where S_t^{d} describes the sought stochastic process of power demand, μ is the percentage drift that describes the rate of growth in the aggregated peak demand that is over the thermal limit, σ is the percentage volatility of the data, and W_t is the Wiener process that describes the stochastic component. Thus, the discretization recursion formula is given by:

$$S_{t+\Delta t}^{\mathrm{d}} = S_t^{\mathrm{d}} e^{\left(\mu - \frac{\sigma^2}{2}\right)\Delta t + \sigma dW_t}. \tag{4.17}$$

The simulation of future power demand takes the historical electricity usage data provided by Ausgrid. The future power demand is simulated for 10,000 MC paths.

On the other hand, diesel fuel price, like all the other bulk commodities such as oil, gas and metal tends to conform to its long-term mean, with stochastic shocks when unforeseen ”events” occur. Given this a mean-reverting process is used to simulate the varying diesel fuel prices; that is:

$$dS_t^{\mathrm{f}} = \beta_{\mathrm{f}}(\hat{S}^{\mathrm{f}} - S_t^{\mathrm{f}})dt + \sigma S_t^{\mathrm{f}} dW_t, \tag{4.18}$$

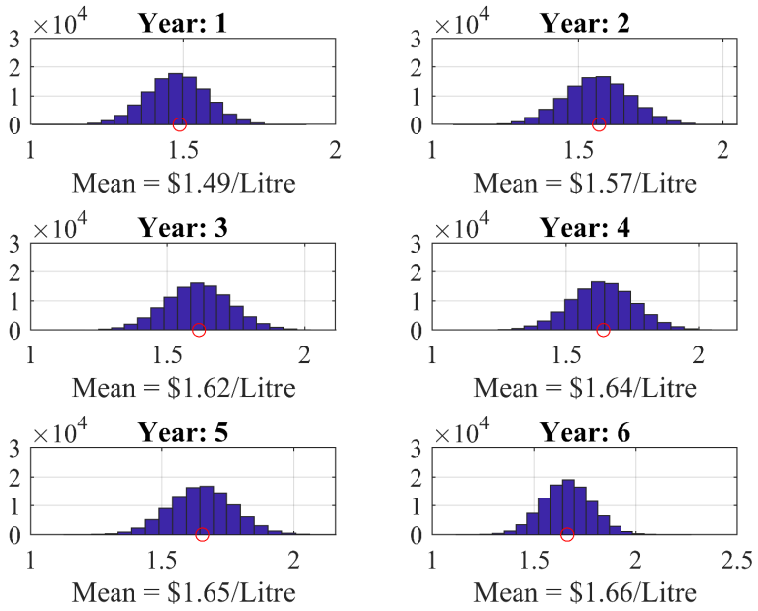

Figure 4.4: Distribution of simulated future diesel price via a mean reverting process (speed of reversion = 5%, reversion level = 2.6, volatility = 4.7%).

where S_t^{f} describes the sought stochastic process for the cost of diesel fuel, β_{f} is the speed of reversion to the mean, and $\hat{S}^{\mathrm{f}}$ is the reversion level. Thus, the discretization recursion formula is given by:

$$S_{t+\Delta t}^{\mathrm{f}} = e^{-\beta_{\mathrm{f}}\Delta t}(S_t^{\mathrm{f}} - \hat{S}^{\mathrm{f}}) + \hat{S}^{\mathrm{f}} + \sigma\varepsilon\sqrt{(1-e^{-2\beta_{\mathrm{f}}\Delta t})/2\beta_{\mathrm{f}}}\,. \tag{4.19}$$

The LSMC approach assumes to be the sample paths of costs of assets (PV-battery systems) over the relevant time horizon are simulated according to the risk-neutral measure[3]. Given this, the evolution of the cost can be described using GBM:

$$dS_t^{\mathrm{PV}} = \mu S_t^{\mathrm{PV}} dt + \sigma S_t^{\mathrm{PV}} dW_t, \tag{4.20}$$

where S_t^{PV} describes the sought stochastic process for the cost of PV-battery systems. Then, I define $dW_t = d\hat{W}_t - \frac{\mu - r}{\sigma}dt$, where $d\hat{W}_t$ is the Brownian motion under risk neutral measure and r is the risk-free rate. Substituting this to (4.20) yields the risk neutral valuation:

$$dS_t^{\mathrm{PV}} = rS_t^{\mathrm{PV}} dt + \sigma S_t^{\mathrm{PV}} d\hat{W}_t. \tag{4.21}$$

[3]This is because these costs depend crucially on their risk as investors typically demand more profit for bearing more risk. It is difficult to adjust the simulated expected values based on an investor's preference, and therefore, risk neutral measure is used.

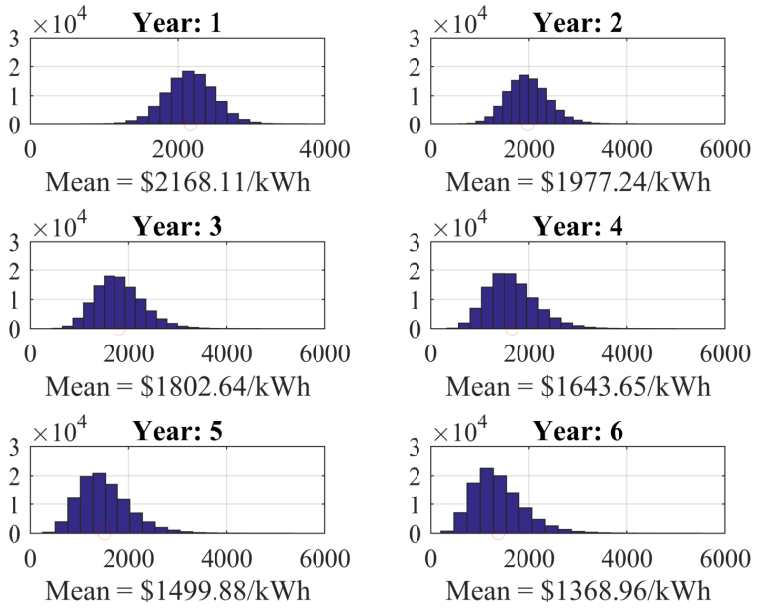

Figure 4.5: Distribution of simulated future cost of PV-battery system via risk neutral valuation (risk-free rate = 0.06, volatility = 9%)

Thus, the discretization formula becomes:

$$S^{\mathrm{PV}}_{t+\Delta t} = S^{\mathrm{PV}}_{t} e^{\left(r-\frac{\sigma^2}{2}\right)\Delta t+\sigma d\hat{W}_t}. \tag{4.22}$$

The historical PV and battery price and diesel price data are obtained from [179] and [180], respectively. The future predictions on diesel fuel cost shown in Fig. 4.4 can be supported by [181]. For brevity, in this work, only 6 years of the simulated future data are shown. It is observed that the electricity usage that is over the thermal limits, $\Delta E^{\mathrm{Cap}}_{t_n,\omega}$, and the cost of diesel fuel $c^{\mathrm{f}}_{t_n,\omega}$ increase gradually in the future, as illustrated in Fig. 4.3 and Fig. 4.4, respectively, while the cost of PV-battery $c^{\mathrm{PV}}_{t_n,\omega}$ continues to decrease (Fig. 4.5).

4.3 Results and Evaluation

This section demonstrates the use of the proposed ROV framework for distribution network investments by evaluating the PV-battery investment considering two interacting options, including (i) the option to defer in the first 5-year decision period, and (ii) the option to expand the investment in the next 5-year decision period. The subsequent option for the investment expansion can only be considered after the investment has been carried out. The option values are calculated via the LSMC approach described in Section 4.1. As previously described, the

expansion of the PV-battery investment aims to cover the further growth in the aggregated peak power demand after the first decision period.

The study period is 10 years, including the two consecutive 5-year decision periods, and the annual risk-neutral discount rate is assumed to be 6%. The diesel generator investment and PV-battery investment are thereafter referred to as P1 and P2, respectively.

The diesel generator used in this case study is the Cummins generator QSK 95 [182]. This generator has a capacity of 3MW and the cost is $500k. In addition, Several other major cost components, including a step-up transformer, cables used for grid connection, civil structure for the generator, professional fees, machinery (Forklifts and Cranes, etc), control panels (including LV and MV breakers), and a contingency cost, are summarised in Table. 4.1.

4.3.1 Diesel Generator Cash Flow Analysis

The NPV for executing P1 in Year 1 is calculated in this subsection. The capital cost of diesel generator is $600 per 1kW [178], while the future electricity generation cost is dependent on the increase in the aggregated peak demand and diesel fuel price simulated using the GBM in Section 4.2.

The average NPV of P1 decreases from –$900k in Year 1 to greater than –$2M by the end of the 10-year study period, as illustrated by Fig. 4.6, left. The cost growth mainly comes from electricity production[4], generator operation and maintenance. Specifically, the cost of generator operation and maintenance is fixed every year, as indicated by Table. 1. The magnitude of the outliers outside the boxes, especially below, increases significantly with respect to time, showing the increasing risks for large investment costs in the case of fast-growing peak demand and diesel fuel cost. This work uses the NPV of P1 in Year 10 in (4.13) to calculate the payoff, $\Pi_{h,t_n,\omega}$, of P2.

4.3.2 PV-Battery Cash Flow Analysis

Compared to the NPV of P1, the average NPV of P2 in Year 1 is roughly –$1.6M, which decreases to just under –$2M in Year 10, assuming P2 is executed in Year 1, as shown in Fig. 4.6, right. The reduction in the NPV is less pronounced because PV-battery systems rely on cost-free solar power, and only the maintenance cost is committed to this investment during the study period.

[4]Per litre of diesel fuel can be used to generate $10kWh of energy, the future cost of diesel fuel has been projected and shown in Fig. 4.4

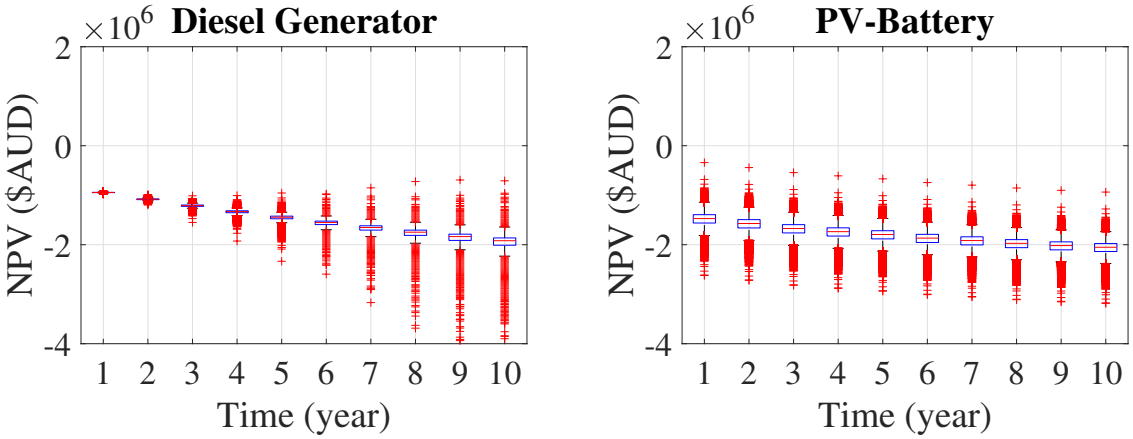

Figure 4.6: Costs for executing the diesel generator investment (left) and the PV-battery investment in Year 1 (right).

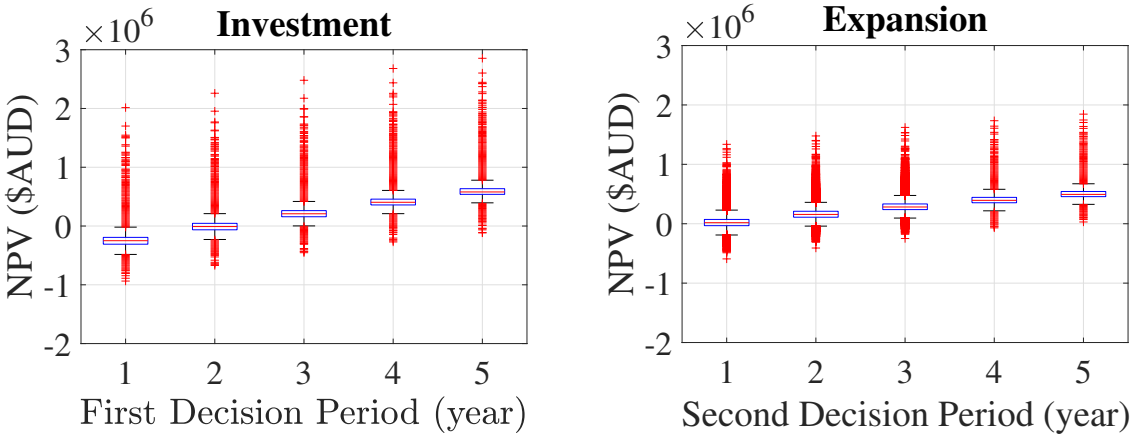

Figure 4.7: Payoffs for executing the PV-battery investment in each of the decision years (left), and for expanding the investment in each of the decision years (right).

Based on the traditional NPV analysis, P2 is not profitable as the NPV in all MC paths are negative, as shown in Fig. 4.6, right, and hence this investment is abandoned. However, ROV creates an opportunity to make profits of this investment by postponing it to a time when the uncertainties turn favourable, and the trade-off to this is the cost to cover the electricity usage that is over the transformer thermal limit, given that neither P1 nor P2 is implemented until the optimal investment timing.

The future payoffs of investing and expanding the PV-battery investment needed for the LSMC approach are shown in Fig. 4.7. Specifically, these costs are calculated using (4.13) and (4.15), respectively, where the cost parameters are shown in Table .4.1 and the simulation of the state variables is described in Section 4.2.2. This work uses the NPV of P1 as the monetary

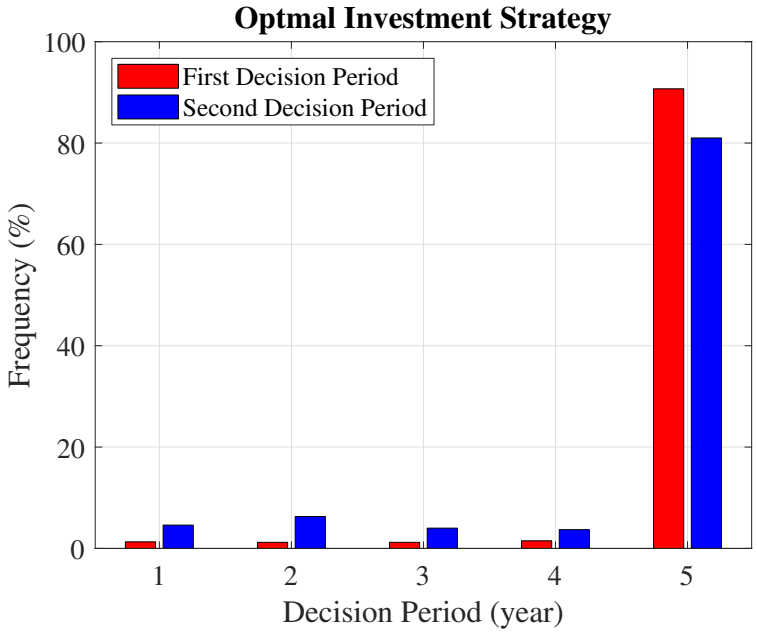

Figure 4.8: Frequency distribution of optimal investment timing for the option to defer the investment in the first decision period, and the option to expand the investment in the second decision period (benchmark).

Table 4.2: ROV results under different scenarios - part I.

Scenario	Description	Year 1 (%)	Year 2 (%)	Year 3 (%)	Year 4 (%)	Year 5 (%)
S1	Benchmark	1.2	1.2	2.3	3.4	90
S2	$\mu_{\mathrm{d}} = 3\%$	8.7	3.1	2.9	5.4	77
S3	$\sigma_{\mathrm{d}} = 20\%$	4.5	4.8	5.5	4.3	80
S4	$\beta_{\mathrm{f}} = 15\%$	2.2	0.5	0.3	0.4	97
S5	$\sigma_{\mathrm{f}} = 20\%$	0.3	6.1	4.8	5.0	84
S6	$\sigma_{\mathrm{pv}} = 20\%$	1.7	1.6	1.7	1.9	92

savings for the NPV calculation of P2. Note that the cash flows calculated in each future year in Fig. 4.7 consider the entire life-cycle of the PV-battery system. Observe that the payoffs for both investing in and expanding in the future gradually increase throughout the decision periods due to the declining cost of the advancing technology. Thus, there exists an opportunity to make the investment profitable in the future via ROV.

4.3.3 PV-Battery Investment: ROV Analysis

The opportunity values provided by future uncertainties are calculated using the proposed ROV framework. Specifically, the ROV suggests to delay the investment and wait for the market conditions to turn favourable if the deferral option value is positive and greater than the payoff

Table 4.3: ROV results under different scenarios - part II.

Scenario	Description	Standard NPV (k$)	ROV (k$)	Flexible NPV (k$)
S1	Benchmark	–240	660	420
S2	$\mu_{\mathrm{d}} = 3\%$	–110	740	630
S3	$\sigma_{\mathrm{d}} = 20\%$	–240	600	360
S4	$\beta_{\mathrm{f}} = 15\%$	–230	690	460
S5	$\sigma_{\mathrm{f}} = 20\%$	–250	640	390
S6	$\sigma_{\mathrm{pv}} = 20\%$	–240	720	480

calculated via the NPV method, and the optimal investment timing is when the payoff exceeds this option value. The flexible investment value is equal to the sum of the option value and the payoff calculated by the NPV analysis.

The LSMC approach for calculating the value of the compound options and the corresponding optimal investment strategies are detailed in Section 4.1: (i) use the payoff ($\Pi_{h+1,t_n,\omega}$) of expanding P2 to calculate the continuation value, $\Phi_{h+1,t_n,\omega}$, via least square regression, (ii) compare the payoff with continuation value for each year during the decision period using (4.6), the optimal timing to execute the investment on the ω^{th} path is when the payoff is greater than the continuation value for the first time, (iii) calculate the investment value considering managerial flexibility using (4.7), and (iv) incorporate the value of the option to expand, F_{h+1}, in the LSMC method to determine the deferral option value, F_h, which helps the DNSP to make a contingent decision for the present year. The options are abandoned in the case of a negative payoff to reduce the computation time.

The average payoff of the investment from the standard NPV analysis is –$240k, as observed in Fig. 4.7, Investment. The value of the compound options calculated using (4.7) is $660k. Therefore, the flexible investment value in this case equals $420k ($660k + (– $240k)), as indicated in Table. 4.3, Benchmark. In this scenario, the drift parameter and volatility of the state variables are given in Table. 4.1. Based on the standard NPV approach, the investment is abandoned immediately because the payoff is negative. However, ROV sees potential hidden within the state variables, and discovers a possible additional benefit of $660k if the investment is postponed to a later year. Given this, the contingent decision in the present year is to delay the PV-battery investment.

To predict the optimal investment timing, the LSMC computes the optimal stopping timing (τ_ω) for each MC path, this extracts the frequency distribution of τ_ω, for the deferral option, as shown in Fig. 4.8, in red. The optimal timing of the investment is indicated by the greatest frequency. Thus, P2 is delayed to Year 5 (90%), despite the fact that the DNSP needs to pay for the additional grid supply that covers the future growth in peak demand, $c^{\mathrm{g}}_{t_n,\omega}$, incurred by

postponing P2.

On the other hand, the option to expand calculated using (4.7) in the second decision period is worth $330k, while the payoff is only $30k in Year 6, as seen in Fig. 4.7, Expansion. In this case, the investment value is already positive before considering the flexibility, thus, based on the NPV analysis, the investment is expanded immediately. However, the ROV sees the potential for the market conditions to become favourable in the future, and hence suggests to delay the expansion. Specifically, based on the frequency distribution extracted from LSMC, as shown in Fig. 4.8, blue, the option to expand is likely to be executed in Year 5 in the second decision period, with a 81% possibility. The future investment possibility given in each year is only an estimate based on the current prediction on future uncertainty. In fact, DNSPs need to repeat ROV in every future year to re-evaluate the options available to make a contingent decision and update future investment possibilities (Fig. 4.7). Overall, these results differentiate ROV from the standard cash flow analysis as ROV accounts for managerial flexibility and promotes/helps DNSPs make contingent decisions in each decision year to maximise the investment value.

If the deferral option is considered independent of the option to expand, the deferral option value is reduced from $660k to only $350k, while the optimal investment timing is kept in Year 5 with a slight decrease in the frequency (84%), compared to Fig. 4.8. Eliminating the option to expand in this calculation means that there is less managerial flexibility considered, leading to a smaller option value. This result shows that properly establish the relation between interacting options leads to a greater option value, and hence significantly increases the investment value.

To summarise, the ROV framework accounts for the opportunity values from executing options under future uncertainties, and properly considers the interaction between these options. By doing so, it reverses the decisions drawn from the traditional NPV analysis. Specifically, the fast-declining PV-battery cost is the main driver to the deferral of the investment. This case serves as the benchmark in this work.

4.3.4 Sensitivity Analysis

The optimal investment strategy can be affected by altering the state variables, including growing power demand, varying diesel fuel price and the declining costs of PV-battery systems. Thus, it is useful to evaluate the sensitivity of the option value and optimal investment timing subject to changing scenarios characterised by these variables. The ROV results are summarised in Table. 4.2 and Table. 4.3.

Overall speaking, increasing the growth rate of future peak demand (S2) leads to a greater operational cost for the diesel generator, and thus a greater standard NPV if the PV-battery

investment is executed in Year 1. Meanwhile, this also means a greater deferral option value, because the payoff increases further by delaying the investment. On the other hand, increasing the volatility of future peak demand shifts the optimal investment timing for some paths to early years, as seen in Table. 4.2, S3. Nevertheless, the option value rises due to the increasing potential for a greater payoff in the future, compared to the benchmark. Increasing the mean reversion speed β_f to 15% means diesel fuel price will reach the reversion level faster. As a result, the market becomes more confident to defer to the investment as the probability to execute the investment in Year 5 nearly reaches 100%.

In more detail, using peak demand growth as an example to demonstrate how changing drift parameter and volatility affect the optimal investment timing. Specifically, the optimal investment timing is kept in Year 5, while the frequency decreases from 97% to just under 50% when μ_d rises from 1% to 5%, as shown in Fig. 4.9, column one, top. As the demand grows faster, greater payoffs are expected. Thus, there is a greater probability for the payoff to exceed the continuation value in early investment years, and it is less confident to execute the investment in Year 5. Further, observe that an increasing deferral option value as there is larger profit in the future with a greater demand growth rate (Fig. 4.9, column one, bottom). Similarly, the value of the option to expand rises with the same increase in μ_d, while the investment frequency in Year 5 is decreased, as shown in Fig. 4.9, column two.

In contrast, as the volatility of demand (σ_d) increases from 10% to 30%, greater payoffs are expected, so are the amount of negative payoff cash flows (due to the increasing uncertainties). Given that all negative cash flows are discarded by the LSMC approach, overall a subtle increasing trend is observed for the option value (Fig. 4.9, column three, bottom). However, even though both the NPV and option value are increasing, the probability to execute P2 has been reduced from 90% to 77% in Year 5 (Fig. 4.9, column three, top) as there is a greater possibility for the payoffs to become negative. Due to the same reasons, similar changes are observed in the case of expanding the investment, as shown in Fig. 4.9, column four.

Therefore, the optimal investment timing and the option value react differently to different values of drift parameter and volatility of the state variables. Interestingly, a greater deferral option value does not necessarily mean that the investment should be further delayed. The results show that the optimal investment timing depends on how payoff and continuation value interact with each other. Meanwhile, it is possible for the option value to decrease as future uncertainties keep increasing, because there will be a greater number of payoffs becoming negative as time moves forward. These payoffs are discarded when calculating the option value. The sensitivity analysis shows how ROV responds to uncertain events in electricity market, and hence increases

the robustness of the decision making process. In general, it is up to the DNSP to check how ROV responds to changing state variables, re-evaluate the investment, and make contingent decisions as time moves forward.

Finally, changing the subsidy levels is expected to significantly impact the NPV of the investment, which can result in less useful outcomes by ROV. This is because, for projects with very high or low NPV, ROV tends to be less useful as the decision is already clear from the standard cash flow analysis.

4.4 Summary

This work proposed a ROV framework that evaluates a distribution network investment that embeds compound options, and derives the optimal investment strategy under uncertain market environment. I demonstrated the characteristics of the framework by determining the optimal strategy for the investment in residential PV-battery systems, and calculating the values of the option to expand, and then the deferral option via the LSMC approach. Through the proposed ROV framework, I demonstrated that delaying the PV-battery investment/expansion to a later year when future uncertainties turned favourable increases the investment value and mitigates the risk of financial losses. Meanwhile, the framework showed that the investment value can be significantly increased when the interaction between the real options are properly considered. More importantly, the framework allowed the managerial flexibility to optimally respond to uncertain events characterised by the underlying state variables. Thus, the proposed ROV framework can be employed in the future to value a distribution network investment with multiple interacting options, and derive the corresponding optimal investment strategy.

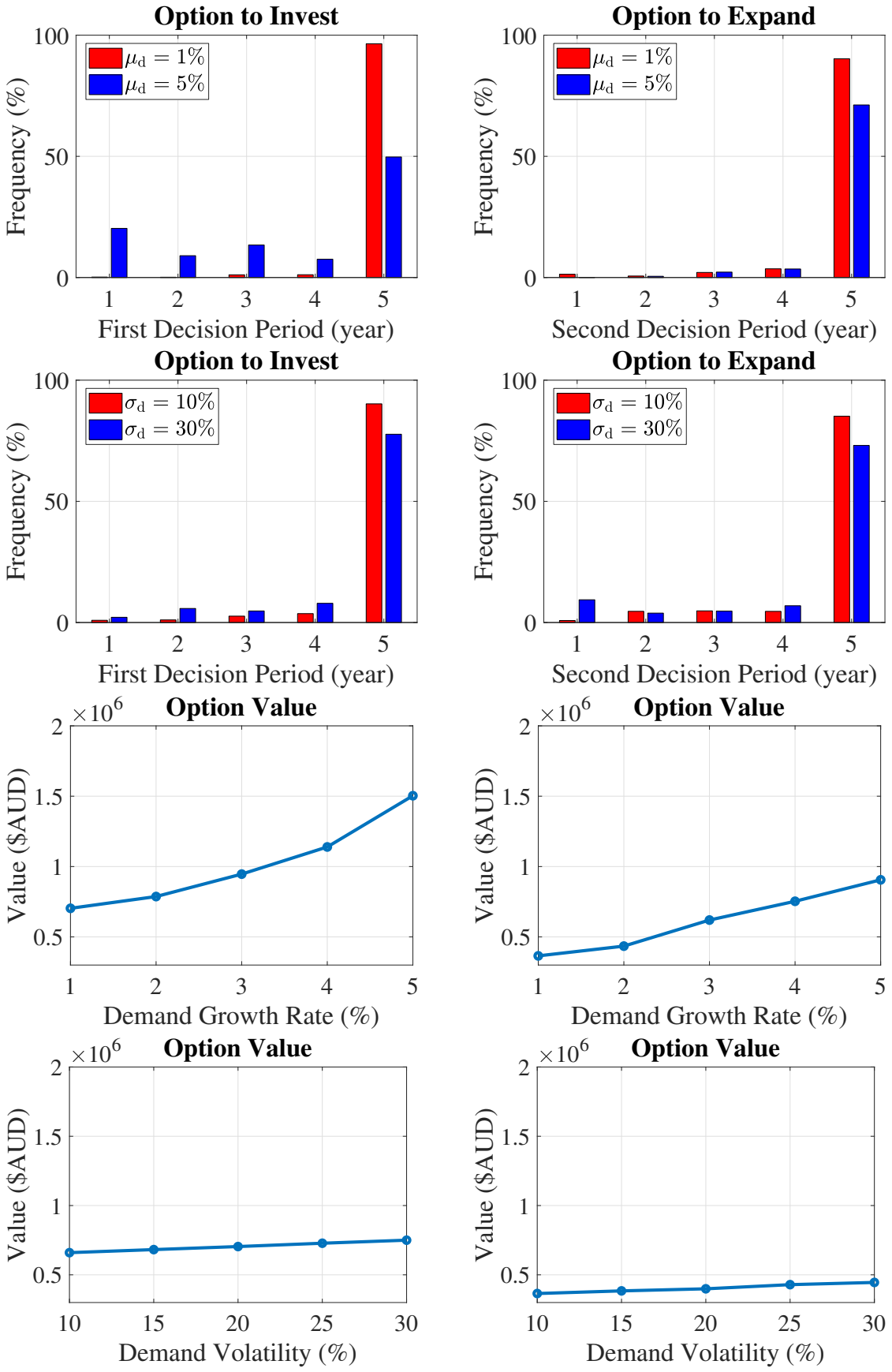

Figure 4.9: Impact on optimal investment timing with respect to changing drift parameter and volatility of the state variables.

Chapter 5

A Novel Real Options Framework to Value Residential Energy Storage Investment

Strategic financial valuation of efficient and well-timed investments in residential energy storage systems (ESS) deployment in distribution networks are challenging, because increasing uncertainties around ESS cost, sizing, location and timing require explicit modeling, typically within a Monte Carlo (MC) framework. The operational profiles of an ESS are usually determined by time-consuming optimization, including it in the MC-based real options valuation (ROV) framework that has been proposed for distribution network investments in Chapter 4 becomes computationally prohibitive.

Therefore, Chapter 5 extends the ROV framework in Chapter 4 based on the probabilistic impact assessment framework presented in Chapter 3, to determine the optimal strategy for distribution network service providers (DNSP) to provide incentives to residential ESS investments, considering compound options associated with the realization of future uncertainty. By doing so, ROV captures the network uncertainties including load behaviour, sizing and placement of distributed energy resources (DER). Specifically, each customer's PV-battery system is formulated as a home energy management (HEM) problem. The HEM problem is solved for all customers and run a probabilistic AC power flow study to determine the impact of residential ESS on network operations.

The interacting options identified in this work are (i) the option to *defer* the initial ESS investment, and (ii) the option to further increase ESS capacity after the initial ESS investment as a subsequent option (option to *expand*). The uncertainties from the network include load behavior, sizing and placement of customer-owned PV-battery systems, while those from the

electricity market include growing power demand, PV uptake and the declining cost of ESS technology.

The rest of the paper is organised as follows. Section 5.1 describes an impact assessment framework which includes synthesis of demand and PV profiles, optimization formulation with PFA, and power flow analysis. Section 5.2 presents the proposed integrated ROV framework which integrates the impact assessment framework to value American compound options. Then, the outcomes are evaluated in Section 5.3, and finally Section 5.4 draws conclusions.

5.1 Impact Assessment framework

To thoroughly examine the value of investing in residential ESS deployment in a distribution system, develop an impact assessment framework that probabilistically determines the increase in network capacity with ESS installations. In more detail, the model integrates three modules in which the first two have been detailed in Chapter 3, namely: (i) a data synthesis model to provide a large pool of demand and PV profiles for MC sampling required by the ROV; (ii) the formulation of a *home energy management* (HEM) system to provide ESS operational profiles for each network customer, and; (iii) power flow analysis to determine the maximum increase in network capacity with ESS deployment during each investment year. The power flow analysis is included in the MC analysis underpinned by the ROV to capture the potential option values hidden under network uncertainties. More details regarding the framework are discussed below[1].

5.1.1 PV and Demand Synthesis

A large pool of demand and PV traces is needed for capturing the uncertainties in a LV network via MC analysis. Therefore, due to the scarcity of smart meter data [18], the framework needs to produce statistically-representative samples. For this, I make use the observed data provided by *Ausgrid Solar Home Electricity Data* [169] as training data for a synthetic data generation method.

This work generate net load traces that have statistically similar behaviors with historical demand and PV generation of the limited observed customers, based on a non-parametric Bayesian model [74].

Specifically, let $o \in \mathcal{O}$ and $m \in \mathcal{M}$ denote the set of observed and unobserved customers, respectively. The module first clusters the observed customers in $\mathcal{O}$ into representative sets

[1]The probabilistic impact assessment framework has been covered in detail in Chapter 3. Therefore, this section only briefly describes each module and their contributions to the financial analysis.

$\gamma \in \Gamma$ according to their features using a clustering technique, namely *maximum a-posteriori Dirichlet process mixtures* [171]. The features of demand are the number of residents and day types (weekday or weekend), while for PV these are the PV panel orientation, capacity and weather information. The data need to be clustered because (i) it is computationally expensive to consider each customer as a single category, and (ii) clustering provides generalizable statistical information as the demand and PV generation in each set are correlated with their features.

Markov Chain Process

After feature assignment, the next step is to synthesise a large pool of net load traces for the unobserved customers that have been clustered using the Dirichlet distribution. To do this, I identify a conditional Markov process for the observed customers from each cluster by constructing a set of state transition matrices. This process is then repeated for the remaining transition frequency matrices to sample a net load trace for one year. For more details regarding the non-parametric Bayesian model, please see Chapter 3, Section 3.2, or [74].

5.1.2 Home Energy Management

ESS operational decisions are a key variable that impacts the technical benefits of ESS on a LV network. This work formulates a HEM system to determine optimal ESS schedules for each customer in both the observed data set and the large pool of synthesised net load traces, generated earlier for unobserved customers. For the observed customers $o \in \mathcal{O}$, *dynamic programming* (DP) is used to determine the optimal ESS schedules for their HEM systems[2]. Then, for the large pool of synthesised customers, an artificial neural network (ANN) is trained as a policy function approximation (PFA), described in the next subsection, to provide fast and close-to-optimal ESS schedules that can be feasibly included within the MC power flow analysis underpinning the ROV.

5.1.3 Policy Function Approximation

The MC-based financial analysis requires sampling from the large data set, synthesised previously. However, determining the optimal ESS schedules using optimization tools for this large data set is computationally prohibitive. In response to this, a PFA algorithm is developed by training an ANN using a smaller set of training data to emulate the output from the ESS scheduling

[2]The choice of the optimization formulation is arbitrary, because none of the existing methods is fast enough to be included directly within a MC framework.

optimization. Given this, it is only needed to solve the HEM system using DP for the observed customers, $o \in \mathcal{O}$. Specifically, the inputs for training include the following state variables — historical demand (s_t^{d}), PV generation (s_t^{pv}), electricity tariff (s_t^{p}), and the SOC with a time delay of 1 (s_{t-1}^{b}); while the target is the SOC at the current time-step (s_t^{b}). In this study, a *recurrent neural network* is used to provide close-to-optimal ESS schedules. The choice of the machine learning technique is arbitrary, because several techniques have been shown to provide close-to-optimal performance on emulating ESS schedules [69].

Then, the trained ANN is used as a PFA which refers to a lookup table and returns an output for a given set of inputs, as shown in the PFA architecture in Fig. 5.1. Specifically, we feed the net load traces synthesised above into the PFA to compute s_t^{b}. A control strategy is overlaid to prevent the outputs from violating the ESS constraints including the maximum charging and discharging power, as well as the maximum and minimum state-of-charge (SOC). This strategy keeps the SOC within its operational limits before feeding it back to the PFA by adjusting the corresponding charging/discharging rates.

5.1.4 Power Flow Analysis

Using the HEM operational decisions provided by the PFA, we conduct power flow analysis to determine the maximum capacity increase in transformer ($\Delta p_t^{\max}$) and reduction in overloading distribution lines (Δl_t) during each investment year, subject to the increasing PV penetration.

The power flow analysis needs to account for the uncertainties in future demand and PV generation. Thus, a new set of state variables is introduced, denoted $s \in \mathcal{S}_{\upsilon} : \mathcal{S}_{\upsilon} \subset \mathcal{S}$, to capture the aggregated growth in power demand $p_{t_n,\omega}^{\mathrm{d}}$ and PV uptake $p_{t_n,\omega}^{\mathrm{pv}}$ for future power flow analysis. Power demand is modelled as a homothetic growth in all loads. That is, the same load growth rate is used for every load.

To ensure the correlation between load, PV and ESS profiles, I first randomly select a set of loads, $\mathcal{D}_{\mathrm{load}}$ from the synthetic data pool. Specific to each PV penetration P_{pv}, a set of loads with a PV system is randomly sampled from $\mathcal{D}_{\mathrm{load}}$, and denoted $\mathcal{D}_{\mathrm{pv}} : \mathcal{D}_{\mathrm{pv}} \subset \mathcal{D}_{\mathrm{load}}$. Then, specific to each ESS penetration P_{b}, a set of ESS systems are randomly sampled from $\mathcal{D}_{\mathrm{pv}}$, and I denote this set $\mathcal{D}_{\mathrm{b}} : \mathcal{D}_{\mathrm{b}} \subset \mathcal{D}_{\mathrm{pv}}$.

The size of individual PV systems from the Ausgrid data set is increased to better represent the average residential PV size, which was around 5.5kW in Australia in 2017. The ESS size is decided based on the size of each PV system. In Australia, 2kWh of ESS is typically used per 1kW of PV installed. The three ESS sizes from LG and Tesla should match the PV size ranges, as shown in Table 5.1.

Table 5.1: Energy storage system specifications

Attached PV size (kW)	≤ 4	5-6	7-10
ESS Capacity (kWh)	6.5	9.8	14.0
ESS Power (kW)	4.2	5.0	5.0
Manufacturer	LG	LG	Tesla

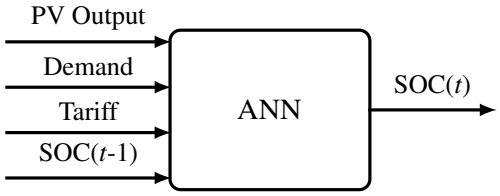

Figure 5.1: The PFA model.

5.2 Integrated ROV Framework

The proposed ROV framework uses the least square Monte Carlo (LSMC) approach that applies recursive backward induction over each MC path to value options obscured by uncertainty. When considering multistage compound options, the first task value the subsequent options (the option to expand), and then incorporate these options in the valuation of the preceding deferral option. Specifically, the option to defer is to be executed within a 5-year decision period, $\mathcal{T}_{\text{inv}}$, while the option to expand is considered in the next 5-year decision period, $\mathcal{T}_{\text{exp}}$. The expansion should only be applied to new PV installations[3] after the initial investment has been executed in $\mathcal{T}_{\text{inv}}$.

In more detail, two subsets of state variables are used to represent the uncertainty in the network and electricity market, respectively. The first subset $\mathcal{S}_{\zeta} \subset \mathcal{S}$ of uncertainties includes load behavior, sizing and placement of customer-owned PV-battery systems, which are incorporated in the MC power flow analysis. The second subset $\mathcal{S}_{\upsilon} \subset \mathcal{S}$ includes the future evolution of random variables in the electricity market, including declining ESS cost $c^{\text{b}}_{t_n,\omega}$, and growing power demand $p^{\text{d}}_{t_n,\omega}$ and PV uptake $p^{\text{pv}}_{t_n,\omega}$.

Specifically, the set of uncertainties from the electricity market $\mathcal{S}_{\upsilon} \subset \mathcal{S}$ is simulated using GBM. Then, the simulated future power demand and PV uptake are considerd as the HEM problem is solved and included in the yearly AC power flow analysis. The dynamic features of these variables are simulated by generating a set of MC realization paths, Ω. Recursive backward induction is used to search through the paths to value the compound options on each path, and thus determine the overall optimal investment strategy. The proposed ROV algorithm

[3] An ESS is only installed in conjunction with an existing PV system

is explained in more detail below. Note that $t_n \in \mathcal{T}_{\text{inv}}$ is used to represent the years to carry out the investment[4], while $t \in \mathcal{T}$ for 48 time intervals in a day.

In more detail, the state variables simulated via *geometric Brownian motion* (GBM) include the aggregated growing power demand $p^{\text{d}}_{t_n,\omega}$ and PV uptake $p^{\text{pv}}_{t_n,\omega}$ for conducting probabilistic power flow analysis[5], and the declining ESS cost $c^{\text{b}}_{t_n,\omega}$ is to be used directly in the ROV.

Given this, the remaining state variables including ESS SOC $s^{\text{b}}_{t,\omega}$, electricity tariff $s^{\text{p}}_{t,\omega}$, grid power $s^{\text{g}}_{t,\omega}$, household electricity demand $s^{\text{d}}_{t,\omega}$ and PV output $s^{\text{pv}}_{t,\omega}$ are governed by the HEM system, as previously discussed. The dynamic features of state variables are simulated by generating a set, $\omega \in \Omega$, of MC realization paths. Then, recursive dynamic programming is used to search through each path to value the compound options, and thus the optimal investment strategy.

The detailed ROV formulation is described in Chapter 4, Section 4.1.

5.2.1 Costs and Benefits Analysis

This subsection discusses the cash flow formulation that converts the outputs from the probabilistic impact assessment framework as the inputs to ROV to evaluate the investment in residential ESS.

The simulation of uncertainty via MC analysis generates Ω paths, and thus, it is necessary to estimate the future payoff at t_n along each $\omega \in \Omega$, considering the set of state variables $\mathcal{S}$. Specifically, each payoff $\Pi_{h,t_n,\omega,\mathcal{S}_{t_n}}$ is given by the cost savings from replacing network augmentation with ESS investment; that is:

$$\Pi_{h,t_n,\omega,\mathcal{S}_{t_n}} = c^{\text{b}}_{t_n,\omega} E^{\text{b}}_{t_n,\omega,\mathcal{S}_{t_n}} - c^{\text{aug}}_{t_n,\omega,\mathcal{S}_{t_n}} + c^{\text{delay}}_{t_n,\omega,\mathcal{S}_{t_n}}, \tag{5.1}$$

where $c^{\text{b}}_{t_n,\omega}$ is the cost per 1kWh of ESS installation, and $E^{\text{b}}_{h,t_n,\omega}$ is the installation size aggregated across all batteries. $c^{\text{delay}}_{t_n,\omega}$ is the cost for overloading the network if the investment is delayed[6], and the augmentation cost $c^{\text{aug}}_{t_n,\omega,\mathcal{S}_{t_n}}$ is given by:

$$c^{\text{aug}}_{t_n,\omega,\mathcal{S}_{t_n}} = c^{\text{trans}} \Delta p^{\text{max}}_{t_n,\omega,\mathcal{S}_{t_n}} + c^{\text{line}} \Delta l_{t_n,\omega,\mathcal{S}_{t_n}}, \tag{5.2}$$

[4] the period $\mathcal{T}$ has been divided into $n \in \mathcal{N}$ intervals whose length equals 1 year

[5] $p^{\text{d}}_{t_n,\omega}$ is modelled as a homothetic growth in all loads. That is, the same load growth rate is used in every load.

[6] In this study, the DNSP will add a grid-scale ESS storage at the substation to store all excessive energy from PV generation, and this work assumes that the ESS size is double the amount of maximum loading that exceeds the transformer capacity.

where c^{trans} is the cost per 1kVA transformer capacity upgrade, and c^{line} is the line reconductoring cost per unit length. $\Delta p^{\max}_{t_n,\omega,\mathcal{S}_{t_n}}$ is the capacity increase in transformer, and $\Delta l_{t_n,\omega,\mathcal{S}_{t_n}}$ is the reduction in line length that requires reconductoring (line loading exceeds the line capacity)[7].

The above equations conduct a cash flow analysis based on the MC simulations of the state variables $\mathcal{S}$. Then, the LSMC approach is applied to recursively value the options at each decision node on each MC path $\omega \in \Omega$ from the maturity T_{inv} to the initial investment year t_0[8]. There are $h \in \mathcal{H}$ options within an investment, and h and $h+1$ are used to represent the options to defer and expand, respectively.

In more detail, to enable the use of ROV, the first task is to estimate the future payoff cash flows of the investment in residential ESS by including the cost of network augmentation as monetary savings, as described by (5.1) and (5.2). This is because the purpose of implementing ESS systems is to delay and/or avoid network augmentation. Meanwhile, this calculation also captures the uncertainties in network augmentation such as the length of overloading cables and transformer loading level. For a more detailed description on the LSMC approach, please see Chapter 4, Section 4.1.

5.2.2 Modelling of Future Uncertainties

The set of state variables $\mathcal{S}_\upsilon$, including growing power demand ($p^{\text{d}}_{t_n,\omega}$), PV uptake ($p^{\text{pv}}_{t_n,\omega}$), and the declining cost of ESS technology ($c^{\text{b}}_{t_n,\omega}$), are simulated by the *geometric Brownian motion* (GBM). This method is employed ahead of other techniques due to its ability to adequately describe the stochasticity and drift of a variable [107]. The GBM model is described by the following equation:

$$ds_t = \mu \mathcal{S}_t dk + \sigma \mathcal{S}_t dW_t, \tag{5.3}$$

where s_{t_n} is the sought stochastic value of a state variable, μ is the percentage drift that describes the rate of growth, σ is the percentage volatility, and W_t is the Wiener process that describes the stochastic component. Thus, the discretization recursion formula is given by:

$$\mathcal{S}_{t+\Delta t} = \mathcal{S}_t e^{\left(\mu - \frac{\sigma^2}{2}\right)\Delta t + \sigma dW_t}. \tag{5.4}$$

Demand data is taken from Ausgrid Solar Home Electricity Data, while the PV uptake and ESS price are obtained from [183] and [179], respectively. The drift parameter and volatility for

[7] In practice, DNSPs apply reconductoring only to the overloaded part of the network. ESS increase network capacity, which reduces the number of lines that requires reconductoring. This reduction is transformed into monetary savings for enabling the use of ROV.

[8] I first divide the investment time-span from t_0 to the maturity time at T_{inv} into $n \in \mathcal{N}$ discrete intervals, representing investment years.

Table 5.2: Drift and volatility of state variables.

	Demand	PV installation	ESS
Drift (%)	2.2	5.2	-8.2
Volatility (%)	3.4	4.9	4.0

each state variable are summarised in Table 5.2. Detailed simulation processes are demonstrated in Chapter 4, Section 4.2.

5.3 Results and Evaluation

The investment in residential ESS deployment is used as a case study to demonstrate the efficacy of the framework, considering compound options, which are (i) the option to defer in $\mathcal{T}_{\text{inv}}$, and (ii) the option to expand the investment in $\mathcal{T}_{\text{exp}}$.

The expansion of the investment only covers new PV installations. Given this, the increase in ESS penetration from the expansion is denoted as P_{b}^{*}, which is the percentage of new PV installations equipped with an ESS. This work assumes that network augmentation is to provide the same network capacity increase as the ESS investment. The DNSP is committed to 50% of total cost for each ESS installation; the rest is paid by the customer[9]. This section demonstrates how to use the proposed methodology to determine the optimal investment strategy for ESS deployment in existing PV installations, assuming that 50% of customers in the network own a PV system (P_{pv} = 50%) in the initial year. 50% is a reasonable assumption given that in some regions in Australia the percentage is expected to reach this level in the near future. At this level of penetration, voltage issues are expected to happen during midday. This work expects voltage and thermal loading issues in the initial year so that DNSPs are required to act now. Detailed results are shown in this section.

5.3.1 Computational Performance

The improvements in computational performance is the linchpin of the proposed methodology. Solving ESS optimization for each net load trace for one year is already time-consuming. Directly include this within the MC simulations underpinned by the ROV is clearly impractical, given a total of 10,000 MC simulation runs for 10 years (1000 for each year) is needed to ensure the

[9] A slightly lower percentage (50%) is set for subsidizing residential ESS investments in Chapter 5 than Chapter 4 (%70), because investing in ESS only is less capital intensive than investing in the hybrid PV-battery systems. Note that these percentages are indicative figures to demonstrate the use of the methodology. DNSPs are free to decide these figures as they feel appropriate in practice and context.

convergence of the ROV solution. By incorporating the PFA algorithm in the ROV to emulate the ESS scheduling policies avoids directly solving optimization within the MC analysis, and due to this, a small set of training data is needed from solving DP[10]. Training the ANN only takes 30 minutes, which is negligible. This process reduces the computation time by 95% for each MC run, and thus, the use of PFAs is essential to making the entire financial analysis computationally feasible.

5.3.2 Test Networks

The test LV feeder which consists of 223 single phase consumers with a total length of 5.6 is adopted from Electricity North West Limited (ENWL), a British network operator [1]. To match the larger air-conditioning loads on typical Australian feeders, this UK test network is transformed into Australian-type LV networks by tripling the transformer and line capacity. The transformer thermal limit is 800kVA, and I sample from the pool of net load traces synthesised in the impact assessment framework for allocation to load points.

5.3.3 Thermal Loading Reduction

ESS reduce network loading level by absorbing excess solar generation, and then discharge during peak periods. I assess the impact of executing the ESS investment in each decision year on transformer loading and line reconductoring, the results are shown in Fig. 5.2 and Fig. 5.3. Specifically, the immediate transformer loading reduction is roughly 100kW if the investment is executed in Year 1 with a 50% PV penetration level. This reduction increases to 120kW if the investment is executed Year 5, because the aggregated ESS capacity rises with increasing P_{pv}. The impact of expanding the investment is much less pronounced, because the network has been equipped with ESS after $\mathcal{T}_{\text{inv}}$, and the expansion only applies to new PV installations in $\mathcal{T}_{\text{exp}}$, denoted P^{*}_{pv}.

The distribution lines with a thermal loading level greater than 100% require reconductoring, as observed in Fig. 5.3; The need for such action decreases when ESS are installed. In this case, the need for reconductoring can be nearly eliminated when the investment is executed in any decision year in $\mathcal{T}_{\text{inv}}$. However, from Year 6 onwards, despite some further reductions, reconductoring is generally required no matter when the DNSP executes the expansion.

[10]Formulating the HEM problem as an MILP would possibly reduce the computational burden of training the PFA, but the MILP approach is still too slow to be directly used in MC analysis.

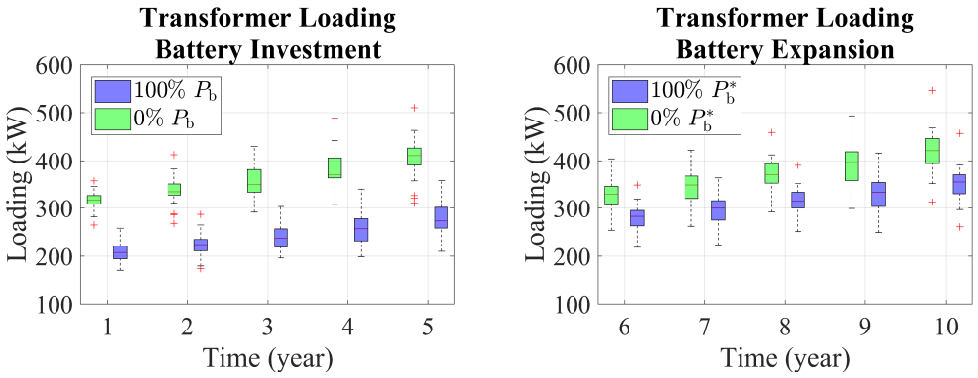

Figure 5.2: Transformer loading before/after executing the ESS investment in each decision year (left); Transformer loading before/after the expansion in ESS capacity in each decision year, assuming the investment has been executed (right). P_b is the percentage of existing PV installations equipped with ESS in $\mathcal{T}_{inv}$. P_b^* is the percentage of new PV installations equipped with an ESS. The increase in the transformer loading is mainly due to the increase in PV penetration levels. Specifically, Fig. 3.1 in Chapter 3 shows the impact of ESS under different PV penetration levels on the same network as the one used in the case study in this Chapter. It shows that the transformer loading level is at 40% when there is no PV, this percentage decreases initially at low PV penetration levels but quickly comes back to just under 50% when PV penetration reaches 50%. Continue increasing the PV capacity would further increase this loading level as more power is flowing back to the transformer.

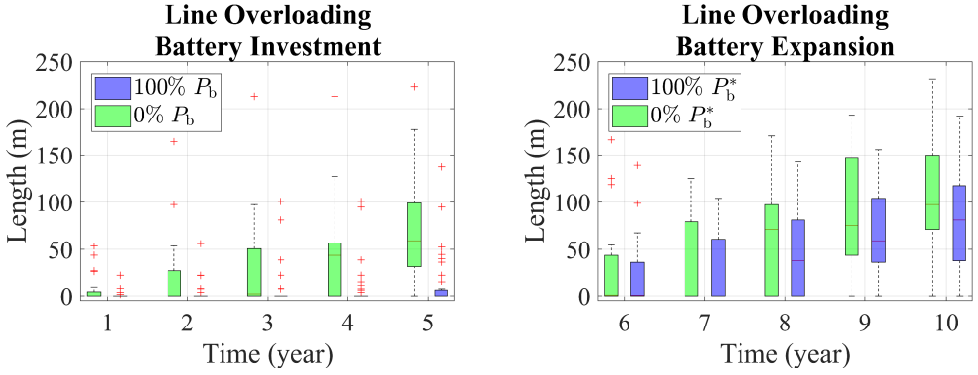

Figure 5.3: Length of overloaded distribution lines with/without ESS. The ESS investment is executed in $\mathcal{T}_{inv}$ (left), and expanded in $\mathcal{T}_{exp}$ (right).

5.3.4 Battery Storage Cash Flow Analysis

This subsection evaluates the investments in network augmentation and ESS via the standard NPV assessment with MC analysis. The capital expenses of transformer and distribution line upgrades are 2k$/kW and 1.5k$/m, respectively, considering system procurement, installation, operation and maintenance costs [184].

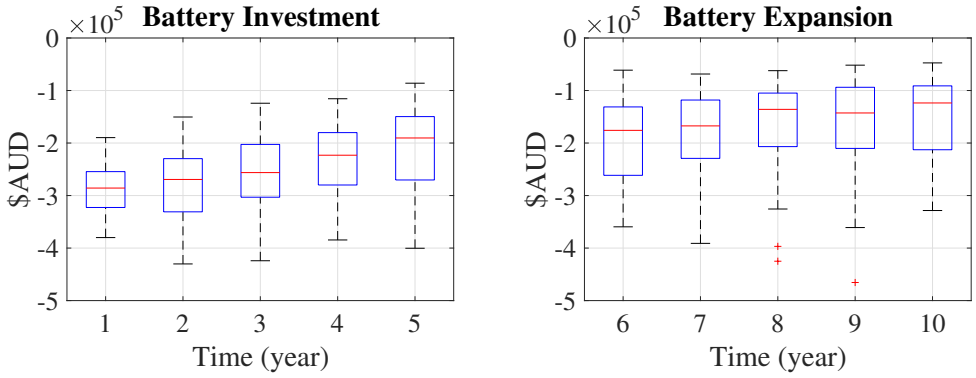

Figure 5.4: Cash flows of ESS investment executed in each decision year in $\mathcal{T}_{\text{inv}}$ (left) and expansion executed in each decision year in $\mathcal{T}_{\text{exp}}$ (right).

The average cost to execute the ESS investment in Year 1 is \$300k, which decreases to \$200k in Year 5 due to the declining cost of the technology (Fig. 5.4). In contrast, network augmentation increases rapidly from \$200k if it is done in Year 1, to \$400k in Year 5, as observed in Fig. 5.5. Thus, network augmentation is clearly cheaper than ESS in Year 1. However, this situation reverses if both investments are deferred to Year 3 as ESS cost continues decreasing and more network augmentation is needed to accommodate new PV installations. Similar trends are observed for expanding the investment, specifically, the cost changes from \$160k in Year 6 to above \$100k in Year 10, while that of the network augmentation for the same capacity increases from \$30k to \$80k.

From Fig. 5.4, observe that negative cash flows for the ESS investment, which renders this investment unsuitable for ROV. In response to this, this work uses the cost of network augmentation as monetary savings (Fig. 5.5), and create payoff cash flows for the ESS investment via (5.1), as shown in Fig. 5.6. The trade-off is the cost of allowing network to overload.

The payoff cash flows might mislead the DNSP to invest in Year 5 and abandon the option to expand in the following decision period, given the impression that Year 5 has the greatest average payoff. This impression is misleading because even though the average payoff increases, it does not mean that all payoffs would follow the same trend. ROV uses recursive backward induction to solve the optimal stopping time for each path, considering the compound options, and provides the optimal investment strategy throughout both decision periods.

5.3.5 Residential ESS Investment: ROV Analysis

The value of managerial flexibility in Year t_n is the difference between the option value $F_{h,t_n,\omega}$ and the initial payoff. Using LSMC, the investment is executed when $\Pi_{h,t_n,\omega}$ exceeds the continuation

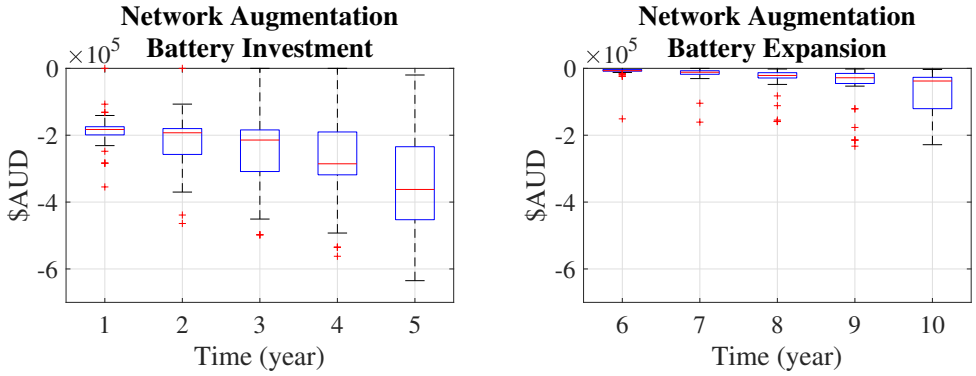

Figure 5.5: Cash flows of network augmentation for the same amount of network capacity increase from ESS systems throughout $\mathcal{T}_{inv}$ (left) and $\mathcal{T}_{exp}$ (right).

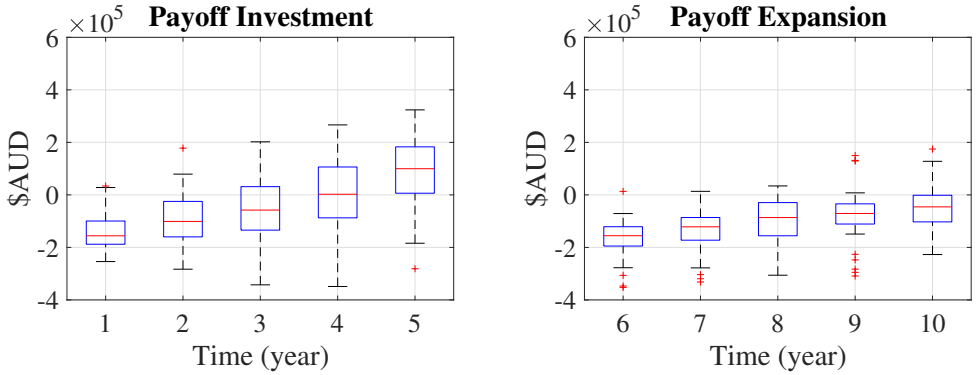

Figure 5.6: Payoff cash flows of the ESS investment executed in each decision year in $\mathcal{T}_{inv}$ (left) and expansion in $\mathcal{T}_{exp}$ (right), considering the cost of network augmentation as monetary savings.

Table 5.3: Frequency distribution of optimal strategy

	Year 1	Year 2	Year 3	Year 4	Year 5	Π	F
Compound	0%	5.1%	8.0%	17.9%	52.5%	–$180k	$130k
Independent	0%	6.8%	6.2%	10.4%	47.1%	–$180k	$80k
Expand	0%	2.5%	7.9%	6.0%	20%	–$170k	$35k

value $\Phi_{h,t_n,\omega}$ (i.e. when the maximum potential of uncertainty is reached on a particular path). ROV integrates all values generated by contingencies to find the optimal investment strategy.

In more detail, the option value for the current year is $130k. The payoff to invest immediately at t_0 is –$180k, so the investment should be delayed. As the optimal stopping problem is solved for each path, 16.5% of the paths recommend abandoning the investment due to a negative cash flow in all decision years. ROV uses backward induction to distribute the remaining 83.5% of the paths based on when the maximum investment value is reached. Observe from Table. 5.3, only 5.1% recommend investing in Year 2, and 78.4% recommend delaying, while nearly 25%

of paths are in profit this year, as shown in Fig. 5.6. By Year 5 (maturity), even though more than 75% paths end up profiting in this year, only the paths remaining (52.5%) will execute the investment. Therefore, ROV explicitly captures the value of contingency, and provides a different strategy from the standard cash flow analysis that also considers future uncertainty.

From ROV, the most likely optimal investment timing is Year 5 with a probability of 52.5%. Given that the investment should definitely be delayed to the future, it is recommended to apply ROV again next year after some uncertainties have unfolded to update the frequency distribution of optimal investment timing, and decide whether to keep delaying.

In contrast, the negative payoff cash flows for expansion indicate immediate abandonment. However, ROV captures the value of making contingent decisions in the future, and provides an option value of $35k. The chances to profit are low, e.g. 20% in Year 5, followed by 11% in Year 4, as illustrated in Table. 5.3, (row *Expand*). With these possibilities, managerial flexibility worth $205k is enough to keep the investment open, just in case market condition turns favourable, given that the average payoff in Year 6 is –$170k.

Considering the options independent of one other decreases the deferral option value from $130k to $80k, and the chance of investing in Year 5 decreases throughout $\mathcal{K}_{\text{inv}}$, as shown in Table. 5.3 (row *Independent*), this is because additional values generated by future contingencies are added to the valuation of the deferral option. Surprisingly, although the expansion is unlikely to be implemented, the option still has great impacts on its prerequisite option. In this case, eliminating the option to expand in the valuation means that less scope for managerial flexibility, leading to a much smaller option value.

5.4 Summary

This work proposed a novel ROV framework that integrates stochastic simulation of power flow analysis with recursive backward induction. It is used to systematically value a set of American compound options in the small-scale ESS investment under uncertainty. The challenge of directly including ESS optimization in the ROV framework is overcome by using a PFA algorithm to provide fast and close-to-optimal ESS schedules, which reduces computation time by greater than 95%. Using the ROV framework, I demonstrate that delaying the ESS investment/expansion to a later year mitigates potential risks and captures the opportunity value under future contingencies. More importantly, the proposed ROV framework provides benefits when systematically considering the interactions between options, beyond those available when the options are calculated individually, even if the subsequent option is unlikely to be executed.

Chapter 6

A Novel Real Options Framework to Value Grid-Scale Energy Storage Investment

The novel integrated real options valuation (ROV) framework proposed in Chapter 5 that formulates a home enegy management (HEM) system for each household so that the investment value of providing incentives for network customers to install behind-the-meter (BTM) distributed network resources (DER) can be captured by ROV. However, to capture the operation of grid-scale DER investments, a different formulation is usually required in ROV. In this regard, Chapter 6 uses ROV to identify possible flexible investment directions in a grid-scale battery energy storage system (ESS) investment in the light of various uncertainties. Different from Chapter 5, the calculations are based on an optimal power flow (OPF) model, run each half hour for the entire decision period, to determine ESS schedules. Solving the OPF determines the optimal size, location and schedules of a grid-scale ESS, and the overall network loading reduction. By incorporating the OPF model within ROV, this Chapter further demonstrates how flexible managerial strategies can be used to increase the value in a distribution network investment.

Within the application of grid-scale ESS investment, growing power demand, varying electricity price and the declining cost of the ESS technology are identified as the main sources of uncertainty. The integrated ROV framework explicitly (i) solves an AC OPF study within the *Monte Carlo* (MC) simulations to capture the uncertainties, and (ii) determine the optimal timing to execute the investment (option to defer). In more detail, the benefits from ESS operations to the network are quantitatively incorporated in the ROV to capture the value of managerial flexibility, and hence the optimal investment strategy. Driven by the declining ESS cost, the results suggest to delay the investment to a later year to maximise the investment value. Furthermore, this

chapter also investigates the impact of different numbers of grid-scale ESS, with the same overall capacity, on distribution networks.

The rest of the chapter is organised as follows. Section 6.1 describes the ESS modelling. Section 6.2 details the optimisation formulations used to (i) study the impact of different numbers of grid-scale ESS on distribution networks; and (ii) determine the optimal sizing of one grid-scale ESS for the ROV analysis. Section 6.3 includes the detailed ROV formulation for valuing the investment in ESS and Section 6.4 includes a detailed explanation of the network model and a discussion on the simulation results. Section 6.5 draws conclusions.

6.1 Energy Storage Modelling

The ESS operation constraints are listed as follows:

$$s^{\mathrm{b}}_{t,i} = s^{\mathrm{b}}_{t-1,i} + 3\big(\eta^{+} x^{b+}_{t,i} - \frac{1}{\eta^{-}} x^{b-}_{t,i}\big)\Delta t. \tag{6.1}$$

The initial state of charge after each cycle, typically one day, must be the same, this is formulated as follows:

$$e_{\Omega} = e_0. \tag{6.2}$$

To ensure that the above constraint can be satisfied, the total charged and discharged power for one cycle must be the same:

$$\sum_{t\in\mathfrak{T}} \Big(\eta^{+} x^{\mathrm{b}+}_{t,i} - \frac{1}{\eta^{-}} x^{\mathrm{b}-}_{t,i}\Big) = 0. \tag{6.3}$$

In addition, charging and discharging rates at each time interval Δt must be constrained by the maximum charging and discharging rates stated by the properties of the ESS:

$$0 \leq 3x^{\mathrm{b}+}_{t,i} \leq \gamma^{\mathrm{c}}. \tag{6.4}$$

$$0 \leq 3x^{\mathrm{b}-}_{t,i} \leq \gamma^{\mathrm{d}}. \tag{6.5}$$

Similarly, the state of charge cannot exceed the minimum and maximum states of charge at all times, indicated by the equation below:

$$s^{\mathrm{b}}_{\min} \leq s^{\mathrm{b}}_{t,i} \leq s^{\mathrm{b}}_{\max}. \tag{6.6}$$

In this study, the charging and discharging efficiencies in the model are neglected.

6.2 Optimal Power Flow Formulation

The optimisation model aims to place and size a CESS and multiple DESS in an unbalanced low-voltage (LV) network in order to minimise annual system losses.

6.2.1 Objective Function

The objective is to minimise system losses, formally stated as:

$$\underset{p^{+}_{t,j},p^{-}_{t,j},B^{\text{loc}}_{t,j},e^{\text{com}},e^{\text{dist}}_{j}}{\text{minimise}} \sum_{d\in\mathcal{D}}\sum_{t\in\mathcal{T}}\sum_{i,j\in\mathcal{L}} p^{\text{loss}}_{t,ij}, \tag{6.7}$$

where $p^{\text{loss}}_{t,ij}$ is given by:

$$p^{\text{loss}}_{t,ij} = \sum_{f\in\mathcal{F}} R_{f,ij}\frac{p^2_{f,t,ij}+q^2_{f,t,ij}}{v^2_{sub}} \quad \forall\, f\in\mathcal{F}. \tag{6.8}$$

This objective function indicates that the overall model is a quadratic problem. It is used with the branch flow constraints in Section 6.2.2 to compare the impacts of different numbers of ESS on distribution networks.

6.2.2 Branch Flow Constraints

Load flows in LV networks with numerous branches can be difficult to solve, especially when the network is unbalanced and each phase must be taken care of individually. In this case, the branch flow model introduced in [36] and [128] is employed, which has been shown to be accurate in modelling power flows in radial distributed networks [132]. The equations in this model show that power flows on each phase from bus i to bus j, can be formulated as a function of power flows and power losses entering bus j, and the generation and consumption at bus j. The modified power flow equations with ESS placed on bus j, phase $f\in\mathcal{F}$ are presented below:

$$\begin{aligned} p_{f,t,ij} = &\sum_{j,k\in\mathcal{L}}\left(p_{f,t,jk}+R_{f,ij}\frac{p^2_{f,t,ij}+q^2_{f,t,ij}}{v^2_{\text{sub}}}\right)\\ &+p^{\text{d}}_{t,j}-p^{\text{g}}_{t,j}+\sum_{j\in\mathcal{E}}(x^{\text{b}+}_{t,j}-x^{\text{b}-}_{t,j}), \end{aligned} \tag{6.9}$$

$$\begin{aligned} q_{f,t,ij} = &\sum_{j,k\in\mathcal{L}}\left(q_{f,t,jk}+X_{f,ij}\frac{p^2_{f,t,ij}+q^2_{f,t,ij}}{v^2_{\text{sub}}}\right)\\ &+q^{\text{d}}_{t,j}-q^{\text{g}}_{t,j}, \end{aligned} \tag{6.10}$$

$$v_{f,t,j}^2 = v_{f,t,i}^2 - 2(p_{f,t,ij}R_{f,ij} + q_{f,t,ij}X_{f,ij}) + (R_{f,ij}^2 + X_{f,ij}^2)\frac{p_{f,t,ij}^2 + q_{f,t,ij}^2}{v_{f,t,j}^2}. \tag{6.11}$$

In this paper, only the active power flow of ESS is considered. It has been clearly illustrated by multiple literature that the nonlinear terms in equations (6.9) and (6.10), representing power losses, can be neglected as the impacts of these terms on the objective function are limited [132]. Under this assumption, the branch flow equations become:

$$p_{f,t,ij} \approx \sum_{j,k\in\mathcal{L}} p_{f,t,jk} + p_{t,j}^{\mathrm{d}} - p_{t,j}^{\mathrm{g}} + \sum_{j\in\mathcal{E}} (x_{t,j}^{\mathrm{b}+} - x_{t,j}^{\mathrm{b}-}) \quad \forall\, f \in \mathcal{F}. \tag{6.12}$$

$$q_{f,t,ij} \approx \sum_{j,k\in\mathcal{L}} q_{f,t,jk} + q_{t,j}^{\mathrm{d}} - q_{t,j}^{\mathrm{g}} \quad \forall\, f \in \mathcal{F}. \tag{6.13}$$

Voltage Constraints

Based on [38] and [132], equation (6.11) can be linearised by assuming voltage variations at an arbitrary bus j are close to 0 at all times, eg. $v_{f,t,j} - v_{\mathrm{sub}} \approx 0$. This assumption leads to the following expression:

$$v_{f,t,j}^2 \approx v_{\mathrm{sub}}^2 + 2v_{\mathrm{sub}}(v_{f,t,j} - v_{\mathrm{sub}}) \quad \forall\, f \in \mathcal{F}. \tag{6.14}$$

The linearised version of the voltage equation can be developed by substituting equation (6.20) to (6.11):

$$v_{f,t,j} \approx v_{f,t,i} - \frac{p_{f,t,ij}R_{f,ij} + q_{f,t,ij}X_{f,ij}}{v_{\mathrm{sub}}} \quad \forall\, f \in \mathcal{F}. \tag{6.15}$$

The accuracy of this equation has been justified by the authors in [128]. In addition, the model should satisfy the voltage limits for all three phases in presence of loads and PV generation:

$$\underline{v} \leq v_{f,t,i} \leq \bar{v} \quad \forall\, f \in \mathcal{F}. \tag{6.16}$$

ESS Location

The following equation assists in deciding the optimal location for the CESS by setting the number of ESS, N_{b}, to 1:

$$\sum_{j\in\mathcal{E}} B_{t,j}^{\mathrm{loc}} = N_{\mathrm{b}}. \tag{6.17}$$

The ESS formulations from (6.1) to (6.6) and the branch flow equations (6.12), (6.13), (6.21), along with votlage and ESS constraints (6.17) and (6.18) formulate a mixed integer quadratic programming model for determining the optimal location and the associated capacity for the CESS.

The study aims to compare the impacts between a CESS and multiple DESS. Therefore, the next step is to determine the optimal locations and capacities for multiple DESS, assuming they have the same aggregated capacity as the CESS.

In this scenario, N in equation (6.17) must be set as a variable instead of a parameter. Meanwhile, the following constraint which equates the aggregated capacity of the DESS to the size of the CESS is added to the optimisation model:

$$\sum_{j \in \mathcal{E}} e_j^{\text{dist}} = e^{\text{com}}. \tag{6.18}$$

6.2.3 Modified Objective Function

The objective function described in Section 6.2.1 is used to study and compare the impact on distribution networks from one grid-scale community ESS and multiple distributed ESS.

However, to evaluate the investment in a grid-scale community ESS, the objective function has to be changed. Specifically, to include the battery schedules within the ROV to determine the optimal investment strategy, the ESS must be optimally operated to maximise the network benefits specific to each MC path of residential power demand growth.

In this context, the objective is now to minimise the grid supply ($\bar{S}$), and the associated ESS size (e^{cap}), formally stated as:

$$\underset{p_{t,j}^{+}, p_{t,j}^{-}, e^{\text{cap}}}{\text{minimize}} \bar{S} + \lambda c^{\text{ESS}}, \tag{6.19}$$

where c^{ESS} is the cost of the ESS. To determine the optimal size that minimises $\bar{S}$, we set the weighting factor, λ, relatively small so that the cost component has limited effect on $\bar{S}$. The optimisation model is formulated to determine the battery schedules for one year, and $\bar{S}$ is therefore the maximum grid power supply within this time horizon.

In addition to the changes made in the objective function, (6.17) and (6.18) should be removed from the constraints listed in Section 6.2.2, because in this Chapter only the investment in a large grid-scale ESS will be evaluated using ROV. On top of this, the constraints in (6.12), (6.13) and (6.20) have been linearised to reduce the computational burden, as shown in Section 6.2.2.

6.3 Valuation of Grid-Scale ESS

This work values the *option to defer* the ESS investment based on future uncertainties, and hence increase the final investment value and determine the optimal investment timing. Specifically, ROV combines a forward-looking model for incorporating uncertainties, and a recursive backward induction and least square regression for determining the optimal investment timing [110]. The mathematical formulation of the least square Monte Carlo (LSMC) method is detailed in Chapter 4, Section 4.1.

In this work, the key to calculating the option value is the payoff from (6.22); or in other words, the profit from investing in ESS. This work assumes that the investment in ESS can be executed in any year from t_0 to the maturity time at T_{mat}. Specifically, the payoff $\Pi_{t_n,\omega}$ is the cost difference from investing in the grid-scale ESS ($c^{\text{ESS}}_{t_n,\omega}$) and network augmentation ($c^{\text{aug}}_{t_n,\omega}$) from each year of the decision period. In this work, the DNSP is responsible for the ESS procurement, installation and operation. Meanwhile, the DNSP is obliged to cover the cost of energy ($c^{\text{g}}_{t_n,\omega}$) delivered through the substation transformer that is above the transformer thermal limit, at the wholesale electricity price, $c^{e}_{t_n,\omega}$[1]. Given this, the annual reduction in grid supply, $\Delta E^{\text{add}}_{t_n,\omega}$ is included in the payoff calculation. Thus, the profit equation for the ω^{th} MC path is shown as follows:

$$\Pi_{t_n,\omega} = c^{\text{ESS}}_{t_n,\omega} - c^{\text{aug}}_{t_n,\omega} + c^{\text{g}}_{t_n,\omega}, \tag{6.20}$$

where $c^{\text{g}}_{t_n,\omega}$ is determined by $c^{e}_{t_n,\omega}$ and $\Delta E^{\text{add}}_{t_n,\omega}$, and $c^{\text{aug}}_{t_n,\omega}$ is:

$$c^{\text{aug}}_{t_n} = c^{\text{trans}} \Delta p^{\text{max}}_{t_n,\omega} + c^{\text{line}} \Delta l_{t_n,\omega}. \tag{6.21}$$

where c^{trans} and c^{line} are the costs for upgrading the transformer and lines, respectively. $\Delta p^{\text{max}}_{t_n,\omega}$ is the reduction in the maximum power supplied from the grid, and $\Delta l_{t_n,\omega}$ is the total length of the cable that requires an upgrade (line loading exceeds the capacity).

Specifically, the capacity to be upgraded in the transformer is equal to the reduction in the grid supply ($\Delta p^{\text{max}}_{t_n,\omega}$) with the ESS, while the cost for upgrading and re-conductoring the cables is decided by the corresponding loading reduction, $\Delta l_{t_n,\omega}$, as shown in (6.21).

Random variables are power demand growth, varying electricity price, and the declining ESS cost, which are governed by *geometric Brownian motion* (GBM) [107]. Specifically, demand growth is modelled as a homothetic growth in all loads. That is, the same load growth rate is used in every load. Demand and PV data are from the Ausgrid *Solar Home Electricity Data*,

[1] In Australia, DNSP-owned and operated assets that have a primary use in providing regulated network services are ring-fenced, and cannot be used to participate in contestable markets, such as wholesale energy and frequency stability services. As such, they face the same energy costs as retail customers.

while wholesale electricity price and the ESS price data are extracted from [185] and [179], respectively. The detailed simulations of these state variables are described in Chapter 4, Section 4.2.

Within the LSMC method, the time span from Year t_0 to the maturity year in T_{inv} is divided into $n \in \mathcal{N}$ intervals, whose length is $\Delta t = (T_{\text{inv}} - t_0)/N$. In this work, one interval is equivalent to one year. The investment value in Year t_n is denoted as $F_{t_n,S_{t_n}}$, where S_{t_n} is the state variable of the ESS investment. In this work, the state variables are the growing power demand, varying electricity price, and the declining ESS cost. Hence, the future discounted value of the investment option can be expressed as follows:

$$F_{t_n,S_{t_n}} = E_{t_n}\left[\Pi_{\tau,S_\tau}\right](1+r)^{-(\tau-t_n)}, \tag{6.22}$$

where τ is the optimal stopping time, $\Pi(\tau,X_\tau)$ is the payoff, $E_{t_n}[\Pi(\tau,X_\tau)]$ is the expectation on the information available in Year t_n, and r is the risk neutral discount rate. The detailed ROV formulation via LSMC is described in Chapter 4, Section 4.1.

Overall, the ROV now can be calculated using a three-step process:

- Use GBM to generate 2500 MC paths of the stochastic variables, and apply each path to the linearised branch flow model to determine the optimal ESS capacity, schedules, $\Delta p^{\max}_{t_n,\omega}$, $\Delta E^{\text{add}}_{t_n,\omega}$ and $\Delta l_{t_n,\omega}$.

- Interpret these values as the payoff, $\Pi_{t_n,\omega}$, using equation (6.20), and serve it as the input to the ROV.

- Apply the LSMC method described in Chapter 4, Section 4.1 to determine the investment value and optimal investment strategy.

6.4 Results and Evaluation

The selected LV feeder consists of 130 single phase consumers with a total length of 3.9km. This is an unbalanced network with 40, 49 and 41 consumers sitting on phase A, B and C, respectively. The feeder is adopted from Electricity North West Limited (ENWL), a British network operator [1]. The network diagram obtained from OpenDSS[2] is shown in Fig. 6.1. To match the larger air-conditioning loads on typical Australian feeders, this UK test network is

[2]Open Distribution System Simulator [172]

transformed into Australian-type LV networks by tripling the transformer and line capacity[3]. Each consumer, which follows a specific demand profile, adopts a single phase PV system. The test feeder is reasonably loaded, presenting great potential for over-loading problems. In addition, the transformer thermal limit is 800kVA, any power transferred through the transformer that has a greater value than this limit is paid by the DNSP. For distribution networks, the R/X ratio is relatively large and usually resistance is considered to be predominant. Mutual impedance that is created by the change in current in a coupled conductor only affects the reactance, not the resistance. Due to this reason, mutual impedance can be neglected in distribution networks. Moreover, this work assumes that most of the customers in Australia are connected in single-phase, which potentially means a less balanced distribution network.

This section first compares the benefits of different numbers of grid-scale ESS on distribution networks. Then, it analyses the valuation results for one grid-scale community ESS investment obtained from the integrated ROV framework. The investment is assumed to be executed within a 5-year decision period, with a 7.5% annual risk-neutral discount rate. The proposed methodology helps the DNSP decide the optimal investment strategy to invest in the ESS considering the value of managerial flexibility in the presence of future uncertainties, and the results are evaluated in this section.

The modified mixed integer quadratic problem (MIQP) with objective given by (6.7), (6.8) and constraints (6.12), (6.13), (6.21), (6.17), (6.18) is modelled in AMPL[4], a software which effectively models mathematical problems. Knitro[5] is used to solve the optimisation problem. Simulation is performed using Matlab, and the optimisation model is accessed via AMPL API[6]. All outcomes from both scenarios are discussed in this section.

Load and PV profiles for one year are generated using the CREST model, which allows one to generate high resolution PV and load profiles [187]. For this study, each individual load and PV system are assigned with unique daily load and PV profiles with 1 hour resolution, respectively. The feeder data from OpenDSS are applied to AMPL when solving the optimisation model. When performing simulations, the base voltage is 0.4kV (1pu) and the phase votlage of transformer secondary winding is fixed at 0.23kV. Further, the results from this work have been validated using OpenDSS.

[3]For transformers, I reduced the impedance, while for transmission lines I only reduced the resistance. The reactance mainly depends on the distance between the conductors, so I left it unchanged.

[4]AMPL - Algebraic Mathematical Programming Language [186]

[5]Knitro - A mixed integer non-linear solver within AMPL

[6]API - Application Programming Interface

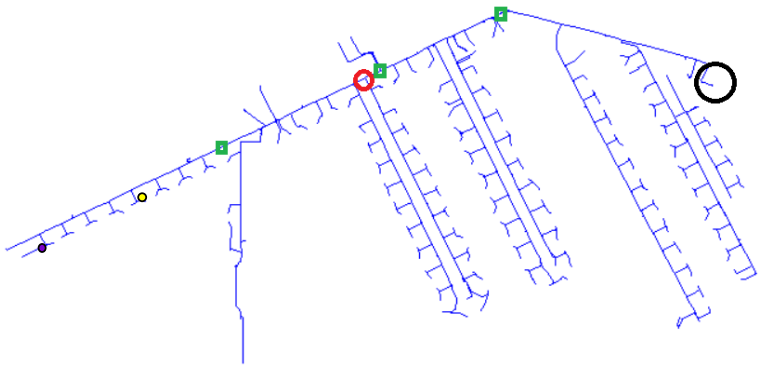

Figure 6.1: The unbalanced LV network, the black and red circles denote the substation transformer (bus 1) and CESS (bus 702), while the three green squares represent DESS (buses 153, 676 and 1786) [1]. The purple and yellow circles indicate the locations for bus 2266 and 1940, respectively.

6.4.1 Computational Performance

The computational performance of the methodology is the key highlight of this work. Specifically, solving the MIQP for each MC path for 1 year requires 30 minutes. Given that the greater the number of MC paths, the more accurate the results become, the simulation becomes impractical given that there is a total of 12,500 MC paths over the 5-year decision period. Specifically, the computation time is greater than 8 months if directly solving the MIQP within the MC analysis. To reduce the computational burden, a linearised branch flow model is used, which speeds up the computation by 90%. It can be further reduced by parallelizing the MC simulations.

6.4.2 Performance Indices

The three performance indices used to compare the impact of different numbers of grid-scale ESS on distribution networks are:

- power losses,
- the hosting capacity[7], and
- network unbalance.

[7]In our study, the hosting capacity is defined as the total amount of new PV production that can be connected to the grid without creating voltage issues.

Power Losses

The primary task of the optimisation model is to reduce annual network energy losses. For the base scenario, without any ESS, simulations are performed for a year. The total network losses in summer, autumn, winter and spring are approximately 2530kWh, 2820kWh, 4660kWh and 2190kWh, respectively. It can be seen that the total energy loss in winter is significantly higher than other seasons due to the employment of heating facilities. The annual network loss is 12200kWh, which is expected to be decreased by implementing the two ESS configurations.

Hosting Capacity

The installed PV capacity is 130kW in the case that all PV system is rated at 1kW. In order to determine the hosting capacity, the rated power generation of PV systems on the entire feeder is gradually increased until the voltage threshold is met. This is most likely to occur at loads towards the end of the feeder. Simulation is performed in OpenDSS in which monitors are placed at all loads. An algorithm, which automatically increases PV generation until the voltage limit is exceeded, is implemented via the common interface shared between OpenDSS and Matlab. A typical summer day is tested using the algorithm since summer usually presents less network loading and reasonably high PV generation. The outcomes indicate that the upper limit is exceeded at bus 2266 at 1pm when each rated PV generation is raised to 2.10kW. This means that the hosting capacity for 100% PV penetration in this network, before installing any ESS, is 368kW.

Network Unbalance

This study also investigates the effects of ESS on the voltage unbalance factor (VUF), which is a measure of the network unbalance [174]. It can be calculated through the following equation:

$$\text{VUF} = 100\frac{v_{t,i}^{-}}{v_{t,i}^{+}}. \tag{6.23}$$

The VUF at each bus is determined in OpenDSS. The maximum and average VUFs of the network without ESS are 0.401% at bus 1940, as shown in Fig. 6.1, and 0.275%, respectively. Altough the VUFs is currrently well below the UK standard of 2%, it can increase in the future as PV penetration increases.

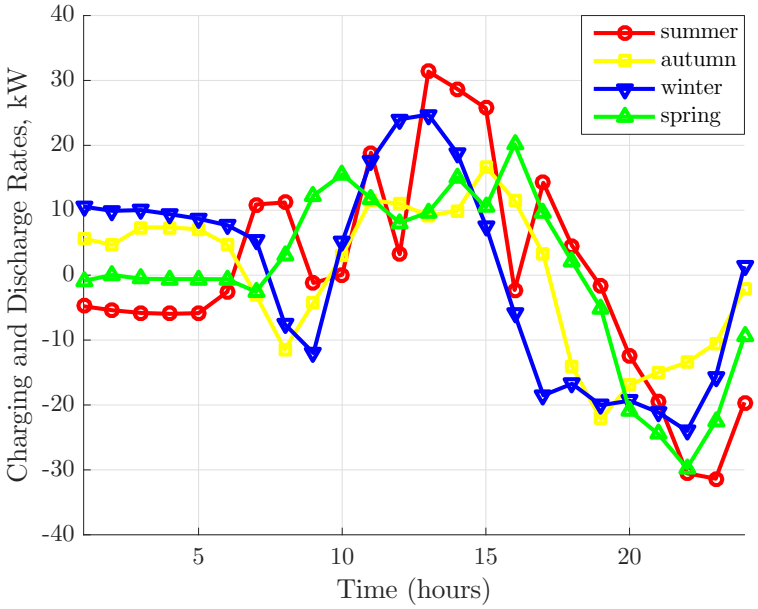

Figure 6.2: Charging and discharging rates on a typical day in each season, given that the maximum charging and discharging rates are 90kW.

6.4.3 Community ESS

The results of installing a CESS in the LV network are shown and analysed in this subsection.

Power Losses

Optimisation-based simulations are performed for one year, and the outcomes suggest an installation at bus 702[8] with the capacity being 942kWh. The initial state of charge for each cycle is 282kWh. The annual network energy loss in this case drops to 9410kWh which shows a 22.9% reduction compared with the base scenario. The detailed charging and discharging patterns of a sample day for each season are observed and presented in Fig. 6.2. It can be seen that summer presents the highest charging rates around mid-day due to high PV penetration. Meanwhile, the discharging period comes at around 4pm in winter as night falls faster, while this time is delayed in summer as expected. Due to the long discharging period in winter, the ESS must charge in early mornings to maintain the state of charge on the pre-defined level at the beginning of each cycle. The corresponding state of charge is illustrated by Fig. 6.3, in which the winter curve reaches its peak at 850kWh at around 5pm, earliest and highest among all, then drops rapidly due to the high energy consumption.

[8]Bus 702 is circled in red in Fig. 6.1. This is the optimal location of the three-phase community ESS decided by solving the OPF described in Section 6.2.

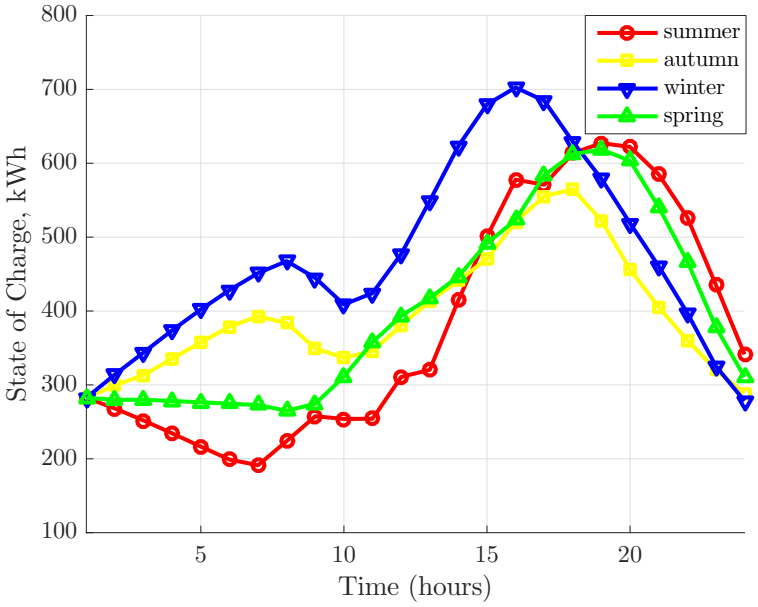

Figure 6.3: State of Charge on a typical day in each season

Hosting Capacity

The ESS with the same charging and discharging patterns is implemented in OpenDSS to quantify the hosting capacity in this scenario. Applying the same method as in the base scenario, an over voltage is discovered at bus 2266 on a typical summer day at 1pm with PV systems at all loads being rated at 2.71kW. This shows that the CESS is capable of increasing the hosting capacity of the network by 27.8%.

Network Unbalance

The maximum VUF in this scenario is improved from 0.401% to 0.381%, and the average VUF is decreased from 0.275% to 0.262%. This improvement can become more helpful when the VUF increases to high levels due to high PV penetration.

6.4.4 Distributed ESS

In this subsection, the results of installing multiple DESS, which have the same aggregated size as the CESS, in the network are detailed and compared with the performance indices and the first scenario.

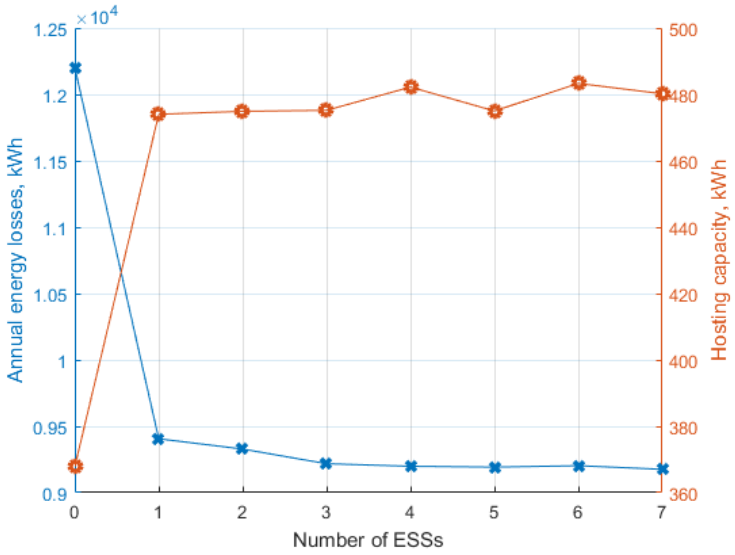

Figure 6.4: Annual energy losses (left) and hosting capacity (right) wrt number of ESSs

Power Losses

Table 6.1 and Fig. 6.4 indicate the improvements in annual energy losses and the hosting capacity with respect to different numbers of DESS. An obvious decrease in energy losses is discovered as the CESS is implemented. However, as the number of ESS continues to rise, the reduction immediately plateaus. When three ESSs are installed, energy loss is decreased only by 190kWh to 9220kWh from the previous scenario. After this, the reduction becomes subtle. This is because the aggregated size is fixed which is limiting the performance of the DESS. Thus, larger numbers of ESSs require further increase in the aggregated capacity to become more effective.

Greater number and size of DESS potentially provide greater power loss reductions, however, these also lead to higher installation cost. Usually, if the installation cost is considerable and the utilities expect the ESS to be up-gradable for greater performance in the future, multiple DESS can be applied. Further, the locations for DESS are fairly uniformly distributed on the main branch of the feeder, which allows the DESS to cover larger areas and become more effective. An example is shown in Fig. 6.1 where the optimal locations of three DESS are indicated by green squares.

Hosting Capacity

The results presented in Table 6.1 and Fig. 6.4 show that there is an obvious increase, 27.8%, in the hosting capacity after the CESS is installed. However, this rate reduces when the large ESS is divided into DESS. Specifically, after two installations, the curve experiences minor fluctuations

Table 6.1: Improvement in energy losses and the hosting capacity wrt different numbers of ESSs

No of ESSs	Locations	Sizes (kWh)	Power loss reduction	Increase in hosting capacity
1	702	942	22.9%	27.8%
2	234, 1704	527, 414	23.6%	29.1%
3	153, 676, 1786	322, 451 169	24.5%	29.2%
4	170, 652, 996, 1786	322, 427, 114, 78.3	24.6%	31.1%
5	153, 429, 728, 996, 1786	179, 269, 312, 63.7, 117	24.7%	29.2%
6	234, 652, 820, 1484, 1851, 2191	320, 346, 114, 57.7, 49.8, 54.9	24.8%	31.4%
7	153, 429, 728, 996, 1484, 1786, 1924	179, 269, 312, 39.3, 34.4, 17.4, 89.7	24.8%	30.6%

and the increase becomes subtle. The utilities must consider this with the trade-off between the ESS costs and performance introduced previously for deciding the most beneficial number of installations.

Network Unbalance

Table 6.3 shows the maximum and average VUFs with respect to different numbers of ESS. The maximum VUF, discovered at bus 1940, remains almost unchanged after replacing the CESS with multiple DESS. Meanwhile, the average VUF drops from 0.262% to 0.261% if three installations are applied. Beyond this number, the average VUF does not change. The difference between the CESS and DESS is almost negligible, and both scenarios present insignificant impacts on the network unbalance because this study adopts three-phase ESS which charge and discharge equal amount of power on each phase. This result is expected to improve when single-phase ESS are used instead.

Table 6.2: Max and average VUFs wrt numbers of ESSs

No of ESSs	Max VUF (%)	Location (bus no.)	Average VUF (%)
0	0.401	1940	0.275
1	0.381	1940	0.262
2	0.382	1940	0.262
3	0.381	1940	0.261
4	0.381	1940	0.261
5	0.381	1940	0.261
6	0.381	1940	0.261
7	0.381	1940	0.261

6.4.5 Comparisons of Community and Distributed ESS

Overall speaking, both CESS and DESS can accomplish the tasks described in this study. Minor improvement can be made when attempting to decrease the VUF by replacing the CESS with multiple DESS, while this improvement is larger regarding power losses and the hosting capacity. It is important to realise that the performance can be improved significantly when increasing the aggregated capacity of distributed ESSs. However, this is not the case for the CESS, for whom a further increase in size will result in more energy losses. Therefore, in general, DESS can be more effective than CESS if the correct number of DESS is placed at optimal locations with reasonable sizes, and consequently, they can make distribution upgrade deferral and increased PV generation a reality.

6.4.6 Community ESS Investment: ROV Analysis

The ROV framework captures the value of managerial flexibility, and therefore determines the optimal timing for the ESS investment. The process follows the LSMC method described in Section 6.3: (i) use the payoff ($\Pi_{t_n,\omega}$) to calculate the *continuation value*, $\Phi_{t_n,\omega,S_{t_n}}$, via least square regression, (ii) compare $\Phi_{t_n,\omega,S_{t_n}}$ with $\Pi_{t_n,\omega}$ using (4.6) in Chapter 4, and decide whether to execute the investment immediately, and (iii) calculate the option value using (4.7) in Chapter 4. The ROV suggests to wait for the market conditions to turn favourable if the deferral option value is positive, and the investment should only be executed when the payoff exceeds this option value.

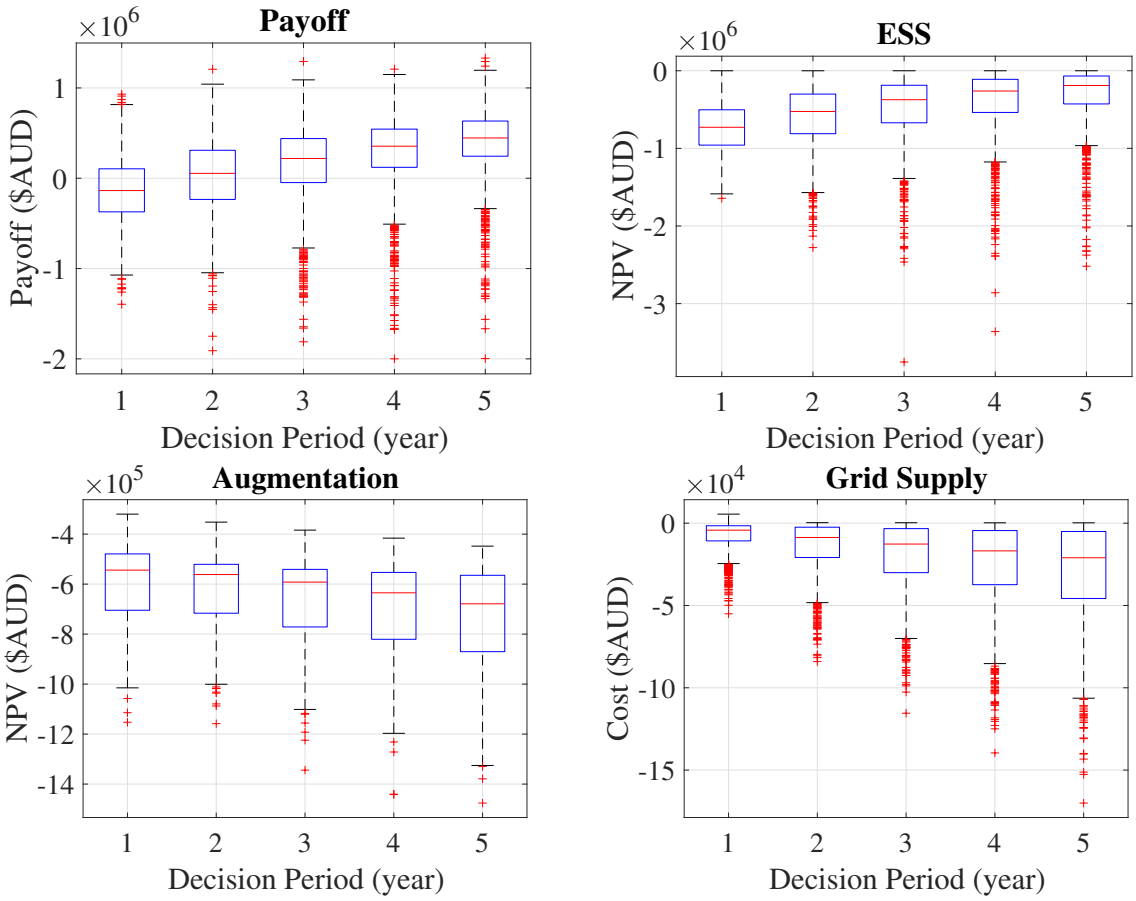

Figure 6.5: This figure shows the payoff for investing in grid-scale ESS in each year (top-left), the cost for investing in grid-scale ESS in each year (top-right), the cost for network augmentation (bottom-left), and the cost for grid supply that is above the transformer limit (bottom-right).

The payoff ($\Pi_{t_n,\omega}$), cost of ESS ($c_t^{\text{ESS}}{}_n$), cost of network augmentation ($c^{\text{aug}}_{t_n,\omega}$) and cost of energy delivered through the transformer that is above the thermal limit ($c^{\text{g}}_{t_n,\omega}$) are shown in Fig. 6.5. The average payoff increases from $-$\$135k in Year 1 to \$295k in Year 5, which is driven by the fast-declining ESS cost (Fig. 6.5, ESS). The amount of increase in the payoff over the decision period is reduced by the cost of annual grid supply reduction, $c^{\text{aug}}_{t_n,\omega}$, incurred by postponing the ESS installation, as shown in Fig. 6.5, Grid Supply. In other words, an early execution of the ESS investment can reduce the grid supply.

Based on the NPV calculated from the DCF, the investment is not profitable as the average payoff in Year 1 is negative, are shown in Fig. 6.5, Payoff, and therefore, this investment is abandoned. However, this decision is changed after taking into account the managerial flexibility under future uncertainties via ROV. Specifically, using the LSMC method, the option to invest is abandoned in the case of a negative payoff to reduce the computation time. Along each of the

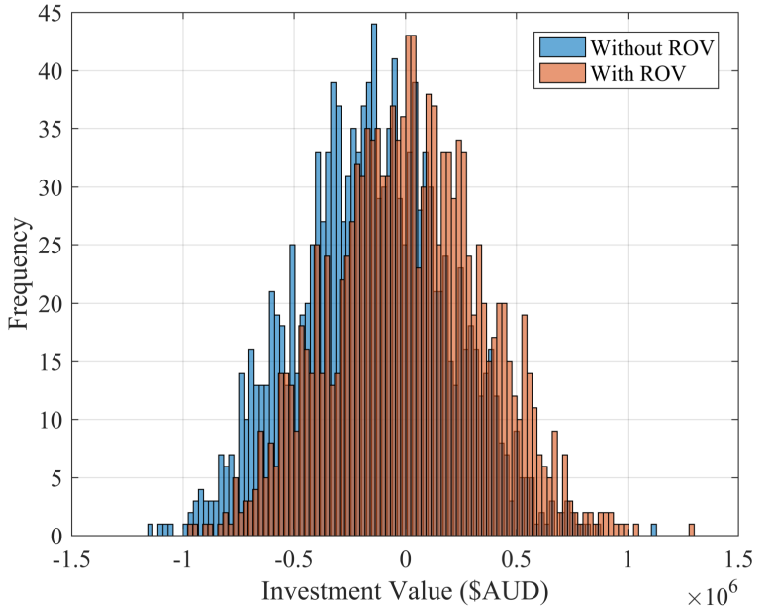

Figure 6.6: NPV distribution with and without flexibility for the deferral option

remaining paths, the optimal timing to execute the ESS investment is when the payoff is greater than the *continuation value* for the first time.

The deferral option value calculated by the ROV that incorporates future uncertainties is \$60k, which increases the payoff calculated from the DCF ($-$\$135k) by \$195k, this increase represents the value of managerial flexibility. This result shows that the ROV accounts for the opportunity values from future uncertainties, and thus draws different conclusions from the DCF analysis. Specifically, the fast-declining ESS cost is the main driver to this option value. Fig. 6.6 illustrates the probability distributions of the NPV from the traditional DCF method (blue) and the ROV (orange), respectively. It is observed that distribution has been shifted towards positive by deferring the investment, and this shift is created by the flexibility that the management holds to defer the investment to a later year when future uncertainties resolve.

Meanwhile, the ROV governed by the LSMC method provides the optimal investment strategy. Specifically, the LSMC computes the optimal investment timing (τ_ω) for each MC path, this extracts the frequency distribution of τ_ω, as shown in Table 6.3. The optimal investment timing is indicated by the greatest frequency. From this distribution, 33.1% of the MC paths have a greater payoff than the *continuation value*, in Year 2, followed by 24.2% in Year 3 and 10.4% in Year 3. The rest of the MC paths (2.5%) are abandoned due to a negative payoff. Thus, the ESS investment is recommended to be delayed to Year 2.

Table 6.3: Frequency distribution of optimal strategy

	Year 1	Year 2	Year 3	Year 4	Year 5	Not to invest
Frequency	6.5%	**33.1%**	24.2%	10.4%	6.5%	2.5%

6.5 Summary

This work proposed a novel methodology that can (i) explicitly incorporate ESS schedules within a MC analysis, and (ii) determine the optimal timing of a distribution network investment considering the option to deferral via ROV. The methodology first models the future stochastic variables, including power demand growth, varying electricity price and the declining ESS cost using the GBM, and then generate a large pool of MC paths characterised by these variables. Second, the framework linearised the branch flow model for computing the optimal ESS schedules. By doing so, the computation time is significantly reduced for solving one MC path, making the incorporation of ESS schedules within the MC analysis feasible. Third, the framework quantified the benefits brought by the ESS to the network, and use this as a measure to evaluate the economic performance of the investment via ROV. To demonstrate the efficacy of the proposed framework, I determined the optimal strategy in investing in a grid-scale ESS on an Australian LV feeder. The results show that the optimal investment timing is Year 2, followed by Year 3. Overall, this work demonstrated how to incorporate ESS operational decisions in a MC study, and hence evaluate the ESS investments in distribution networks considering future uncertainties via ROV. In addition, the method shows that grid-scale ESS can sufficiently increase network capacity, and therefore improve the hosting capacity of renewable generation in distribution networks.

Chapter 7

PV Investment Game

The rapid rise of photovoltaic (PV) installations in low-voltage (LV) distribution networks means that they are likely to exceed network hosting capacity. For this reason, distribution network service providers (DNSPs) have begun to mandate connection codes, such as inverter Volt/Var control (VVC) and/or PV active power curtailment (APC), to mitigate the resulting network problems. This approach manages the network state, but may cause an existing PV system to become inefficient as it is curtailed more often. Different from the previous chapters where DNSP is the main investor, in Chapter 7 network customers independently invest in their own PV systems.

In more detail, this work investigates the effects on overall economic efficiency and individual customer welfare of natural uncoordinated rooftop PV investment processes that arise when customers invest in PV systems independently to maximise their individual welfare. To do this, a novel game-theoretic framework is proposed to compute the annual payoffs to customers for different PV investment sizes, given the installations of other customers. This calculation is based on an optimal AC power flow model that includes inverter connection standards that link customers' annual payoffs via their effects on AC network voltages and consequent PV curtailment responses. The game shows that the interaction of PV investments produces a concave potential game with continuous action sets, which has a pure Nash equilibrium (NE) that can be found using an adaptive learning process. Then, to evaluate the efficiency of the investments under the game model, a centrally-coordinated PV investment profile is computed by solving an optimal PV sizing problem that maximises social welfare across all customers. Comparing the value of investment patterns for the game and the centrally-coordinated optimization shows: (i) the inefficiency of Nash equilibrium is 1.4, which indicates the efficiency loss resulting from uncoordinated PV investments, and (ii) the inequity of a skewed distribution of benefits,

penalising customers closer to the distribution transformer and benefiting those towards the end of the feeder. This model provides a quantitative tool for evaluating policies and regulations that improved coordination and allocation of PV hosting capacity (and that of other energy distributed energy resources (DER)) between customers on LV feeders.

The remainder of the paper is organised as follows. Section 7.1 formulates the PV investment game. Section 7.2 details the formulation of the optimal PV sizing problem that maximises social welfare across all customers. The inverter VVC and APC functions are included within this centrally-coordinated approach. Section 7.3 describes the adaptive learning algorithm that determines the NE. The proposed game is played on a typical Australian LV feeder and the results are discussed and compared with the centrally-coordinated solution in Section 7.4. Section 7.5 draws conclusions.

7.1 Preliminaries

This section provides details and characteristics of the proposed PV investment game. Formally, this work considers a class of *potential games*, which are a natural model for resource allocation in large networks [188]. In our work, the payoff of each player depends on the hosting capacity required by its PV installation and the number of players who are competing in the same distribution network with limited hosting capacity.

7.1.1 Concave Potential Games

This work focuses on games played by a finite set of players. We consider a repeated game $\mathcal{G} = \{\mathcal{I}, \Upsilon, u\}$, where $\mathcal{I} = \{1, ..., \imath\}$ is the set of players (network customers), $\Upsilon_\imath \subset R$ is a continuous normed action space. An action $\upsilon_\imath \in \Upsilon_\imath$ is regarded as an investment size chosen by individual players. Finally, $\xi = (\xi_\imath)_{\imath \in \mathcal{I}}$ is the vector of payoff functions, where $\xi_\imath$ is assumed to be differentiable in $\upsilon_\imath$ and strictly concave in $upsilon_\imath$.

Players aim to maximise their payoff by choosing an investment size, but they do not know their payoff functions $\xi = (\xi_\imath)_{\imath \in \mathcal{I}}$. As the game progresses, each player selects an action $\upsilon_\imath \in \Upsilon_\imath$ to update their payoff, which is determined by all players' action profile $\upsilon = \{\upsilon_1, ..., \upsilon_\imath\} \equiv (\upsilon_\imath; \upsilon_{-\imath})$, where $-\imath = \mathcal{I} \setminus \{\imath\}$. I wish to analyse how the interaction of customers on the LV network affects their incentives and their choice of PV investment sizes, with an objective to improving overall system efficiency. To do this, a stable pattern of PV investment is characterised as the *Nash equilibrium* of the PV investment game. Although the NE is an idealised solution concepts, which assumes flexibility in investment sizing, strong rationality

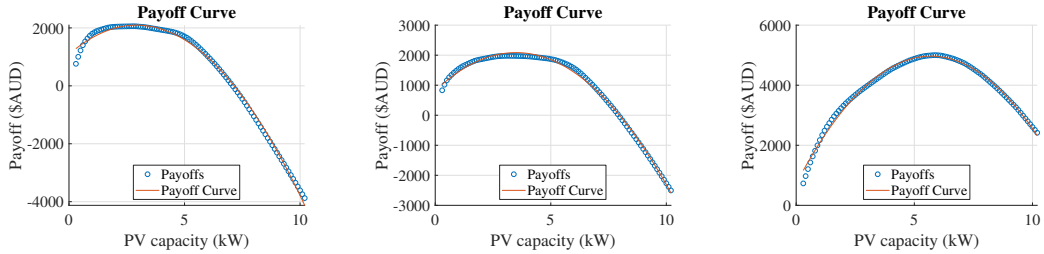

Figure 7.1: Payoff curves for three network customers who have a different payoff trajectory with respect to their PV investment size. Each player's payoff regression curve is approximated by increasing its own investment size, while others remain fixed.

of electricity customers and perfect monitoring of other customers actions', it is still useful for us to understand any *systematic* failures in the incentive design implicit in the combination of electricity pricing and connection codes. Such failures of incentive design can lead to significant inefficiencies in the pattern of rooftop PV investment; but models like the one developed in this chapter can be used to identify reforms and policy changes that reduce these inherent flaws (noting that it may not be possible to completely remove them, nor to change the behaviour of sometime economically-irrational electricity customers).

The game is in a pure NE (i.e. non-randomised) when no player has any incentive to change its (pure) action. This solution concept can be formally stated as:

$$u_\iota(\upsilon*_\iota;\upsilon*_{-\iota}) \geq u_\iota(\upsilon_\iota;\upsilon*_{-\iota}) \quad \forall \upsilon_\iota \in \Upsilon_\iota, \iota \in \mathcal{I}. \tag{7.1}$$

where $(\upsilon*_\iota)_{\iota\in\mathcal{I}}$ is the set of actions played in the NE.

This work relies on a well-known result that a pure NE exists if all players' payoff functions are *concave*. Following [189], it is shown that the game $\mathcal{G}$ is concave because the payoff functions are concave (and the action sets are convex).

In the absence of an analytic representation of the payoff function, I demonstrate payoff concavity in our game as follows. A player's payoff is computed as the sum of their energy costs over the year. Each time-slot's energy production is computed using an AC power flow model to calculate the payoff. This power flow model, run each half hour for a year, includes real-world characteristics such as inverter connection standards that link customers' annual payoffs via their effects on AC network voltages and consequent PV curtailment responses. Thus, on average over a year's operating conditions, the PV investment payoff is expected to be concave with respect to the PV installation capacity.

In more detail, the game setting is designed such that all systems on the same phase in the network will be curtailed by similar amount when over-voltage appears, as encoded in the

AS4777 connection code. PV generation is more frequently curtailed when large installations are present in the network. To illustrate this, the player's investment size increases, while others remain fixed, and calculate the corresponding payoff. Fig. 7.1 shows three players' payoff trajectories. Observe that the payoff regression line is concave over the domain of reasonable PV investment sizes. This shows that the game is concave and a pure NE exists.

Now that it is shown that the game is concave, an adaptive learning algorithm can be used to compute the NE of the PV investment game [163]. In this process, the game is repeated for $\psi \in \Psi$ iterations, and at each iteration, ψ, the players adapt by updating their current choice of action according to their previous action and how the previous payoff has varied. In brief, the players investment size move in the same direction as the previous iteration if their previous payoff has increased. Conversely, they move in the opposite direction if the payoff has decreased. The step size of these moves is proportional to the variation in payoff, and every player uses the same rule simultaneously. Details of this algorithm are provided in Section 7.3, but the important feature of this learning algorithm is that the magnitude by which player ι changes its action is proportional to the variation in payoff from the previous iteration.

Before outlining the learning algorithm used to compute the NE, the next section describes the socially-optimal PV sizing problem, making use of the tools of optimal power flow (OPF).

7.2 Optimal Power Flow Formulation

This section formulates the PV inverter VVC function with APC for all consumers in a distribution network as a constrained OPF problem. The main objective is to minimise the sum of all customers' cost, given the PV investment size as a decision variable. This is considered as the socially-optimal solution. This solution is used to calculate the inefficiency of the uncoordinated PV investment game, which is the ratio of socially-optimal solution from the OPF and the game's NE solution.

Specifically, the VVC function specified in AS4777 aims to regulate voltage at each connection point, and allows for a greater installation capacity and payoff. On the other hand, the APC function curtails PV generation when the reactive power support is insufficient to eliminate all over-voltages. Incorporating these functions within the centralised OPF releases more hosting capacity to the network.

7.2.1 Objective Function

The objective of the social welfare maximising problem is to minimise the sum of all customers' energy cost (c^{e}) and the investment cost (c^{inv}). A fair allocation of curtailment across the network also requires to minimise the maximum APC ($\hat{p}^{\mathrm{c}}$) in the same objective function; that is:

$$\underset{S_{\mathrm{pv}},q_g,p_{\mathrm{g}}}{\text{minimise}} \quad \sum_{t=1}^{T}(c^{\mathrm{e}}+c^{\mathrm{inv}}+\hat{p}^{\mathrm{c}}), \tag{7.2}$$

where p_g and q_g are active and reactive power from each PV system.

7.2.2 Branch flow Constraints

Load flows in LV networks with numerous branches can be difficult to solve, especially when the network is unbalanced and each phase must be taken care of individually. In this case, the branch flow constraints are employed to accurately model power flows in distributed networks. Specifically, let $G(\mathcal{K},\mathcal{L})$ be a graph representing a radial distribution circuit. Each node in $\mathcal{K}$ is a bus and each link $(i,j)\in\mathcal{L}$ is a line. In addition, $\mathcal{D}_{\mathrm{load}}$ is denoted as the set of buses that are assigned with a load in the network.

$$p_{t,ij}=\sum_{jk\in\mathcal{L}}p_{t,jk}+R_{ij}l_{t,ij}+p^{\mathrm{d}}_{t,j}-p^{\mathrm{g}}_{t,j}, \tag{7.3}$$

$$q_{t,ij}=\sum_{jk\in\mathcal{L}}q_{t,jk}+X_{ij}l_{t,ij}+q^{\mathrm{d}}_{t,j}-q^{\mathrm{g}}_{t,j}, \tag{7.4}$$

$$p^{\mathrm{g}}_{t,j}=p^{\mathrm{pv}}_{t,j}-p^{\mathrm{c}}_{t,j} \quad \forall j\in\mathcal{D}_{\mathrm{load}}, \tag{7.5}$$

$$0\le p^{\mathrm{c}}_{t,j}\le p^{\mathrm{pv}}_{t,j} \quad \forall j\in\mathcal{D}_{\mathrm{load}}, \tag{7.6}$$

$$v_{t,i}l_{t,ij}\ge p^2_{t,ij}+q^2_{t,ij}, \tag{7.7}$$

$$\rho_{t,j}\ge (p^{\mathrm{g}}_{t,j})^2+(q^{\mathrm{g}}_{t,j})^2, \tag{7.8}$$

$$0\le\rho_{t,i}\le\bar{S}_i^2 \quad \forall i\in\mathcal{D}_{\mathrm{load}}, \tag{7.9}$$

$$v_{t,j}=v_{t,i}-2\left(p_{t,ij}R_{ij}+q_{t,ij}X_{ij}\right)+\left(R^2_{ij}+X^2_{ij}\right)l_{t,ij}, \tag{7.10}$$

$$V^2\le v_{t,i}\le\bar{V}^2, \tag{7.11}$$

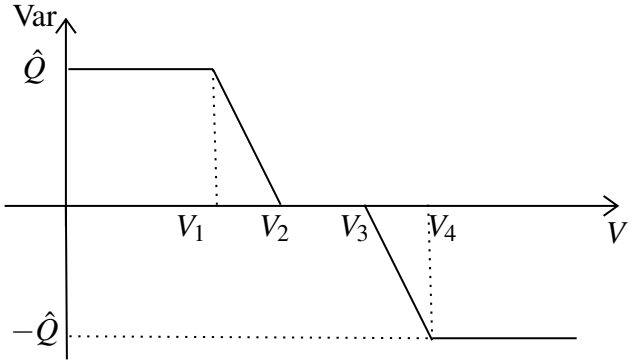

Figure 7.2: The Volt/Var control curve.

$$\hat{p}^{\mathrm{c}}_t \geq p^{\mathrm{c}}_{t,i} \quad \forall i \in \mathcal{D}_{\mathrm{load}}. \tag{7.12}$$

The branch flows are governed by (7.3) and (7.4), where the active power flow $p_{t,ij}$ on each phase from bus i to bus j is formulated as a function of power flow ($p_{t,jk}$) and power loss entering bus j, and the generation ($p^{\mathrm{g}}_{t,j}$) and consumption ($p^{\mathrm{d}}_{t,j}$) at bus j. I set the constraints for PV curtailment $p^{\mathrm{c}}_{t,j}$ using (7.5) and (7.6). The voltage constraints are described by (7.10) and (7.11). Given by (7.12), the maximum PV curtailment ($\hat{p}^{\mathrm{c}}$) should be greater or equal to all network curtailments. By minimising $\hat{p}^{\mathrm{c}}$, PV curtailment is fairly curtailed across the network.

The maximum available reactive power is fed to the droop control method detailed below to determine the reactive power output from an inverter. As shown in Fig. 7.2, this droop control curve, given by the AS 4777 standard, specifies the amount of Q injection/absorption based on the voltage level calculated by (7.10) and the maximum reactive power $\bar{Q}$, which is normally defined as a percentage of the inverter's maximum capacity $\bar{S}_i$ at the point of connection. The droop curve is described mathematically as follows:

$$Q^*(V_{t,i}) = \begin{cases} \bar{Q} & V_{t,i} \leq V_1 \\ \bar{Q}\frac{V_{t,i}-V_1}{V_1-V_2} & V_1 \leq V_{t,i} \leq V_2 \\ 0 & V_2 \leq V_{t,i} \leq V_3 \\ \bar{Q}\frac{V_{t,i}-V_3}{V_4-V_3} & V_3 \leq V_{t,i} \leq V_4 \\ -\bar{Q} & V_4 \leq V_{t,i} \end{cases}$$

The set points, V_1, V_2, V_3 and V_4 are the voltages which define the dead-band (between V_2 and V_3) and the active bands of the VVC curve. The above formulation introduces mixed integers and non-convexity to the problem which is already nonlinear. Thus, incorporating it within the OPF

model for assessing the impact of the VVC function creates a non-convex MINLP. In this regard, this work uses constraints (7.7) and (7.8) to relax and transform the non-convex optimization model into a *mixed integer second order cone program* (MISOCP), and CPLEX has been used to solve this problem.

7.3 Methodology

This section details the steps taken to assess the cost-reflectivity in the allocation of distribution network hosting capacity to LV residential consumers. The method to calculate each player's payoff is explained, followed by the algorithm that leads the game to the NE.

7.3.1 Payoff Calculation

The future costs of the PV investment need to be discounted via the traditional net present value (NPV) method as follows before calculating the payoffs:

$$NPV = \sum_{n=1}^{N} \frac{c_{t_n}}{(1+r)^{t_n}}. \tag{7.13}$$

where r is the risk-free discount rate[1]. The life time of each PV system is denoted as $t_n \in \mathcal{T}_{\text{pv}}$, where $n \in \mathcal{N}$ is the set of years in $\mathcal{T}_{\text{pv}}$.

The OPF analysis is run for the investment profile $\upsilon_\iota \in \Upsilon_\iota$ in each round of play. The equation that computes each player's payoff Π_ι can be formally stated as:

$$\Pi_\iota(\upsilon) = \sum_{n=1}^{\iota} (c_\iota^{\text{pv}}(\upsilon)) - c_\iota^{\text{inv}}(\upsilon). \tag{7.14}$$

where c_ι^{inv} is the cost of PV procurement and installation and c_ι^{pv} can be stated as:

$$c_\iota^{\text{pv}}(\upsilon) = c_\iota^{\text{r}}(\upsilon) - \hat{c}_\iota^{\text{e}}(\upsilon) + c_\iota^{\text{e}}(\upsilon), \tag{7.15}$$

where c_ι^{r} is the revenue from exporting to the grid, $\hat{c}_\iota^{\text{e}}$ and c_ι^{e} is the electricity cost with and without PV system. The payoff after each iteration of the game is obtained, which enables us to draw the payoff trajectory for each player $\iota \in \mathcal{I}$.

[1]This work assumes that the future costs are risk free. Thus, this value is fixed to be a constant (0.06).

Algorithm 4 Potential Game Solver

Start the game.
for $\psi \in \Psi$ **do**
  Run yearly optimal power flow simulations.
  for $\iota \in \mathcal{I}$ **do**
    Calculate $\Pi_{\iota,\psi}$ using (7.14) and (7.16).
    Calculate the change in payoff $\bigtriangledown \Pi_{\iota,\psi}$.
    if $\Pi_{\iota,\psi} \geq \Pi_{\iota,\psi-1}$ **then**
      $\upsilon_{\iota,\psi+1} = \upsilon_{\iota,\psi} + b_{\iota,\psi}(\gamma \bigtriangledown \Pi_{\iota,\psi})$.
    else if $\Pi_{\iota,\psi} < \Pi_{\iota,\psi-1}$ **then**
      $\upsilon_{,\psi+1} = \upsilon_{\iota,\psi} - b_{\iota,\psi}(\gamma \bigtriangledown \Pi_{\iota,\psi})$.
    end if
  end for
  if $\bigtriangledown \Pi_{\iota,\psi} < \theta \quad \forall \iota \in \mathcal{I}$ **then**
    The game has reached the NE.
    End the game.
  end if
end for

7.3.2 Computing the Nash Equilibrium

The algorithm that finds find the NE is detailed in Algorithm 4. Specifically, in each iteration of the game, each player decides their investment size based on how their payoff has varied from the previous iteration $\bigtriangledown \Pi_{\iota,\psi}$. In this regard, if the investment payoff has increased because the player raised its investment size in the previous iteration, then it should move in the same direction (increase the investment size) in the current iteration. In contrast, the player should move in the opposite direction when the payoff has decreased compared to the previous iteration. According to this rule, a player's next action can be formally stated as:

$$\upsilon_{\iota,\psi+1} = \upsilon_{\iota,\psi} + b_{\iota,\psi}(\lambda \bigtriangledown \Pi_{\iota,\psi}), \tag{7.16}$$

where $b_{\iota,\psi}$ is a variable which indicates the direction of the player's previous move and λ is a scaling factor. The payoffs are expected to reach a state where each payoff trajectory remains on the same level as the game continues progressing. While this, the game has reached the NE because there is no incentive for any player to make a move. In our game, the stopped criteria is when the variations in all players' payoff are consistently less than a threshold θ for a set of the most recent iterations in Ψ.

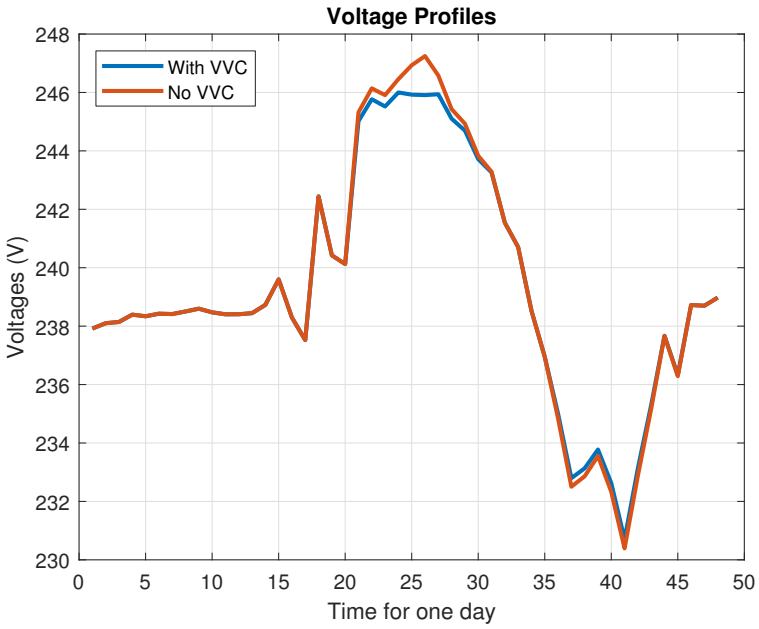

Figure 7.3: Voltage profiles on a randomly selected day for a consumer with 2kW PV system with (blue) and without (red) the VVC function.

7.4 Results and Evaluation

This section evaluates the proposed PV investment game on a typical Australian LV network. First, the impact of the VVC function with APC is assessed on voltage regulation with different levels of PV penetration. Second, the results are compared from the natural uncoordinated process simulated by the game model and the centrally-coordinated approach.

7.4.1 Test Networks

An LV test network adopted from Electricity North West Limited (ENWL), a British network operator [1] is used to examine the efficacy of the method. Typically, Australian LV networks are designed to have higher capacity than the UK ones, mainly due to much larger air-conditioning loads. To match this design, the UK test network is transformed into an Australian-type LV network by tripling the transformer and line capacity[2]. This feeder is supplied by a 400kVA 11kV/0.4kV 3-phase transformer. In total, 39 customers reside on the feeder, with 14 on phase A, 12 on phase B and 13 on phase C.

[2]For transformers, I reduced the impedance, while for transmission lines I only reduced the resistance. The reactance mainly depends on the distance between the conductors, so I left it unchanged.

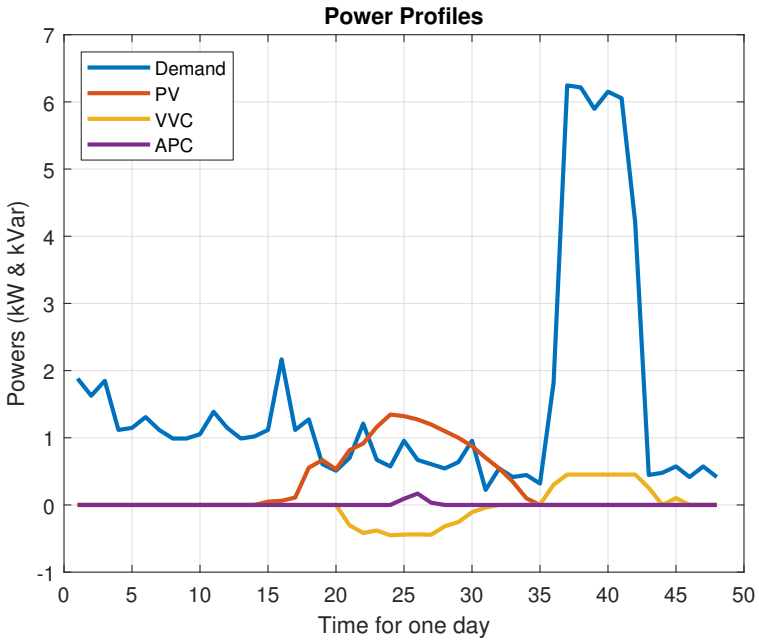

Figure 7.4: Demand, PV generation, reactive power output and PV curtailment on a randomly selected day for a consumer with 2kW PV system.

7.4.2 Impact of the VVC function

This subsection demonstrates the efficacy of the VVC function with APC specified by AS4777 on voltage regulation. In our work, the voltage set points from $\hat{V}_1$ to $\hat{V}_4$ are 234V, 237V, 243V and 246V, respectively.

Here, I assess the efficacy of the inverter VVC and APV functions within a centralised OPF detailed in Section 7.2 and obtain the centrally-coordinated solution. Specifically, Fig. 7.3 shows the voltage profile with/without the inverter VVC function, and Fig. 7.4 shows the demand, PV generation & curtailment and reactive power profiles for a network customer who has a PV system. The PV investment size is 2kW and the generation reaches just under 1.5kW at around 12:00pm. Because of the low demand and high PV generation (Fig. 7.4, blue and red curves), over-voltage appears and reaches 247V (Fig. 7.3, red curve), which is above the pre-defined limit at 246V. Consequently, VVC absorbs roughly 0.5kVar reactive power and APC curtails only 0.2kW PV generation to eliminate the over-voltage, as seen in Fig. 7.4, yellow and purple curves. Thus, the VVC and APC functions work together to ensure that the voltages are within the pre-defined limits at all times.

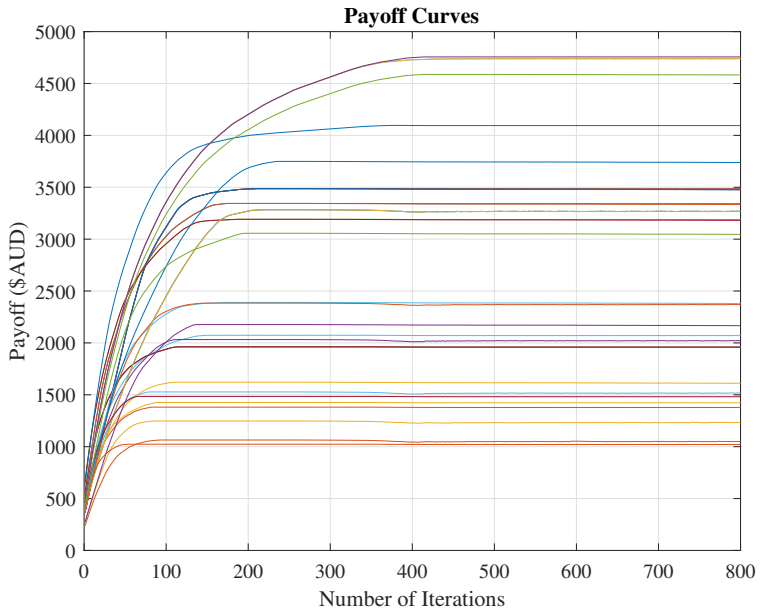

Figure 7.5: Payoff curves with respect to the number of iterations for all 39 players.

7.4.3 PV Investment Game

This subsection analyses the NE results from the PV investment game and compare them against the centrally-coordinated solution.

The first task is to examine the payoff curves for all players with respect to the number of iterations, as plotted in Fig. 7.5. While playing, each player's payoff increase until finding the maximum, they remain on the same level of payoff. This happens because the players attempt to stay at the maximum payoff by adjusting its action based on how their payoff has varied from the previous iteration, as specified in Algorithm 4. Alongside Fig. 7.5, similar trends are observed for the increase in the individual investment sizes (Fig. 7.6). As the payoff variation decreases, the incremental step in the investment size decreases. When this step size for every player is less than a threshold, all players are assumed to have no incentive to change their actions and the game has reached the NE. As observed in Fig. 7.6, the game has reached the NE after 500 iterations.

It is observed that for some customers, their PV size continues to increase after reaching the maximum payoff, as shown in Fig. 7.5 and Fig. 7.6. This is because the PV systems that reach the maximum payoff early will likely be curtailed more as the surrounding PV systems continue to increase in size. Then, if these customers hope to maintain the maximum payoff they will need to increase their size by a little as well. This means that they will get curtailed more on some days, but they are also generating more (greater savings) on other days.

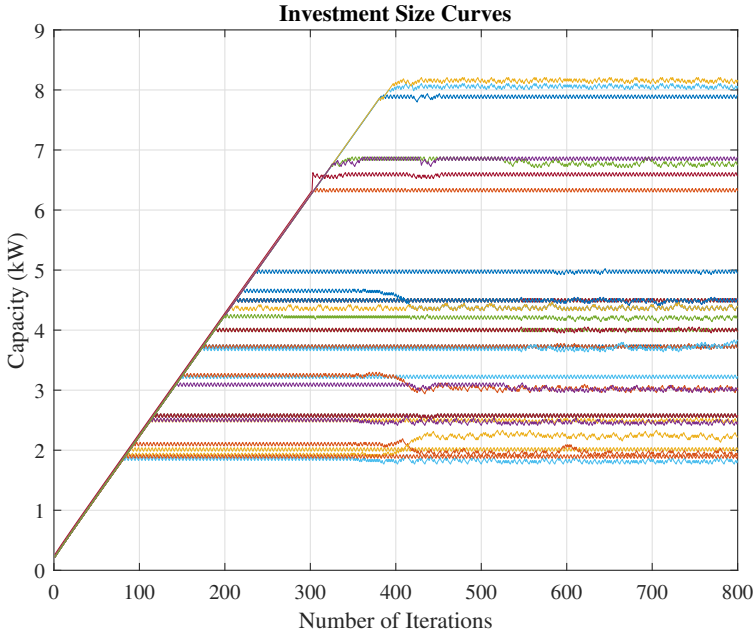

Figure 7.6: PV investment size curves with respect to the number of iterations for all 39 players.

From the centrally-coordinated solution, more than 60% of the network customers experience an reduction in their investment size, as seen in Fig. 7.7[3]. This mostly happens to the customers towards the end of the feeder. On the other hand, customers that are closer to the transformer see their sizes increase. This is because the natural uncoordinated process simulated by the game allows each customer to selfishly increase their size to improve payoff but neglects the larger impacts that the end-of-line investments have on network operations. For example, if one customer, by selfishly increasing its PV capacity, limits the capacity or curtails the output of others to the point where more is imported from the grid overall, their investment payoffs will decrease. Because of this, curtailments happen more frequently under the game, and the investments become inefficient.

Thus, under the game, the aggregated investment size increases by roughly 20% compared to the centrally-coordinated solution. This selfish behaviour of the end-of-line customers disproportionately affect customers near the feeder head.

Looking at the investment payoffs, the aggregated annual investment payoff is roughly 60% of the centrally-coordinated solution, in which nearly all customers have their payoffs increased. Greater improvements are observed for those that are closer to the feeder head, as seen in Fig. 7.8. This is an expected result because the natural uncoordinated process allows the end-of-feeder customers to selfishly increase their PV size, which limits the potential for those closer to the

[3]From Fig. 7.7 to Fig. 7.10, the customers are ordered by the distance to the transformer.

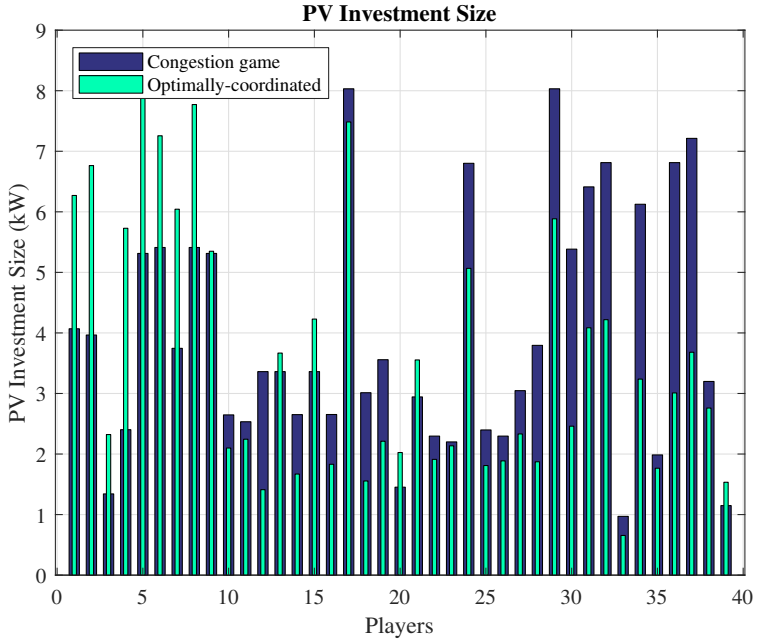

Figure 7.7: PV investment sizes from the game and the centrally-coordinated solution.

feeder head. Interestingly, the annual payoffs of the end-of-line customers are also improved under central coordination. This is because their large PV systems are getting more frequently curtailed under the game. As a result, overall, the uncoordinated melee leads to less total generation and less total investment payoff.

In addition, the total PV generation shown in Fig. 7.9 follows the investment sizes in Fig. 7.7. Under the centrally-coordinated approach, customers sitting on a shorter distance to the transformer are able to utilise a greater total PV capacity, which leads to larger PV generation. Further, energy cost is reduced for only about half of the customers, as observed in Fig. 7.10. This shows that the additional payoff obtained by the centrally-coordinated approach is mostly contributed by the revenue earned by feeding energy to the grid. In contrast, although the end-of-line customers are able to generate more due to their larger installation sizes under the game, their energy cost is sometimes higher because of a more frequent curtailment, and their payoffs are lower because of a greater capital cost.

The inefficiency of Nash Equilibrium given the ratio between the total investment payoff from the centrally-coordinated solution and the NE solution is nearly 1.4. This shows that even assuming hyper-rational and flexible customers, the nature of the setting is the one that leads to inefficiency. This indicates a failure in the incentive design inherent in the interaction of pricing and PV inverter control, and motivates a deeper investigation of pricing and inverter connection code redesign.

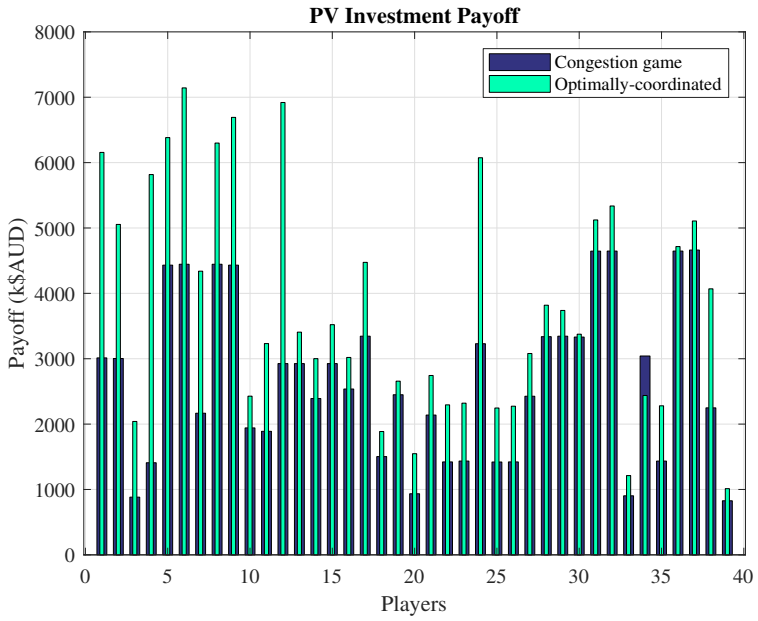

Figure 7.8: Investment payoffs from the game and the centrally-coordinated solution.

7.5 Summary

This chapter proposed a game theoretic approach to simulate the natural uncoordinated process for customers investing in PV systems in a distribution network. The game considered the customers unsophisticated but having flexibility to selfishly improve their own payoff. Specifically, they had no information regarding the rest of the network and can only decide their own investment size based on how their previous payoffs have varied. The game had a pure NE because the investment payoff was concave in the installation capacity. To demonstrate the efficiency of this natural uncoordinated process, this work formulated a centrally-coordinated optimal sizing problem considering both the VVC and APC functions to determine the optimal investment profile for each customer. Solving both the game and the centrally-coordinated approach showed that the uncoordinated melee leads to less total generation and less total investment payoff. Then, the inefficiency of Nash equilibrium of 1.4 was obtained, which indicated the efficiency loss from uncoordinated PV investments. This result demonstrated that even assuming hyper-rational and flexible customers, the nature of the problem was the one that leads to inefficiency. In addition, the game and the centrally-coordinated models that were developed in this work helped us to understand any systematic failures in the incentive design implicit in the combination of electricity pricing and connection codes (i.e. the VVC and APC functions specified by AS4777). Inefficient rooftop PV investments were shown as an example that is led by these failures. In this regard, the models developed can be used to identify reforms and policy changes that reduced

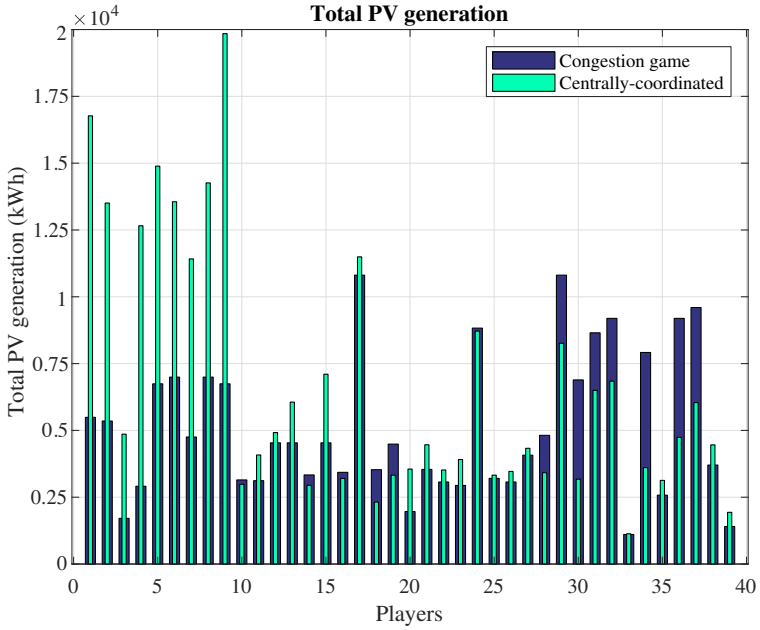

Figure 7.9: Annual PV generation from the game and the centrally-coordinated solution.

inherent flaws.

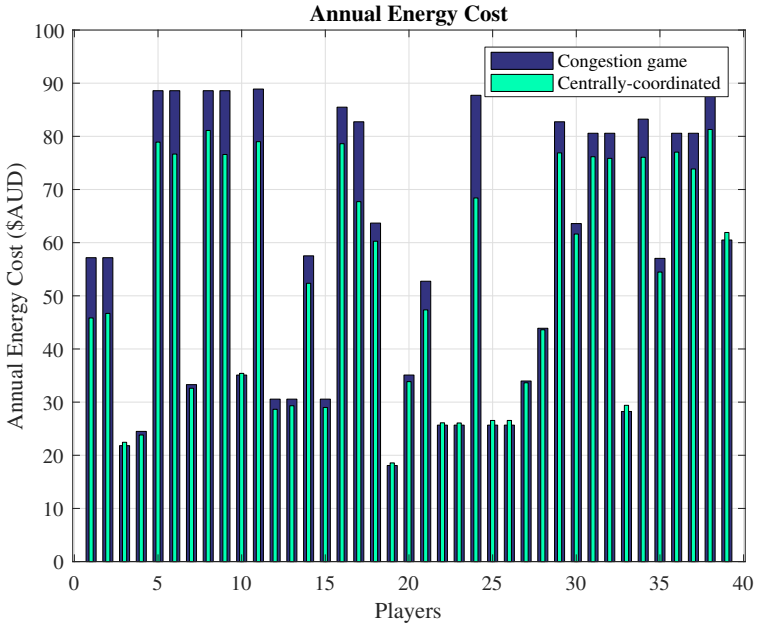

Figure 7.10: Annual Energy cost from the game and the centrally-coordinated solution.

Chapter 8

Conclusions

This chapter presents an overview of the contributions made in this thesis in light of the research objectives outlined earlier in Chapter 1. Section 8.1 summarises the technical contributions and results discussed in the preceding technical chapters.

8.1 Summary of Results

The main aim of this thesis was to develop new methods and tools to capture the technical and economic benefits of distributed energy resources (DER) for both residential customers and distribution network service providers (DNSPs). From the review of the existing literature in Chapter 2, it is challenging for DNSPs to assess the benefits from investing in residential and grid-scale DER projects due to two reasons: (i) including flexible DER such as battery energy storage systems (ESS), electric vehicles and loads with thermal inertial into a probabilistic analysis based on Monte Carlo (MC) simulation for studying their impact on the network is computationally impractical, because their operational profiles need to be determined in each MC simulation by computationally intensive optimization; (ii), MC analysis requires a large pool of statistically-representative demand profiles to sample from, but in many jurisdictions smart metering data are scarce; and (iii), financial appraisals involve real options valuation (ROV) is generally not applicable for this type of investments because the net present value (NPV) is always negative and not close to zero, and the uncertainties around sizing, location and operation of DER are difficult to capture. Due to these challenges, the current literature lacks a comprehensive methodology that evaluates the technical and economic benefits of DER investments. Moreover, it is also important to visualise and understand any systematic failures in

policies and regulations that are involved in these DER investments, such as DER connection standards, for improving network resource allocation.

This thesis developed a list of tools and methods to overcome the above challenges. First, Chapter 3 presented a probabilistic framework for assessing the impacts of schedulable DER at different uptake rates in LV networks. Residential PV-battery systems were used as an example DER to demonstrate the efficacy of the proposed framework. Specifically, the framework incorporated home energy management (HEM) operational decisions within a Monte Carlo (MC) power flow analysis comprising three parts. First, due to the unavailability of a large number of load and PV traces required for MC analysis, a maximum a-posteriori Dirichlet process was used to generate statistically representative synthetic profiles. Second, a policy function approximation (PFA) that emulates the outputs of the HEM solver was implemented to provide battery operational decisions for the large pool of synthesised customers, making the simulation of optimization-based HEM feasible within MC studies. Third, the resulting net loads were used in a MC power flow time-series study. The efficacy of the method was shown on three typical LV feeders. Our assessment found that uncoordinated PV-battery systems have little beneficial impact on LV networks, which was against the conjecture that the prevalence of batteries will serendipitously mitigate the technical problems induced by PV penetration.

Second, this thesis developed a financial appraisal that enables the application of ROV and considers network uncertainties for valuing the investment in DER projects. Three case studies were used to examine the efficacy of the proposed framework. In particular, Chapter 4 compared the investment in subsidizing PV-battery systems to the investment in a diesel generator for injecting power at the substation for peak demand support. Specifically, a ROV framework was proposed to determine the optimal plan for executing multiple interacting options to increase the investment value. Chapter 5 evaluated the investment in residential ESS, considering network uncertainties and the operation of ESS by incorporating the impact assessment framework developed in Chapter 3. Similarly, Chapter 6 assessed the investment in grid-scale ESS by integrating an AC optimal power flow model within the ROV framework.

The results indicated that developing an optimal strategy to execute the options upon the realisation of future uncertainties increases the investment value and mitigates the risk of financial losses. More importantly, supported by numerous case studies in this thesis, the proposed framework can be used by DNSPs to perform technical and economic assessments on different network investments in schedulable DER. These case studies showed that following appropriate investment plans proposed by ROV makes DER investments more appealing than investment applications such as diesel generators and network augmentations. Moreover, ROV

provides benefits when systematically considering the interactions between options, beyond those available when the options are calculated individually, even if the subsequent option is unlikely to be executed.

Finally, this thesis proposed a game-theoretic model in Chapter 7 to simulate the uncoordinated process that the network customers undertake to invest in PV systems under recent standards in AS4777 on PV inverters, including the Volt-Var control (VVC) and active power curtailment (APC) functions. The loss of efficiency for PV investments under these standards was calculated by comparing against a centrally-coordinated solution from solving an optimal PV sizing problem. The case study shows that the proposed game and the centrally-coordinated models can help DNSPs understand any systematic failures in policies and regulations for improving network resource allocation. Inefficient rooftop PV investments were shown as an example that was led by these failures caused by the inverter connection standards specified in AS4777.

8.2 Future Research

The methods and tools proposed in this thesis is a step towards the efficient use of financial assessment tools such as ROV on the investments in emerging DER technologies. Given the topics covered in this thesis, there still remain other issues that need investigation and further research. In this section, a list of further works specific to each technical contribution discussed earlier is described below.

- **Probabilistic Impact Assessment Framework:** The main future works involved are to (i) investigate further on the accuracy of the PFA using other machine techniques; (ii) study the technical benefits of other schedulable DER, such as electrical vehicles, that are equipped by HEM; (iii) apply coordination to DER scheduling for improving the technical benefits; and (iv) study the effectiveness of peer-to-peer trading with network constraint envelops on improving the technical benefits from schedulable DER [190].

- **Financial Assessment on DER investments via ROV:** Use the integrated ROV framework proposed in Chapters 4 to 6 to study the economic benefits of the investments in other emerging DER technologies and design the optimal plan to maximise the investment value for the DNSP.

- **Game-theoretic Framework:** Further research regarding this topic includes (i) examining the efficiency of flat limits on export or PV capacity; (ii) altering the network tariff a

customer pays based on their effect on the hosting capacity, the challenge is to explicitly consider the network charges by studying the effect of each customer on peak demand; and (iii) adding battery storage to the model. The inclusion of battery storage would make the OPF problem with VVC constraints computationally challenging. In response to this, a distributed approach could be used, as shown in [191].

Bibliography

[1] Electricity North West Limited. (2014) Low voltage network solutions. [Online]. Available: https://www.enwl.co.uk/go-net-zero/innovation/smaller-projects/low-carbon-networks-fund/low-voltage-network-solutions/

[2] Ineternational Energy Agency, "Trends in Photovoltaic Applications," Tech. Rep., 2018.

[3] AEMO, "Projections of uptake of small-scale systems," Tech. Rep., 2017.

[4] ——, "Technical integration of distributed energy resources," Tech. Rep., 2019.

[5] R. Tonkoski, D. Turcotte, and T. H. El-Fouly, "Impact of high PV penetration on voltage profiles in residential neighborhoods," *IEEE Trans. Sustainable Energy*, vol. 3, no. 3, pp. 518–527, 2012.

[6] G. Shrestha and P. Fonseka, "Flexible transmission and network reinforcements planning considering congestion alleviation," *IEE Proceedings-Generation, Transmission and Distribution*, vol. 153, no. 5, pp. 591–598, 2006.

[7] NREL, "The cost of distribution system upgrades to accommodate increasing penetrations of distributed photovoltaic systems on real feeders in the united states," Report, 2018.

[8] Clean Energy Council, "The Clean Energy Australia Report 2018," Report, 2018.

[9] Y. Ma, D. Azuatalam, T. Power, A. C. Chapman, and G. Verbič, "A novel probabilistic framework to study the impact of photovoltaic-battery systems on low-voltage distribution networks," *Applied Energy*, vol. 254, p. 113669, 2019.

[10] Climate Change Council, "Fully Charged: Renewables and Storage Powering Australia," Tech. Rep., 2018.

[11] AEMO, "AEMO observations: Operational and market challenges to reliability and security in the NEM," Report, 2018.

[12] ——, "Projections of uptake of small-scale systems," Report, 2017.

[13] T. Brinsmead, P. Graham, and J. Qiu, "Economic benefits of the electricity network transformation roadmap," CSIRO report for Energy Networks Australia, Tech. Rep., 2017.

[14] P. Kodukula and C. Papudesu, *Project valuation using real options: a practitioner's guide*. J. Ross Publishing, 2006.

[15] S. Vlaović-Begović, M. Momčilović, and S. Jovin, "Advantages and limitations of the discounted cash flow to firm valuation," *Škola biznisa*, no. 1, pp. 38–47, 2013.

[16] G. Verbič and C. A. Canizares, "Probabilistic optimal power flow in electricity markets based on a two-point estimate method," *IEEE Trans. Power Systems*, vol. 21, no. 4, pp. 1883–1893, 2006.

[17] AEMO and Energy Networks Australia, "Open Energy Networks Consultation Paper," Tech. Rep., 2018.

[18] CIGRE, "Smart Metering, Regulatory Aspects, Standards and Development Status," CIGRE Report No. 678, 2017.

[19] Y. Ma, K. Swandi, A. C. Chapman, and G. Verbič, "Multi-stage compound real options valuation in residential PV-battery investment," *Energy*, vol. 191, p. 116537, 2020.

[20] AEMO, "Energy supply outlook, for eastern and south-eastern Australia," Report, 2017.

[21] P. Scott, D. Gordon, E. Franklin, L. Jones, and S. Thiébaux, "Network-aware coordination of residential distributed energy resources," *IEEE Trans. Smart Grid*, 2019.

[22] E. Franklin, "Agents of change: Making batteries go extra mile," *ReNew*, vol. 136, pp. 56–58, 2016.

[23] Y. Ma, A. C. Chapman, and G. Verbič, "Strategic valuation of compound options for the investment in residential battery systems," *Under review by IEEE Trans. Power Systems*, 2020.

[24] Y. Ma, M. S. S. Abad, D. Azuatalam, G. Verbič, and A. C. Chapman, "Impacts of community and distributed energy storage systems on unbalanced low voltage networks," in *2017 Australasian Universities Power Engineering Conference (AUPEC)*. IEEE, 2017, pp. 1–6.

[25] V. G. Ma, Yiju and A. C. Chapman, "Estimating the option value of grid-scale battery systems to distribution network service providers," in *PowerTech, Milan*. IEEE, 2019, pp. 1–6.

[26] ——, "Optimal investment strategy in grid-scale energy storage systems," in *Asia-Pacific Solar Research Conference*, 2018, pp. 1–10.

[27] Y. M. Atwa and E. El-Saadany, "Optimal allocation of ess in distribution systems with a high penetration of wind energy," *IEEE Trans. Power Systems*, vol. 25, no. 4, pp. 1815–1822, 2010.

[28] J. Eyer and G. Corey, "Energy storage for the electricity grid: Benefits and market potential assessment guide," *Sandia National Laboratories*, vol. 20, no. 10, p. 5, 2010.

[29] D. Condon, D. McPhail, and D. Ingram, "Customer and grid impacts of solar, storage and cost reflective tariffs," in *Power Engineering Conference (AUPEC), 2016 Australasian Universities*. IEEE, 2016, pp. 1–6.

[30] G. Celli, S. Mocci, F. Pilo, and M. Loddo, "Optimal integration of energy storage in distribution networks," in *PowerTech, Bucharest*. IEEE, 2009, pp. 1–7.

[31] Y. Ma, D. Gebbran, A. C. Chapman, and G. Verbič, "A photovoltaic system investment game for assessing network hosting capacity allocations," in *The Eleventh ACM International Conference on Future Energy Systems (e-Energy'20)*, June 2020, pp. 1–9.

[32] M. H. Bollen and F. Hassan, *Integration of distributed generation in the power system*. John Wiley & Sons, 2011, vol. 80.

[33] *Australia and New Zealand Standard for Grid connection of energy systems via inverters*, Standards Australia and Standards New Zealand Std. AS/NZS 4777.2:2015, 2015.

[34] H. Zhu and H. J. Liu, "Fast local voltage control under limited reactive power: Optimality and stability analysis," *IEEE Trans. Power Systems*, vol. 31, no. 5, pp. 3794–3803, 2015.

[35] E. Demirok, P. C. Gonzalez, K. H. Frederiksen, D. Sera, P. Rodriguez, and R. Teodorescu, "Local reactive power control methods for overvoltage prevention of distributed solar inverters in low-voltage grids," *IEEE Journal of Photovoltaics*, vol. 1, no. 2, pp. 174–182, 2011.

[36] M. Farivar, R. Neal, C. Clarke, and S. Low, "Optimal inverter var control in distribution systems with high PV penetration," in *Power and Energy Society General Meeting, 2012 IEEE*. IEEE, 2012, pp. 1–7.

[37] Z. Tian, W. Wu, B. Zhang, and A. Bose, "Mixed-integer second-order cone programing model for var optimisation and network reconfiguration in active distribution networks," *IET Generation, Transmission & Distribution*, vol. 10, no. 8, pp. 1938–1946, 2016.

[38] Y. Xu, Z. Y. Dong, R. Zhang, and D. J. Hill, "Multi-timescale coordinated voltage/var control of high renewable-penetrated distribution systems," *IEEE Trans. Power Systems*, 2017.

[39] C. J. Bennett, R. A. Stewart, and J. W. Lu, "Development of a three-phase battery energy storage scheduling and operation system for low voltage distribution networks," *Applied Energy*, vol. 146, pp. 122–134, 2015.

[40] M. R. Jannesar, A. Sedighi, M. Savaghebi, and J. M. Guerrero, "Optimal placement, sizing, and daily charge/discharge of battery energy storage in low voltage distribution network with high photovoltaic penetration," *Applied Energy*, vol. 226, pp. 957–966, 2018.

[41] M. Kabir, Y. Mishra, G. Ledwich, Z. Xu, and R. Bansal, "Improving voltage profile of residential distribution systems using rooftop PVs and battery energy storage systems," *Applied Energy*, vol. 134, pp. 290–300, 2014.

[42] K. Petrou, L. F. Ochoa, A. T. Procopiou, J. Theunissen, J. Bridge, T. Langstaff, and K. Lintern, "Limitations of residential storage in pv-rich distribution networks: An australian case study," in *2018 IEEE Power Energy Society General Meeting (PESGM)*, 2018, pp. 1–5.

[43] A. T. Procopiou, K. Petrou, L. F. Ochoa, T. Langstaff, and J. Theunissen, "Adaptive decentralized control of residential storage in pv-rich mv–lv networks," *IEEE Transactions on Power Systems*, vol. 34, no. 3, pp. 2378–2389, 2019.

[44] X. Liu, A. Aichhorn, L. Liu, and H. Li, "Coordinated control of distributed energy storage system with tap changer transformers for voltage rise mitigation under high photovoltaic penetration," *IEEE Trans. Smart Grid*, vol. 3, no. 2, pp. 897–906, 2012.

[45] P. Fortenbacher, J. L. Mathieu, and G. Andersson, "Modeling and optimal operation of distributed battery storage in low voltage grids," *IEEE Trans. Power Systems*, vol. 32, no. 6, pp. 4340–4350, 2017.

[46] P.-C. Chen, R. Salcedo, Q. Zhu, F. De Leon, D. Czarkowski, Z.-P. Jiang, V. Spitsa, Z. Zabar, and R. E. Uosef, "Analysis of voltage profile problems due to the penetration of distributed generation in low-voltage secondary distribution networks," *IEEE Trans. Power Delivery*, vol. 27, no. 4, pp. 2020–2028, 2012.

[47] A. Navarro-Espinosa and P. Mancarella, "Probabilistic modeling and assessment of the impact of electric heat pumps on low voltage distribution networks," *Applied Energy*, vol. 127, pp. 249–266, 2014.

[48] A. Navarro-Espinosa and L. F. Ochoa, "Probabilistic impact assessment of low carbon technologies in LV distribution systems," *IEEE Trans. Power Systems*, vol. 31, no. 3, pp. 2192–2203, 2016.

[49] C. Protopapadaki and D. Saelens, "Heat pump and PV impact on residential low-voltage distribution grids as a function of building and district properties," *Applied Energy*, vol. 192, pp. 268–281, 2017.

[50] M. Kolenc, I. Papič, and B. Blažič, "Assessment of maximum distributed generation penetration levels in low voltage networks using a probabilistic approach," *International Journal of Electrical Power & Energy Systems*, vol. 64, pp. 505–515, 2015.

[51] Z. Rahimpour, A. Faccani, D. Azuatalam, A. Chapman, and G. Verbič, "Using thermal inertia of buildings with phase change material for demand response," *Energy Procedia*, vol. 121, pp. 102–109, 2017.

[52] A. Barbato and A. Capone, "Optimization models and methods for demand-side management of residential users: a survey," *Energies*, vol. 7, no. 9, pp. 5787–5824, sep 2014.

[53] G. Lorenzi and C. A. S. Silva, "Comparing demand response and battery storage to optimize self-consumption in PV systems," *Applied Energy*, vol. 180, pp. 524–535, 2016.

[54] R. Velik, "Renewable energy self-consumption versus financial gain maximization strategies in grid-connected residential buildings in a variable grid price scenario," *IJARER International Journal of Advanced Renewable Energy Research*, vol. 2, no. 6, 2013.

[55] J. Widén, "Improved photovoltaic self-consumption with appliance scheduling in 200 single-family buildings," *Applied Energy*, vol. 126, pp. 199–212, 2014.

[56] R. Luthander, J. Widén, D. Nilsson, and J. Palm, "Photovoltaic self-consumption in buildings: A review," *Applied Energy*, vol. 142, pp. 80–94, 2015.

[57] J. Moshövel, K.-P. Kairies, D. Magnor, M. Leuthold, M. Bost, S. Gährs, E. Szczechowicz, M. Cramer, and D. U. Sauer, "Analysis of the maximal possible grid relief from PV-peak-power impacts by using storage systems for increased self-consumption," *Applied Energy*, vol. 137, pp. 567–575, 2015.

[58] R. Thygesen and B. Karlsson, "Simulation and analysis of a solar assisted heat pump system with two different storage types for high levels of PV electricity self-consumption," *Solar Energy*, vol. 103, pp. 19–27, 2014.

[59] Z. Chen, L. Wu, and Y. Fu, "Real-time price-based demand response management for residential appliances via stochastic optimization and robust optimization," *IEEE Trans. Smart Grid*, vol. 3, no. 4, pp. 1822–1831, 2012.

[60] O. Erdinc, N. G. Paterakis, I. N. Pappi, A. G. Bakirtzis, and J. P. Catalão, "A new perspective for sizing of distributed generation and energy storage for smart households under demand response," *Applied Energy*, vol. 143, pp. 26–37, 2015.

[61] M. C. Bozchalui, S. A. Hashmi, H. Hassen, C. A. Canizares, and K. Bhattacharya, "Optimal operation of residential energy hubs in smart grids," *IEEE Trans. Smart Grid*, vol. 3, no. 4, pp. 1755–1766, 2012.

[62] F. De Angelis, M. Boaro, D. Fuselli, S. Squartini, F. Piazza, and Q. Wei, "Optimal home energy management under dynamic electrical and thermal constraints," *IEEE Trans. Industrial Informatics*, vol. 9, no. 3, pp. 1518–1527, 2012.

[63] J. Wang, Z. Sun, Y. Zhou, and J. Dai, "Optimal dispatching model of smart home energy management system," in *IEEE PES Innovative Smart Grid Technologies*. IEEE, 2012, pp. 1–5.

[64] M. Killian, M. Zauner, and M. Kozek, "Comprehensive smart home energy management system using mixed-integer quadratic-programming," *Applied Energy*, vol. 222, pp. 662–672, 2018.

[65] C. Keerthisinghe, G. Verbič, and A. C. Chapman, "Addressing the stochastic nature of energy management in smart homes," in *2014 Power Systems Computation Conference*. IEEE, 2014, pp. 1–7.

[66] H. Tischer and G. Verbič, "Towards a smart home energy management system a dynamic programming approach," in *Innovative Smart Grid Technologies Asia (ISGT), 2011 IEEE PES*. IEEE, 2011, pp. 1–7.

[67] K. Garifi, K. Baker, B. Touri, and D. Christensen, "Stochastic model predictive control for demand response in a home energy management system," in *2018 IEEE Power & Energy Society General Meeting (PESGM)*. IEEE, 2018, pp. 1–5.

[68] C. Keerthisinghe, G. Verbič, and A. C. Chapman, "A fast technique for smart home management: ADP with temporal difference learning," *IEEE Trans. Smart Grid*, vol. 9, no. 4, pp. 3291–3303, 2016.

[69] C. Keerthisinghe, A. C. Chapman, and G. Verbič, "Energy management of PV-storage systems: Policy approximations using machine learning," *IEEE Trans. Industrial Informatics*, vol. 15, no. 1, pp. 257–265, 2019.

[70] J. Widén, A. M. Nilsson, and E. Wäckelgård, "A combined Markov-chain and bottom-up approach to modelling of domestic lighting demand," *Energy and Buildings*, vol. 41, no. 10, pp. 1001–1012, 2009.

[71] J. Widén and E. Wäckelgård, "A high-resolution stochastic model of domestic activity patterns and electricity demand," *Applied Energy*, vol. 87, no. 6, pp. 1880–1892, 2010.

[72] J. Widén, M. Lundh, I. Vassileva, E. Dahlquist, K. Ellegård, and E. Wäckelgård, "Constructing load profiles for household electricity and hot water from time-use data—modelling approach and validation," *Energy and Buildings*, vol. 41, no. 7, pp. 753–768, 2009.

[73] A. Capasso, W. Grattieri, R. Lamedica, and A. Prudenzi, "A bottom-up approach to residential load modeling," *IEEE Trans. Power Systems*, vol. 9, no. 2, pp. 957–964, 1994.

[74] T. Power and G. Verbič, "A nonparametric Bayesian model for forecasting residential solar generation," in *2017 Australasian Universities Power Engineering Conference (AUPEC)*. IEEE, 2017, pp. 1–6.

[75] A. Soroudi, M. Ehsan, R. Caire, and N. Hadjsaid, "Possibilistic evaluation of distributed generations impacts on distribution networks," *IEEE Trans. Power Systems*, vol. 26, no. 4, pp. 2293–2301, 2011.

[76] Y. M. Atwa and E. F. El-Saadany, "Probabilistic approach for optimal allocation of wind-based distributed generation in distribution systems," *IET Renewable Power Generation*, vol. 5, no. 1, pp. 79–88, 2011.

[77] J. von Haebler, M. Osthues, C. Rehtanz, and G. Blanco, "Investment strategies as a portfolio of real options for distribution system planning under uncertainty," in *PowerTech, Grenoble*. IEEE, 2013, pp. 1–6.

[78] S. C. Myers, "Determinants of corporate borrowing," *Journal of Financial Economics*, vol. 5, no. 2, pp. 147–175, 1977.

[79] L. Trigeorgis, "Real options and investment under uncertainty: What do we know?" Working Paper Research, Tech. Rep., 2002.

[80] H. Salazar, C.-C. Liu, and R. F. Chu, "Decision analysis of merchant transmission investment by perpetual options theory," *IEEE Trans. Power Systems*, vol. 22, no. 3, pp. 1194–1201, 2007.

[81] R. Pringles, F. Olsina, and F. Garcés, "Real option valuation of power transmission investments by stochastic simulation," *Energy Economics*, vol. 47, pp. 215–226, 2015.

[82] B. Fernandes, J. Cunha, and P. Ferreira, "The use of real options approach in energy sector investments," *Renewable and Sustainable Energy Reviews*, vol. 15, no. 9, pp. 4491–4497, 2011.

[83] G. Kumbaroğlu, R. Madlener, and M. Demirel, "A real options evaluation model for the diffusion prospects of new renewable power generation technologies," *Energy Economics*, vol. 30, no. 4, pp. 1882–1908, 2008.

[84] S.-E. Fleten and E. Näsäkkälä, "Gas-fired power plants: Investment timing, operating flexibility and co2 capture," *Energy Economics*, vol. 32, no. 4, pp. 805–816, 2010.

[85] B. Zou, J. Wang, and F. Wen, "Optimal investment strategies for distributed generation in distribution networks with real option analysis," *IET Generation, Transmission & Distribution*, vol. 11, no. 3, pp. 804–813, 2017.

[86] K. Linnerud, A. M. Andersson, and S.-E. Fleten, "Investment timing under uncertain renewable energy policy: An empirical study of small hydropower projects," *Energy*, vol. 78, pp. 154–164, 2014.

[87] T. K. Boomsma, N. Meade, and S.-E. Fleten, "Renewable energy investments under different support schemes: A real options approach," *European Journal of Operational Research*, vol. 220, no. 1, pp. 225–237, 2012.

[88] T. Bøckman, S.-E. Fleten, E. Juliussen, H. J. Langhammer, and I. Revdal, "Investment timing and optimal capacity choice for small hydropower projects," *European Journal of Operational Research*, vol. 190, no. 1, pp. 255–267, 2008.

[89] D. Eryilmaz and F. R. Homans, "How does uncertainty in renewable energy policy affect decisions to invest in wind energy?" *The Electricity Journal*, vol. 29, no. 3, pp. 64–71, 2016.

[90] I. Ritzenhofen and S. Spinler, "Optimal design of feed-in-tariffs to stimulate renewable energy investments under regulatory uncertainty — a real options analysis," *Energy Economics*, vol. 53, pp. 76–89, 2016.

[91] T. K. Boomsma and K. Linnerud, "Market and policy risk under different renewable electricity support schemes," *Energy*, vol. 89, pp. 435–448, 2015.

[92] E. A. Martinez-Cesena, B. Azzopardi, and J. Mutale, "Assessment of domestic photovoltaic systems based on real options theory," *Progress in Photovoltaics: Research and Applications*, vol. 21, no. 2, pp. 250–262, 2013.

[93] M. Zhang, P. Zhou, and D. Zhou, "A real options model for renewable energy investment with application to solar photovoltaic power generation in china," *Energy Economics*, vol. 59, pp. 213–226, 2016.

[94] M. R. Gahrooei, Y. Zhang, B. Ashuri, and G. Augenbroe, "Timing residential photovoltaic investments in the presence of demand uncertainties," *Sustainable Cities and Society*, vol. 20, pp. 109–123, 2016.

[95] M. Zhang, D. Zhou, P. Zhou, and H. Chen, "Optimal design of subsidy to stimulate renewable energy investments: The case of china," *Renewable and Sustainable Energy Reviews*, vol. 71, pp. 873–883, 2017.

[96] M. A. Eissa and B. Tian, "Lobatto-Milstein numerical method in application of uncertainty investment of solar power projects," *Energies*, vol. 10, no. 1, p. 43, 2017.

[97] D. Lončar, I. Milovanovič, B. Rakič, and T. Radjenovič, "Compound real options valuation of renewable energy projects: The case of a wind farm in Serbia," *Renewable and Sustainable Energy Reviews*, vol. 75, pp. 354–367, 2017.

[98] F. Black and M. Scholes, "The pricing of options and corporate liabilities," *Journal of Political Economy*, vol. 81, no. 3, pp. 637–654, 1973.

[99] J. de Moraes Marreco and L. G. T. Carpio, "Flexibility valuation in the Brazilian power system: A real options approach," *Energy Policy*, vol. 34, no. 18, pp. 3749–3756, 2006.

[100] S. L. MacDougall, "The value of delay in tidal energy development," *Energy Policy*, vol. 87, pp. 438–446, 2015.

[101] E. A. Martinez-Cesena, "Real options theory applied to renewable energy generation projects planning," *The University of Manchester, Manchester, UK*, 2012.

[102] R. C. Merton, "An intertemporal capital asset pricing model," *Econometrica: Journal of the Econometric Society*, pp. 867–887, 1973.

[103] ——, "Theory of rational option pricing," *The Bell Journal of economics and management science*, pp. 141–183, 1973.

[104] S. P. Mason and R. C. Merton, "The role of contingent claims analysis in corporate finance," *In Recent Advances in Corporate Finance*, 1985.

[105] L. Chorn and S. Shokhor, "Real options for risk management in petroleum development investments," *Energy Economics*, vol. 28, no. 4, pp. 489–505, 2006.

[106] M. J. Brennan and E. S. Schwartz, "Evaluating natural resource investments," *Journal of business*, pp. 135–157, 1985.

[107] S.-E. Fleten, K. M. Maribu, and I. Wangensteen, "Optimal investment strategies in decentralized renewable power generation under uncertainty," *Energy*, vol. 32, no. 5, pp. 803–815, 2007.

[108] O. Sezgen, C. Goldman, and P. Krishnarao, "Option value of electricity demand response," *Energy*, vol. 32, no. 2, pp. 108–119, 2007.

[109] D. Möst and D. Keles, "A survey of stochastic modelling approaches for liberalised electricity markets," *European Journal of Operational Research*, vol. 207, no. 2, pp. 543–556, 2010.

[110] J. Schachter and P. Mancarella, "A critical review of real options thinking for valuing investment flexibility in smart grids and low carbon energy systems," *Renewable and Sustainable Energy Reviews*, vol. 56, pp. 261–271, 2016.

[111] J. C. Cox, S. A. Ross, and M. Rubinstein, "Option pricing: A simplified approach," *Journal of Financial Economics*, vol. 7, no. 3, pp. 229–263, 1979.

[112] J. Munoz, J. Contreras, J. Caamano, and P. Correia, "Risk assessment of wind power generation project investments based on real options," in *PowerTech, Bucharest*. IEEE, 2009, pp. 1–8.

[113] E. M. Ceseña, J. Mutale, and F. Rivas-Dávalos, "Real options theory applied to electricity generation projects: A review," *Renewable and Sustainable Energy Reviews*, vol. 19, pp. 573–581, 2013.

[114] S. Mathews and J. Salmon, "Business engineering: a practical approach to valuing high-risk, high-return projects using real options," in *OR Tools and Applications: Glimpses of Future Technologies*. Informs, 2007, pp. 157–175.

[115] M. C. Fu, S. B. Laprise, D. B. Madan, Y. Su, and R. Wu, "Pricing american options: A comparison of Monte Carlo simulation approaches," *Journal of Computational Finance*, vol. 4, no. 3, pp. 39–88, 2001.

[116] F. A. Longstaff and E. S. Schwartz, "Valuing american options by simulation: a simple least-squares approach," *The Review of Financial Studies*, vol. 14, no. 1, pp. 113–147, 2001.

[117] G. Blanco, F. Olsina, F. Garces, and C. Rehtanz, "Real option valuation of facts investments based on the least square Monte Carlo method," *IEEE Trans. Power Systems*, vol. 26, no. 3, pp. 1389–1398, 2011.

[118] H. Pandžić, Y. Wang, T. Qiu, Y. Dvorkin, and D. S. Kirschen, "Near-optimal method for siting and sizing of distributed storage in a transmission network," *IEEE Trans. Power Systems*, vol. 30, no. 5, pp. 2288–2300, 2015.

[119] W. Min and L. Shengsong, "A trust region interior point algorithm for optimal power flow problems," *International Journal of Electrical Power & Energy Systems*, vol. 27, no. 4, pp. 293–300, 2005.

[120] E. C. Baptista, E. A. Belati, and G. R. da Costa, "Logarithmic barrier-augmented lagrangian function to the optimal power flow problem," *International journal of electrical power & energy systems*, vol. 27, no. 7, pp. 528–532, 2005.

[121] S. H. Low, "Convex relaxation of optimal power flow—part i: Formulations and equivalence," *IEEE Trans. Control of Network Systems*, vol. 1, no. 1, pp. 15–27, 2014.

[122] X. Bai and H. Wei, "Semi-definite programming-based method for security-constrained unit commitment with operational and optimal power flow constraints," *IET Generation, Transmission & Distribution*, vol. 3, no. 2, pp. 182–197, 2009.

[123] X. Bai, H. Wei, K. Fujisawa, and Y. Wang, "Semidefinite programming for optimal power flow problems," *International Journal of Electrical Power & Energy Systems*, vol. 30, no. 6, pp. 383–392, 2008.

[124] B. C. Lesieutre, D. K. Molzahn, A. R. Borden, and C. L. DeMarco, "Examining the limits of the application of semidefinite programming to power flow problems," in *Communication, Control, and Computing (Allerton), 2011 49th Annual Allerton Conference on*. IEEE, 2011, pp. 1492–1499.

[125] S. Bose, D. F. Gayme, K. M. Chandy, and S. H. Low, "Quadratically constrained quadratic programs on acyclic graphs with application to power flow," *IEEE Trans. Control of Network Systems*, vol. 2, no. 3, pp. 278–287, 2015.

[126] B. Zhang and D. Tse, "Geometry of injection regions of power networks," *IEEE Trans. Power Systems*, vol. 28, no. 2, pp. 788–797, 2013.

[127] L. Gutierrez-Lagos, M. Z. Liu, and L. F. Ochoa, "Implementable three-phase opf formulations for mv-lv distribution networks: Milp and miqcp," in *2019 IEEE PES Innovative Smart Grid Technologies Conference - Latin America (ISGT Latin America)*, 2019, pp. 1–6.

[128] M. E. Baran and F. F. Wu, "Optimal capacitor placement on radial distribution systems," *IEEE Trans. power Delivery*, vol. 4, no. 1, pp. 725–734, 1989.

[129] M. Farivar and S. H. Low, "Branch flow model: Relaxations and convexification—part i," *IEEE Transactions on Power Systems*, vol. 28, no. 3, pp. 2554–2564, 2013.

[130] M. Farivar, C. R. Clarke, S. H. Low, and K. M. Chandy, "Inverter var control for distribution systems with renewables," in *Smart Grid Communications (SmartGridComm), 2011 IEEE International Conference on*. IEEE, 2011, pp. 457–462.

[131] Z. Wang, H. Chen, J. Wang, and M. Begovic, "Inverter-less hybrid voltage/var control for distribution circuits with photovoltaic generators," *IEEE Trans. Smart Grid*, vol. 5, no. 6, pp. 2718–2728, 2014.

[132] H.-G. Yeh, D. F. Gayme, and S. H. Low, "Adaptive var control for distribution circuits with photovoltaic generators," *IEEE Trans. Power Systems*, vol. 27, no. 3, pp. 1656–1663, 2012.

[133] R. Cespedes, "New method for the analysis of distribution networks," *IEEE Trans. Power Delivery*, vol. 5, no. 1, pp. 391–396, 1990.

[134] R. A. Jabr, "Radial distribution load flow using conic programming," *IEEE Trans. Power Systems*, vol. 21, no. 3, pp. 1458–1459, 2006.

[135] R. Baldick, B. H. Kim, C. Chase, and Y. Luo, "A fast distributed implementation of optimal power flow," *IEEE Trans. Power Systems*, vol. 14, no. 3, pp. 858–864, 1999.

[136] T.-H. Chen, M.-S. Chen, K.-J. Hwang, P. Kotas, and E. A. Chebli, "Distribution system power flow analysis-a rigid approach," *IEEE Trans. Power Delivery*, vol. 6, no. 3, pp. 1146–1152, 1991.

[137] L. Gan and S. H. Low, "Convex relaxations and linear approximation for optimal power flow in multiphase radial networks," in *Power Systems Computation Conference (PSCC), 2014*. IEEE, 2014, pp. 1–9.

[138] Q. Peng and S. H. Low, "Distributed algorithm for optimal power flow on an unbalanced radial network," in *Decision and Control (CDC), 2015 IEEE 54th Annual Conference on*. IEEE, 2015, pp. 6915–6920.

[139] M. Zidar, P. S. Georgilakis, N. D. Hatziargyriou, T. Capuder, and D. Škrlec, "Review of energy storage allocation in power distribution networks: applications, methods and future research," *IET Generation, Transmission & Distribution*, vol. 10, no. 3, pp. 645–652, 2016.

[140] C. Abbey and G. Joós, "A stochastic optimization approach to rating of energy storage systems in wind-diesel isolated grids," *IEEE Trans. Power Systems*, vol. 24, no. 1, pp. 418–426, 2009.

[141] V. Poulios, E. Vrettos, F. Kienzle, E. Kaffe, H. Luternauer, and G. Andersson, "Optimal placement and sizing of battery storage to increase the PV hosting capacity of low voltage grids," in *International ETG Congress 2015; Die Energiewende-Blueprints for the new energy age; Proceedings of.* VDE, 2015, pp. 1–8.

[142] M. Nick, R. Cherkaoui, and M. Paolone, "Optimal allocation of dispersed energy storage systems in active distribution networks for energy balance and grid support," *IEEE Trans. Power Systems*, vol. 29, no. 5, pp. 2300–2310, 2014.

[143] M. Zidar, T. Capuder, P. Georgilakis, and D. Škrlec, "Convex ac optimal power flow method for definition of size and location of battery storage systems in the distribution grid," in *Proc. of the Ninth Conf. on Sustainable Development of Energy, Water and Environment System–SDEWES'(University of Zagreb Faculty of Mechanical Engineering and Naval Architecture, 2014)*, 2014, pp. 1–23.

[144] S. W. Alnaser and L. F. Ochoa, "Optimal sizing and control of energy storage in wind power-rich distribution networks," *IEEE Transactions on Power Systems*, vol. 31, no. 3, pp. 2004–2013, 2016.

[145] M. S. S. Abad, M. K. Gharigh, A. Safdarian, and J. N. Zaeem, "Optimal sizing of distributed energy storage with consideration of demand response in distribution systems," in *Electrical Engineering (ICEE), 2016 24th Iranian Conference on*. IEEE, 2016, pp. 1181–1186.

[146] S. Kahrobaee, S. Asgarpoor, and W. Qiao, "Optimum sizing of distributed generation and storage capacity in smart households," *IEEE Trans. Smart Grid*, vol. 4, no. 4, pp. 1791–1801, 2013.

[147] P. Fortenbacher, M. Zellner, and G. Andersson, "Optimal sizing and placement of distributed storage in low voltage networks," in *Power Systems Computation Conference (PSCC), 2016*. IEEE, 2016, pp. 1–7.

[148] M. Zeraati, M. E. H. Golshan, and J. Guerrero, "Distributed control of battery energy storage systems for voltage regulation in distribution networks with high PV penetration," *IEEE Trans. Smart Grid*, 2016.

[149] W. W. Weaver and P. T. Krein, "Game-theoretic control of small-scale power systems," *IEEE Trans. Power Delivery*, vol. 24, no. 3, pp. 1560–1567, 2009.

[150] S. Mei, Y. Wang, and F. Liu, "A game theory based planning model and analysis for hybrid power system with wind generators-photovoltaic panels-storage batteries," *Dianli Xitong Zidonghua(Automation of Electric Power Systems)*, vol. 35, no. 20, pp. 13–19, 2011.

[151] M. Fahrioglu and F. L. Alvarado, "Designing cost effective demand management contracts using game theory," in *IEEE Power Engineering Society. 1999 Winter Meeting (Cat. No. 99CH36233)*, vol. 1. IEEE, 1999, pp. 427–432.

[152] C. Ibars, M. Navarro, and L. Giupponi, "Distributed demand management in smart grid with a congestion game," in *2010 First IEEE International Conference on Smart Grid Communications*. IEEE, 2010, pp. 495–500.

[153] U. Berger, "Fictitious play in $2\times$ n games," *Journal of Economic Theory*, vol. 120, no. 2, pp. 139–154, 2005.

[154] D. Monderer and L. S. Shapley, "Fictitious play property for games with identical interests," *Journal of economic theory*, vol. 68, no. 1, pp. 258–265, 1996.

[155] R. S. Sutton and A. G. Barto, "Reinforcement learning: An introduction," 2011.

[156] J. R. Marden and J. S. Shamma, "Revisiting log-linear learning: Asynchrony, completeness and payoff-based implementation," *Games and Economic Behavior*, vol. 75, no. 2, pp. 788 – 808, 2012.

[157] P. Mertikopoulos and W. H. Sandholm, "Learning in games via reinforcement and regularization," *Mathematics of Operations Research*, vol. 41, no. 4, pp. 1297–1324, 2016.

[158] P. Zhou, Y. Chang, and J. A. Copeland, "Reinforcement learning for repeated power control game in cognitive radio networks," *IEEE Journal on Selected Areas in Communications*, vol. 30, no. 1, pp. 54–69, 2011.

[159] J. R. Marden, S. D. Ruben, and L. Y. Pao, "A model-free approach to wind farm control using game theoretic methods," *IEEE Trans. Control Systems Technology*, vol. 21, no. 4, pp. 1207–1214, July 2013.

[160] A. C. Chapman, D. S. Leslie, A. Rogers, and N. R. Jennings, "Learning in Unknown Reward Games: Application to Sensor Networks," *The Computer Journal*, vol. 57, no. 6, pp. 875–892, 2013.

[161] ——, "Convergent learning algorithms for unknown reward games," *SIAM Journal on Control and Optimization*, vol. 51, no. 4, pp. 3154–3180, 2013.

[162] S. Bervoets, M. Bravo, and M. Faure, "Learning and convergence to nash in games with continuous action sets," Working paper, Tech. Rep., 2016.

[163] P. Mertikopoulos and Z. Zhou, "Learning in games with continuous action sets and unknown payoff functions," *Mathematical Programming*, vol. 173, no. 1-2, pp. 465–507, 2019.

[164] X. Su, M. A. Masoum, and P. J. Wolfs, "Optimal PV inverter reactive power control and real power curtailment to improve performance of unbalanced four-wire lv distribution networks," *IEEE Trans. Sustainable Energy*, vol. 5, no. 3, pp. 967–977, 2014.

[165] P. Jahangiri and D. C. Aliprantis, "Distributed volt/var control by PV inverters," *IEEE Trans. Power Systems*, vol. 28, no. 3, pp. 3429–3439, 2013.

[166] H. Li, F. Li, Y. Xu, D. T. Rizy, and S. Adhikari, "Autonomous and adaptive voltage control using multiple distributed energy resources," *IEEE Trans. Power Systems*, vol. 28, no. 2, pp. 718–730, 2012.

[167] P. Šulc, S. Backhaus, and M. Chertkov, "Optimal distributed control of reactive power via the alternating direction method of multipliers," *IEEE Trans. Energy Conversion*, vol. 29, no. 4, pp. 968–977, 2014.

[168] C. Zhang, Y. Xu, Z. Dong, and J. Ravishankar, "Three-stage robust inverter-based voltage/var control for distribution networks with high-level PV," *IEEE Trans. Smart Grid*, vol. 10, no. 1, pp. 782–793, 2017.

[169] Ausgrid, "Ausgrid Solar Home Electricity Data," http://data.worldbank.org/indicator/SP.DYN.LE00.FE.IN.

[170] T. Power, G. Verbič, and A. C. Chapman, "A nonparametric bayesian methodology for synthesizing residential solar generation and demand data," *IEEE Trans. Smart Grid*, vol. 11, no. 3, pp. 2511–2519, 2020.

[171] Y. P. Raykov, A. Boukouvalas, F. Baig, and M. A. Little, "What to do when k-means clustering fails: a simple yet principled alternative algorithm," *PloS one*, vol. 11, no. 9, p. e0162259, 2016.

[172] EPRI, "Open distribution system simulator," Online, Report. [Online]. Available: http://electricdss.sourceforge.net

[173] British Standards Institution, "BS EN 50160: Voltage Characteristics of Electricity Supplied by Public Distribution Systems," Report, 2000.

[174] P. Pillay and M. Manyage, "Definitions of voltage unbalance," *IEEE Power Engineering Review*, vol. 21, no. 5, pp. 50–51, 2001.

[175] P. Scott and S. Thiebaux, "Distributed multi period optimal power flow for demand response in microgrids," in *ACM e-Energy*, 2015.

[176] P. Scott, D. Gordon, E. Franklin, L. Jones, and S. Thiébaux, "Network-aware coordination of residential distributed energy resources," *IEEE Trans. Smart Grid*, vol. online, 2019.

[177] A. Papavasiliou, "Analysis of distribution locational marginal prices," *IEEE Trans. Smart Grid*, vol. 9, no. 5, pp. 4872–4882, sep 2018.

[178] W. El-Khattam, Y. Hegazy, and M. Salama, "An integrated distributed generation optimization model for distribution system planning," *IEEE Trans. Power Systems*, vol. 20, no. 2, pp. 1158–1165, 2005.

[179] K. Joshi, "Four charts that show the future of battery storage," *Australian Renewable Energy Agency*, 2017. [Online]. Available: https://arena.gov.au/blog/arenas-role-commercialising-big-batteries/

[180] Bureau of Infrastructure, "Petrol prices and diesel prices in Australia," *Department of Infrastructure, Regional Development and Cities, Australian Government*, 2018. [Online]. Available: https://bitre.gov.au/publications/2017/is_082.aspx

[181] Global Petrol Prices. (2021) Download gasoline and diesel price forecasts. [Online]. Available: https://www.globalpetrolprices.com/forecast.php

[182] Generator Power. (2021) Cummins diesel generators. [Online]. Available: https://generatorpower.com.au/generator-product-category/diesel-generators/generator-brands/cummins-diesel-generators/

[183] Australian PV Institute, "Australian PV Market since April 2001." [Online]. Available: http://pv-map.apvi.org.au/analyses

[184] K. A. W. Horowitz, F. Ding, B. Mather, and B. Palmintier, "The cost of distribution system upgrades to accommodate increasing penetrations of distributed penetrations of distributed photovoltaic systems on real feeders in the United States," National Renewable Energy Laboratory, Tech. Rep., 2018.

[185] AEMO. Market Data. [Online]. Available: http://www.nemweb.com.au

[186] R. Fourer, D. M. Gay, and B. Kernighan, *A Mathematical Programming Language (AMPL)*. Boyd & Fraser Danvers, MA, 1993, vol. 117.

[187] I. Richardson, M. Thomson, D. Infield, and C. Clifford, "Domestic electricity use: A high-resolution energy demand model," *Energy and Buildings*, vol. 42, no. 10, pp. 1878–1887, 2010.

[188] H. Ackermann, H. Röglin, and B. Vöcking, "Pure nash equilibria in player-specific and weighted congestion games," in *International Workshop on Internet and Network Economics*. Springer, 2006, pp. 50–61.

[189] J. B. Rosen, "Existence and uniqueness of equilibrium points for concave n-person games," *Econometrica*, vol. 33, no. 3, pp. 520–534, 1964.

[190] J. Guerrero, A. C. Chapman, and G. Verbič, "Decentralized P2P energy trading under network constraints in a low-voltage network," *IEEE Trans. Smart Grid*, 2018, , Early Access.

[191] D. Gebbran, S. Mhanna, Y. Ma, A. C. Chapman, and G. Verbič, "Fair coordination of distributed energy resources with volt-var control and pv curtailment," *Applied Energy*, vol. 286, p. 116546, 2021.

Thank you.

Do what you can with all you have, wherever you are.
Theodore Roosevelt